

FMH606 Master's Thesis 2017

Industrial IT and Automation

# **Characterization of Ultrasonic Waves in Various Drilling Fluids**

Kenneth Nonso Mozie

Faculty of Technology, Natural sciences and Maritime Sciences  
Campus Porsgrunn

**Course:** FMH606 Master's Thesis, 2017

**Title:** Characterization of Ultrasonic Waves in various Drilling Fluids

**Number of pages:** 78

**Keywords:** Acoustics, Attenuation, impedance, Sound speed.

**Student:** Kenneth Nonso Mozie  
**Supervisor:** Håkon Viumdal  
**Co-Supervisor:** Kanagasabapath Mylvaganam  
**External partner:** Geir Elseth  
**2<sup>nd</sup> External partner:** Tor Inge Waag  
**3<sup>rd</sup> External partner:** Espen Oland  
**Availability:** Open/Confidential

**Approved for archiving:** \_\_\_\_\_

(supervisor signature)

The aim of this master thesis is to characterize ultrasonic wave propagation in different mud samples with respect to propagation distance using three different transducers frequency, this is expected to be an introduction to utilizing ultrasonic Doppler measurements for determining mud flow rate in the test rig at USN.

The experiments were carried out to determine the amplitude attenuation coefficient of the different fluid samples while comparing it to their acoustic properties at different frequencies.

The transducers were operated in through transmission mode while taking apart along an axial propagation distances. A pulser device was employed to drive the transducers at their various designed frequencies, and the amplitude decay from the ultrasonic beam were observed and recorded at several points within the distances between the emitter and the receiver. Results were obtained by estimating the exponential function that described the attenuation coefficient of the fluid sample and multivariate data analysis was used in analyzing the correlations between the fluid samples.

The sound speed of the materials was also calculated but the obtained values for sound speed in water did not completely show concordance with the one defined by literature. This could be due to errors related to the discrepancies associated with the frequencies involved but they have not been completely identified. Nevertheless, experiments yielded successively better results.

It was observed that highly viscous fluid samples with particle composition attenuations more than denser fluid with soluble salt contents.

# Preface

I would like to express my appreciation to Håkon Viumdal my supervisor for his support, guidance and constant encouragement throughout the course of this thesis and for making the resources available at right time, through provision of valuable insights leading to the successful completion of my project.

I would also use this opportunity to express a deep sincere gratitude to Geir of Statoil, Kanagasabapath, Morten and Khim at USN for their cordial supports, which has helped me in completing this task through various stages.

Lastly, I thank almighty God, my family and friends for their constant encouragement without which this project would have not been possible.

Porsgrunn, 14/05/2017

Kenneth Nonso Mozie

# Nomenclature

---

Symbols	Explanations
BHA	Bottom-Hole Assembly
BHA	Bottom hole assembly
ECD	Equivalent circulating density
ESD	Equivalent static density
LWD	Logging While Drilling
MWD	Measurement While Drilling
OBFs	Oil-based fluids
ROP	Rate of penetration
Tf	Transducer frequency
USPD	Ultrasonic Pulse Doppler
PCA	Principal Component Analysis
PLS-R	Partial Least Square Regression
RMSE	Root Mean Square error
NDE	Non-Destructive Evaluation
NDT	Non-Destructive Test

# Overview of Tables and Figures

## List of Figures

Figure 2.1: Drilling Fluid Circulation System.[11]	14
Figure 2.2: Functions of Drilling Fluid.[12]	14
Figure 2.3: Effect of Blowout in the Gulf of Mexico Deep Water Horizon.[13]	15
Figure 2.4: Operating Window for Drilling Operation.[12]	16
Figure 2.5: Mud Balance as used in Measuring Specific Gravity of Drilling Mud.[16]	19
Figure 2.6: March Funnel and Graduated Cup for Quick Test of Viscosity of Drilling Mud[17]	20
Figure 2.7: Multi-rate Viscometer for more Accurate Representation of Viscosity Measurement[17]	20
Figure 2.8: Filter Press Apparatus for Filtrate Verification [17]	21
Figure 2.9: Cutting Bed Formation while Drilling that Results to Hole[19]	22
Figure 2.10: Sand content Apparatus for Measuring the Amount of Sand present in the Mud[17]	22
Figure 3.1: A Longitudinal Wave, The particles move in a direction parallel to the direction of wave propagation	26
Figure 3.2: Shear Wave; as particle vibration is perpendicular to wave direction	26
Figure 3.3: Medium propagation of wave velocity[29]	27
Figure 3.4: Sound Ranges and its Applications	28
Figure 3.5: Sound Beam as it travels from a transducer probe [31]	29
Figure 3.6: Ultrasonic Field Presentation[31]	30
Figure 3.7: Ultrasonic Beam Control	31
Figure 3.8: Wave Attenuation as it is propagated over distance[28]	32
Figure 3.9: Effect of scattering from particle, as can be applicable to mud system[30]	33
Figure 3.10: Viscosity of Newtonian, shear thinning and shear thickening fluids as a function of shear rate.[33]	34
Figure 3.11: Shear stress versus shear rate for Newtonian (a) and non-Newtonian (b) fluid	35
Figure 3.12: Doppler Effect measuring principle basic technique	37
Figure 3.13: Pulsed Doppler principle: initial pulse and echoes from particles[39]	38
Figure 3.14: Interpretation of acoustic raw data	39
Figure 4.1: Setup of the Ultrasonic Measurement for both Axial and Transversal Direction	40
Figure 4.2: Modified image of an Immersion transducer of 1inch element diameter[41]	43
Figure 4.3: Ultrasonic Transceiver	43

Figure 4.4: Container for the Fluid Samples (a) was used for water and (b) was used for Drilling Fluids	44
Figure 4.5: Confidence Interval for t-distribution	46
Figure 4.6: Presentation of Data in Unscrambler Software	47
Figure 5.1: Regression plot for Linear (a) and Logarithmic Scale (b) of Amplitude Variation of 0.5MHz Transducer versus Distance	49
Figure 5.2: Regression plot for Linear (a) and Logarithmic scale (b) of Amplitude Variation of 1MHz Transducer versus Distance	50
Figure 5.3: Regression plot for Linear (a) and Logarithmic Scale (b) of Amplitude Variation of 2.25MHz Transducer versus Distance	51
Figure 5.4: Combined plots of Amplitude Changes in Propagation Distances for the Various Ultrasonic Transducer in Water	51
Figure 5.5: Attenuation of Ultrasonic Wave in Water versus Propagation Distance	52
Figure 5.6: Regression plot for Linear (a) and Logarithmic scale (b) of Amplitude Variation of 0.5MHz Transducer versus Distance	53
Figure 5.7: Regression plot for Linear (a) and Logarithmic Scale (b) of Amplitude Variation of 1MHz Transducer versus Distance	53
Figure 5.8: Regression plot for Linear (a) and Logarithmic Scale (b) of Amplitude Variation of 2.25MHz Transducer versus Distance	54
Figure 5.9: Combined plots for Amplitude Changes with Propagation Distances for the Various Ultrasonic Transducers in Simulated mud	55
Figure 5.10: Attenuation of Ultrasonic Wave in Simulated Mud versus Propagation Distance	55
Figure 5.11: Regression plot for Linear (a) and Logarithmic Scale (b) of Amplitude Variation of 0.5MHz Transducer versus Distance	56
Figure 5.12: Regression plot for Linear (a) and Logarithmic Scale (b) of Amplitude Variation of 1MHz Transducer versus Distance	57
Figure 5.13: Regression plot for Linear (a) and Logarithmic Scale (b) of Amplitude Variation of 2.25MHz Transducer versus Distance	57
Figure 5.14: Combined plot for Amplitude Change with Propagation Distances for the various Ultrasonic Transducer in Mud	58
Figure 5.15: Attenuation of Ultrasonic Wave in Mud versus Propagation Distance	58
Figure 5.16: Matrix Plot of Data set	59
Figure 5.17: Explained Variance for the Decomposed Dataset	60
Figure 5.18: Scores and Loading plot	61
Figure 5.19: Root Mean Square Error Plot	62
Figure 5.20: X- and Y- Loadings Plot	63

Figure 5.21: Loading Weight 64

Figure 5.22: Predicted vs. Reference Plot of 0.5MHz 65

Figure 5.23: Predicted vs. Reference Plot of 1MHz 65

Figure 5.24: Predicted vs. Reference of 2.25MHz 65

Figure 5.25: The plot of the collective fluids attenuation and frequency versus distance 65

**List of Tables**

Table 3.1: Summary of Wave Types used in Non-destructive Testing .....26

Table 4.1: Fluid Composition used .....41

Table 4.2: Experimental Test Matrix .....42

Table 4.3: Calculated details of the transducer in water at sound speed of 1480 [m/s].....43

Table 5.1: Regression Result in Water Sample for the Different Transducers.....49

Table 5.2: Regression Result in Simulated Mud Sample for the Different Transducers.....52

Table 5.3: Regression result in Real mud sample for the different transducers .....56

Table 5.4: Summary of Sound speed Results for the Various Fluid samples, Transducers  
attenuation values and Near zone Distances .....60



# Contents

Preface .....	4
Nomenclature .....	5
Contents.....	9
<b>1 ..Introduction .....</b>	<b>11</b>
1.1 Previous Works.....	11
1.2 Project Scope .....	12
1.3 Organization of the Report .....	12
<b>2 ..Drilling Operations.....</b>	<b>13</b>
2.1 Circulation of Drilling Fluids.....	13
2.2 Basic functions of drilling fluids .....	14
2.2.1 <i>Controlling Formation Pressures</i> .....	15
2.2.2 <i>Removing Cuttings from the Borehole</i> .....	16
2.2.3 <i>Cooling and Lubricating the Bit</i> .....	16
2.2.4 <i>Transmitting Hydraulic Energy to the Bit and Downhole Tools</i> .....	16
2.2.5 <i>Preserving Wellbore Stability</i> .....	17
2.3 Drilling Fluid Types.....	17
2.3.1 <i>Non-Dispersed Systems</i> .....	18
2.3.2 <i>Dispersed Systems</i> .....	18
2.4 Drilling Fluid Properties and Measuring Devices .....	18
2.4.1 <i>Density (Specific gravity)</i> .....	18
2.4.2 <i>Viscosity and GEL Strength</i> .....	19
2.4.3 <i>Filtration Loss</i> .....	20
2.4.4 <i>Solids Content</i> .....	21
2.4.5 <i>Sand Content</i> .....	22
2.5 Acoustic Properties of Drilling Fluids .....	23
2.5.1 <i>Biot Theory</i> .....	24
<b>3 ..Ultrasonic Measurement Technique.....</b>	<b>25</b>
3.1 Wave Propagation and Particle Motion .....	25
3.1.1 <i>Longitudinal Wave</i> .....	25
3.1.2 <i>Shear Wave</i> .....	26
3.2 Properties of Acoustic Wave .....	27
3.2.1 <i>Wave Velocity</i> .....	27
3.2.2 <i>Frequency of Sound</i> .....	27
3.2.3 <i>Wavelength and Defect Detection</i> .....	28
3.3 Ultrasonic Field Analysis .....	29
3.3.1 <i>Ultrasonic Waveform Field Pressure</i> .....	29
3.3.2 <i>Computational Model of a Single Point Source</i> .....	30
3.3.3 <i>Interference Effect</i> .....	30
3.4 Additional parameters of wave propagation.....	31
3.4.1 <i>Attenuation</i> .....	31
3.5 Material Properties Affecting Speed of Sound in Drilling Mud .....	33
3.5.1 <i>Acoustic Impedance</i> .....	35
3.5.2 <i>Viscosity and Thermal Conductivity</i> .....	35
3.6 Measuring Principle of Ultrasonic.....	36
3.6.1 <i>Doppler Effect</i> .....	36
3.6.2 <i>Transit Time Difference</i> .....	37
3.6.3 <i>Pulsed Measurement Principle</i> .....	38

3.7 Interpretation of the Acoustic Spectrometer Raw Data ..... 38

    3.7.1 *Time of the Pulse Flight t* ..... 39

    3.7.2 *Phase of Sound after Propagation* ..... 39

4.. Experiments ..... 40

    4.1 Setup ..... 40

    4.2 Procedure ..... 41

        4.2.1 *Experimental Test Matrix*..... 42

        4.2.2 *Devices used* ..... 42

    4.3 Description of Statistical Analysis Tools Used ..... 44

        4.3.1 *Univariate Linear Regression* ..... 44

        4.3.2 *Multivariate Data Analysis*..... 46

        4.3.3 *Multivariate Data Presentation*..... 47

5.. Results and Discussions..... 48

    5.1 Ultrasonic Propagation in Water ..... 48

        5.1.1 *Measurements with 0.5MHz Transducer in Water* ..... 49

        5.1.2 *Measurements with 1MHz Transducer in Water* ..... 50

        5.1.3 *Measurements with 2.25MHz Transducer in Water* ..... 50

        5.1.4 *Combined Results of the Measurements in Water* ..... 51

    5.2 Ultrasonic Propagation in Simulated Mud ..... 52

        5.2.1 *Measurements with 0.5MHz Transducer in Simulated Mud*..... 53

        5.2.2 *Measurements with 1MHz Transducer in Simulated Mud*..... 53

        5.2.3 *Measurements with 2.25MHz Transducer in Simulated Mud*..... 54

        5.2.4 *Combined Result of the Measurements in Simulated Mud* ..... 54

    5.3 Ultrasonic Propagation Result in Mud..... 55

        5.3.1 *Measurements with 0.5MHz Transducer in Water-based Mud* ..... 56

        5.3.2 *Measurements with 1MHz Transducer in Water-based Mud* ..... 57

        5.3.3 *Measurements with 2.25MHz Transducer in Water-based Mud* ..... 57

        5.3.4 *Combined Result of the Measurements in Real Mud* ..... 58

    5.4 Multivariate Data Analysis ..... 59

        5.4.1 *PCA Results*..... 60

        5.4.2 *PLS-R Results*..... 62

6.. Conclusion ..... 66

    6.1 Further Works ..... 66

References ..... 67

Appendices ..... 70

# 1 Introduction

Optimization of drilling operations has been an ongoing advancement in technology as different strategies are being employed using adequate instrumentations having a distinct focus of minimizing down-time in operations while maximizing profit which collectively is expected to account for both security and safety requirement of personnel and equipment's.

Drilling fluids (mud) are known to be the most important variables to always consider in drilling operations looking at the various functions of it, which amongst many are that it facilitates the drilling of boreholes, provides hydrostatic pressure to prevent formation fluids from entering into the well bore, cooling, cleaning and lubricating of drill bit, transporting of cuttings to surface and serving as a great barrier to hydrocarbon blow out while drilling. This collectively covers the main goals in drilling with controlling of well kicks and prevention of loss of circulation at the top of it.[1, 2]

For successful explorations various considerations are made when controlling the varying constituencies of mud as used by the oil and gas industries which essentially are involved with detection of the different rheological parameters of the drilling fluid and in many cases are unresolved. Study have shown that measurement of delta flow (outflow minus inflow) are seen as the best traditional options for timely diagnosis of kicks and lost circulation while drilling[2]. However, it is significant to develop high-performance flowmeter of drilling mud and the gas-liquid two-phase flow, hence the use of ultrasonic Doppler's for measurement for it accounts for the propagation speed, time, and phase difference of sound waves in the whole system of drilling fluid. As this provides accuracy and response time in detection of influx or loss in a drilling process.

In this thesis some of the physical properties of ultrasonic transducers are exploited taking into considerations ultrasonic field parameters as near field and angle of divergence are tested out and the signal attenuations of the acoustic beam of the transducers observed as the they are taking apart over varying distances and angles while aligning in axial and lateral resolutons and are equally compared with the acoustic properties of different fluid systems.

The information's gathered from ultrasonic field analysis is expected to present some tangible information with regards to downhole conditions. Nevertheless, the state of the drilling process can be known through the analysis of the acoustic properties from the drilling fluids conditions while improving performance by decisions made in real time as flow rates are estimated using ultrasonic Doppler measurements as evaluated in mud flow applications.

## 1.1 Previous Works

Several research and experimental works in different applications has being carried out with ultrasonic Doppler's, taking advantage of it's special features that allows for it to measure instantaneous velocity profile in a very fast response time. (Fischer et al., 2012) used an approach with applicability to hydraulic fluids (in many ways like drilling fluid) where performances are observed through hydraulic pipes and the response from ultrasonic Doppler were compare with other classical flow meter technologies.

The author presented that other flow technologies such as differential pressure, magnetic, turbine and propellers are not well adapted to measure fluctuating flows in hydraulic machines, however by using ultrasonic Doppler, allows for instantaneous velocity profiles in a very short time. They also infer that

Coupling ultrasonic measurement with pressure measurement, one can quantify the unsteady flow in pipes.[3] This essentially can be related to an open Venturi loop with similar transfer function of hydraulic components.

(Zhou. Et al., 2013) used traditional export flow method of early kick detection in verification of their feasibility study on the application of ultrasonic flow measurement technology in drilling mud flow detection based on the Doppler Effect. Even though they obtained good experimental results but they still have severe lag in real time when detecting gas invasion and kicks and concluded that further research needs to be done.[4]

In the paper by (S. A. Africk. et al., 2010) The author used ultrasonic pulse doppler (USPD) for characterizing suspensions of particles using ultrasound. In his study, invasive and non-invasive measurements of velocity components normal to the transducer face in a flowing liquid (milk) similar to mud were demonstrated in measuring flow velocities in a particle suspension using ultrasonic backscatter, where the doppler shifts indicate that flow against the direction of primary flow are functions of the secondary flow. It was also observed that the smallest velocities measured were on the order of 1 cm/s or less. [5]

Furthermore (Mohanarangam et al. 2012). Also, stated that advancement in ultrasonic Doppler measurement technique can replace the previously laser-based techniques used in velocity measurements for large scale process vessels, due to their size and the non-transparent nature of slurries. Ultrasonic Doppler enables quantification of highly turbulent and unsteady flows with useful insight in flow behaviors.[6]

## 1.2 Project Scope

Feasibility study on ultrasonic Doppler flow rate measurement in drilling mud

- Literature research on Ultrasonic Doppler flow rate measurements and its usage in mud flow.
- Experimental research on acoustic properties in water, artificial drilling fluid (from test rig) and actual drilling fluid(s), with three different ultrasonic transducers.
- Analyzing the experimental results and characterizing the wave propagation in the fluids with respect to the propagated distance and transducer frequency.
- Submitting a report with respect to the guidelines of USN with a systematic documentation of codes developed and data gathered

## 1.3 Organization of the Report

The report is divided into six chapters. A preface and introduction to this thesis is given in first two chapters, followed by a chapter briefly describing drilling operations and the applicability of drilling fluid systems, then a chapter where ultrasonic measurement techniques is generally described with emphases on some key parameters such as attenuation and sound speed in a medium. The fourth chapter described how the experiments was carried out, the setup and procedure of the test devices. In the fifth chapter, The results and analysis of the wave characterizations was presented. Chapter six covers the conclusion from the thesis work with some suggestions for further works.

## 2 Drilling Operations

Oil well drilling are essentially performed in creating wells that extend several kilometers into the the earth crust which could be on land or below sea bed in the case of offshore drilling. There are numerous complexity associated with drilling operation which among many involves managing the hydraulic pressures while determining the pressure limits of the open hole of a wellbore, and achieving effective hole cleaning all in the verge of maintaining wellbore integrity.

In optimization of drilling operation, drilling fluid is probably the most crucial variable to be observed, where its selections are based on its corresponding ability to drill the expected formations, effectively clean the hole and still maintain the stabilization of the wellbore.[7]

In this report acoustic properties of drilling fluid will be observed as it has great influence on ultrasonic techniques of oil-well inspection as they are useful in monitoring the physical properties of the fluid.[8]

This chapter focuses on a brief understanding of the fundamentals in drilling operations, where topics such as circulation of drilling fluids, the functions of drilling fluids, types of drilling fluids and drilling fluid properties are discussed.

### 2.1 Circulation of Drilling Fluids

In drilling operation, the drilling fluid are subjected to several processes in its circulations, which in the long run affect its physical properties such as density, viscosity, gel strength and percentage of sand content, this collectively defines the criteria that certifies how efficient and safe the drilling operation is. Adequate strategies must be employed in monitoring and controlling the mud in ensuring that it satisfies the various physical requirements.[9]

Figure 2.1, Shows the description of the life cycle of a drilling mud as its being pumped from the suction tank, up the standpipe, down the Kelly and through the drill pipe as it flows downhole to the bit. The rate of flow of the mud tend to have shear and temperature effect on its properties because of high velocity and pressure.

More also additional shear effects occur as the mud passes through the bit jets and impacts the formation, on returning up the annulus they are also subjected to degradations resulting from downhole conditions loaded with rock cuttings from the formation.

At the surface, the mud flows down the flowline to the shale shakers where larger formation solids are removed. further cleaning occurs as the fluid flows through the mud tank system.

At the suction or mixing tank, fresh additives are mixed into the system, the continuous phase is replenished and the mud weight adjusted, preparing the fluid for its trip back down the hole.[10]

The pressure at the bottom hole is associated with the amount of drilling mud present in the annulus. The larger the drill mud within the annulus, the greater the hydrostatic pressure which essentially results to the increase at bottom hole pressure of the well. Monitoring and controlling the drill mud flowrate aids therefore in maintaining the bottom hole pressure window.

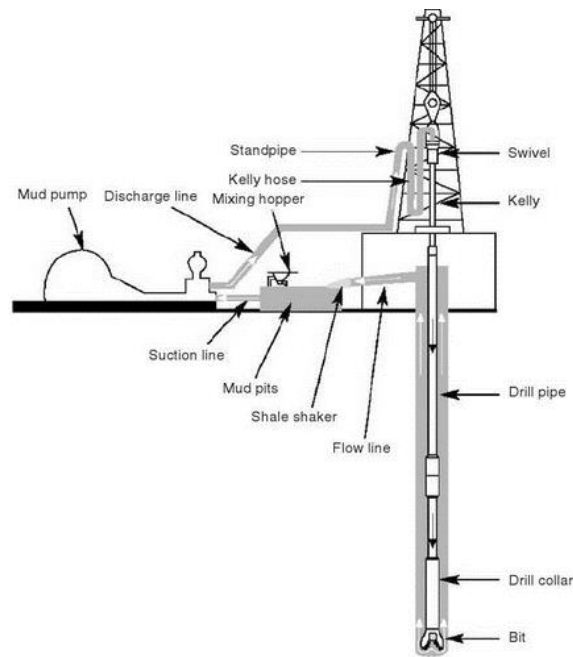


Figure 2.1: Drilling Fluid Circulation System.[11]

## 2.2 Basic functions of drilling fluids

In achieving a set goal for well various fluids are used during the drilling and completion process, these fluids are usually formulated based on the requirements from each wellbore where the mud Engineers designs the composition often with compromise between various fluid properties. The essence of the drilling fluid (mud) design is to serve several functions such as transporting drilled formation out of the wellbore, controlling the formation pressure, avoiding loss of fluid to the formation etc. as can be seen in Figure 2.2. They are usually accompanied with addition of solids to the fluid to prevent fluid loss to the formation, which can eventually lead to increase in viscosity and corresponding excess pump pressures due to flow resistance, on the other hand if the formation fails to withstand the increase in pressure, this results to the fluid being lost into generated fractures in formation. Key performance characteristics of drilling fluids are the following:

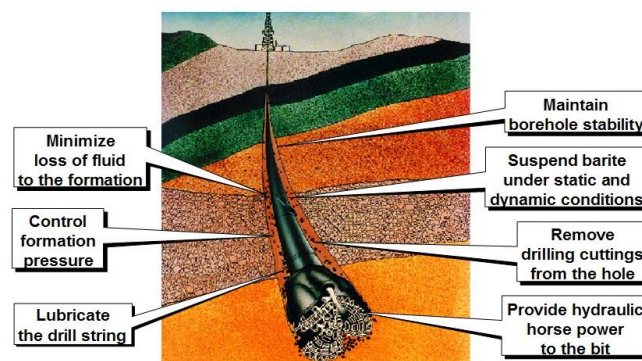


Figure 2.2: Functions of Drilling Fluid.[12]

## 2.2.1 Controlling Formation Pressures

In controlling of well, drilling fluids play an important role, where formation pressure of the well is essentially counterbalanced by the hydrostatic pressure exerted by the drilling fluid as it is being circulated in an open hole, this would otherwise cause loss of well control. However, it is very important to avoid conditions known as lost in circulation - a situation where the drilling fluid flows into generated fractures in the borehole, by always ensuring that the pressure exerted by the drilling fluid must never be higher than the fracture pressure of the rock itself. Operational pressure window must always be maintained while drilling, this is usually achieved by observing the limits for fracturing and pore pressure as shown in Figure 2.4

More also to prevent influx of gas or liquid into the wellbore, the wellbore pressure must always be higher than the pore pressure and the resultant pressures must be kept within the window. This is usually achieved by maintaining an appropriate fluid density for the wellbore pressure regime. As the formation pressure increases, the density of the drilling fluids is increased to help in maintaining a safe margin that would prevent “kicks” or “blowouts” The effect of blowouts can be seen in Figure 2.3. However, the formation may also break down if the density of the fluid becomes too heavy leading to loss of drilling fluid to the resultant fractures, a corresponding reduction of hydrostatic pressure occurs as this reduction can equally lead to an influx from a pressure formation. Static fluid column pressure is described in terms of equivalent static density (ESD), while the sum of all other pressures that includes frictional pressure loss during pumping, makes up the equivalent circulating density (ECD). [9-12]



Figure 2.3: Effect of Blowout in the Gulf of Mexico Deep Water Horizon.[13]

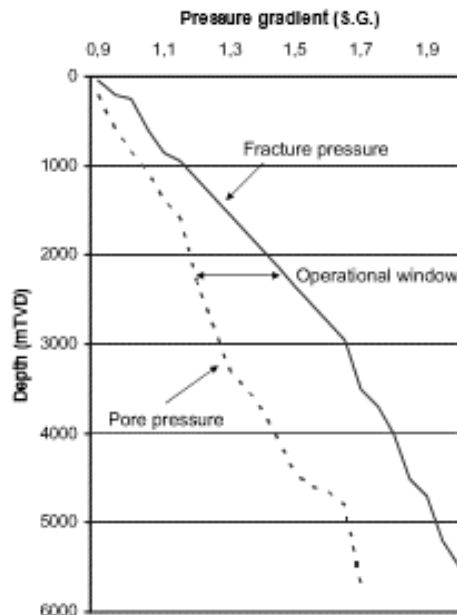


Figure 2.4: Operating Window for Drilling Operation.[12]

## 2.2.2 Removing Cuttings from the Borehole

In the process of drilling, a lot of cutting of rock fragments will occur as the drill bit is moving downwards in the pipe, this will always be carried to the surface by circulating drilling fluid to prevent drilling operation from being stuck due to accumulated particles from rock fragments. Drilling fluid specialist works with the drillers in designing mud rheology and balancing fluid flow rate to achieve an appropriate carrying capacity for the fluid in removing cuttings while avoiding high equivalent circulation density (ECD). Loss of circulation can result from unchecked, high ECD. [9, 12]

## 2.2.3 Cooling and Lubricating the Bit

As the drill pipe are rotating, usually at high revolution per minutes during drilling operations, thermal energy is usually accumulated as result of frictional forces existing between the drilling bit and cuttings as it impacts the well in creating a bore. The circulation of drilling fluid through the drill string up the wellbore annular space helps in minimizing the effect of the friction. The drilling fluid tends to absorb the thermal energy resulting from frictional forces and carries it to the surface. Heat exchanger may be used in extremely hot drilling environments in cooling the fluids at the surface. [9] The drilling fluid lubricates and cool the drill bit as well as provide some amount of lubricity in the movement of the drill pipe and bottom hole assembly (BHA) through planned angles for directional drilling and/or through tight spots that can result from swelling shale.

Oil-based fluids (OBFs) and synthetic-based fluids (SBFs) offer a high degree of lubricity, and as such are preferable fluid types for high-angle directional wells. Some water-based polymer systems also provide lubricity similar to that of the oil and synthetic-based systems.[12]

## 2.2.4 Transmitting Hydraulic Energy to the Bit and Downhole Tools

In drilling operations, the rate of penetration (ROP) of drilling bits are maximized by the hydraulic energy transmitted by drilling fluids with improved cuttings removal at the bit. This



is usually accomplished while the fluids are being discharged through nozzles at the face of the bit, the hydraulic energy released against the formation loosens and carries cuttings away from the formation.

The energy also provides power for downhole motors to rotate the bit and for Measurement While Drilling (MWD) and Logging While Drilling (LWD) tools, that are essentially used in obtaining drilling or formation data in real time. The hydraulic energy effect of the drilling fluid is equally being used in transmitting data gathered downhole to the surface using mud pulse telemetry which relies on pressure pulses through the mud column[10].

### 2.2.5 Preserving Wellbore Stability

The stability of wellbore is preserved by drilling fluids, as the density of the fluids is constantly being regulated through overbalancing the weight of the drilling mud column as against formation pore pressure, this would otherwise help in containing formation pressures and prevention of hole collapse and shale destabilization.

Furthermore, the properties of drilling fluids can also be modified in controlling clay. This are usually complex situations in minimizing hydraulic erosion. Mud engineers ensures that fluid's effect on the formation are always regulated and maintained [9, 11].

## 2.3 Drilling Fluid Types

There are different types of drilling fluids available and are used depending on their compositions, having the key focus of cost, technical performance and environmental impact for any specific well.

This are categorized into nine distinct types which includes:[14]

- Freshwater systems
- Saltwater systems
- Oil- or synthetic-based systems
- Pneumatic (air, mist, foam, gas) “fluid” systems

**Water-based fluids:** With reduced cost water-based fluids (WBFs) also known as invert-emulsion systems and are the most widely used systems and are formulated to withstand relatively high downhole temperatures.

**Oil-based fluids:** The oil-based fluids (OBFs) or synthetic-based fluids (SBFs) also known as invert-emulsion systems this are often recommended when well conditions require excellent lubricity. They are more expensive than most water-based fluids.

**Pneumatic systems:** At the region where formation pressures are relatively low with high risk of loss of circulation, the use of pneumatic systems are usually more beneficial. This involves specialized pressure-management equipment to help prevent the development of hazardous conditions when hydrocarbons are encountered.

The oil and water system can be classified as Mud systems, where water based mud or oil based mud systems are often used in drilling operation which essentially involves exploration of crude oil which are material of great value. In this process, complex equipment is used to filter and process the sludge that emerges as a by-product of the drilling process.

For this project water-based fluid was used with the ultrasonic signal in determining how the signal attenuates with propagation distance, this fluid is categorized into non-dispersed and dispersed system[14].

### 2.3.1 Non-Dispersed Systems

Non-dispersed systems are simple gel and water systems used for top-hole drilling. Flocculation and dilution are used to manage the natural clay that are used in formulating the non-dispersed systems. The efficiency of drilling can be maintained by using an adequate formulated solids control system in removing fine solids from the drilling fluid system

### 2.3.2 Dispersed Systems

The dispersed systems are treated with chemical dispersants that are designed to deflocculate clay particles, that increases the fluid acceptance of solids in controlling mud rheology in the case of higher density muds. This typically require maintaining of pH level of 10.0 to 11.0 by additions of caustic soda (NaOH).

## 2.4 Drilling Fluid Properties and Measuring Devices

The phenomenon of gas invasion which can result in well-blowout while drilling, can easily be detected once the properties of the drilling fluid are clearly understood and maintained.

Mud properties are regularly measured by Engineers as they are designed with different types and quantities of solids (insoluble components) for it to perform a given function, for this reason influences on the distinct property of the designed mud can be resolved. Sound wave principle used by ultrasonic is based on the varying propagation velocity between the different types of mud as this will alert the driller once there is a two-phase flow due to gas influx. The different properties of drilling fluid that are constantly monitored while drilling are:

### 2.4.1 Density (Specific gravity)

Density is defined as weight per unit volume and is reported in any of the following units; ppg (lbs gallons), pound per cubic feet ( $\text{lb}/\text{ft}^3$ ),  $\text{kg}/\text{m}^3$ ,  $\text{gm}/\text{cm}^3$  or compared to the weight of an equal volume of water as specific gravity. This is measured using mud balance as can be seen in Figure 2.5 it is based on the same principle as a beam balance.

The starting point of pressure control while drilling is to ensure that the Mud density is always controlled, for the weight of a column of mud in the hole is necessary to balance formation pressure. However complete mud check generally requires the measurements of both physical and compositional properties of drilling fluid. Some functions are controlled directly by the mud composition, and additive such as calcium carbonate, barite, and hematite are added when required to control the density of the drilling fluids.[15, 16]

The weight of mud columns defines the density of the mud at any specific case. Frequent mistakes in measuring density account for most of the inaccuracies such as:

- Improperly calibrated balance
- Entrained air or gas in the mud
- Failure in filling the balance to exact volume
- Dirty mud balance

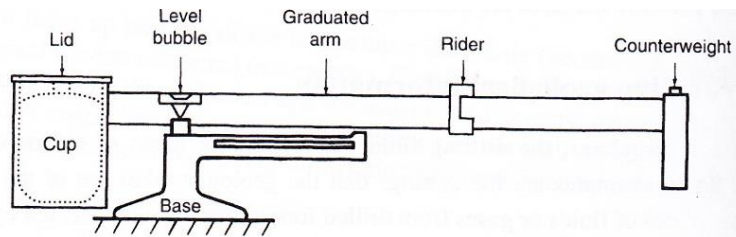


Figure 2.5: Mud Balance as used in Measuring Specific Gravity of Drilling Mud.[16]

## 2.4.2 Viscosity and GEL Strength

Viscosity is defined as the resistance to flow while the gel strength is the thixotropic property of mud since some mud tends to thicken up overtime when not disturbed or placed in motion. The suspension properties of a drilling fluid are measured as Gel strength. This is performed with a rheometer or shearometer and are expressed in pounds per 100 square feet. Mud additives commonly used in imparting viscosity and reducing viscosity are: Bentonite clay, Attapul-Gite, Asbestos, Carboxy, and Methyl cellulose.

As a timed rate of flow, viscosity is measured in seconds per quart. Two methods are commonly used on the rig to measure viscosity:

**Marsh funnel:** as seen in Figure 2.6 is used to make a very quick test of the viscosity of the drilling mud as it measures the time it takes for a given volume of fluid to drain out through the calibrated orifice of a funnel. However, this device only gives an indication of changes in viscosity which is not completely the actual viscosity representation of the mud and cannot be used to quantify the rheological properties of the mud, such as the *yield point* or *plastic viscosity*. It is mainly used in providing a rough but rapid evaluation of any contamination that might drastically modify the fluid's properties.

**Viscometer:** Figure 2.7 shows a multi-rate viscometer, this gives a more accurate representation of viscosity and its control, following rotational principle of its measurement. It can be used in determining drilling fluid rheogram, i.e. the flow law that is represented by the function as expressed in Equation 2.1:

Equation 2.1, Shows the expression of the flow law of viscometer

$$t = f(\gamma) \quad (2.1)$$

Where;  $t$  is the shear stress and  $\gamma$  is the shear rate.

Viscosity and gel strength increases during drilling penetration of the formations by the bit, where cuttings from the drilling process add to the active solids, inert solids and contaminants of the system. This can cause increased viscosity and/or gel strength to level, which may not be acceptable for pressures can be generated by higher viscosity in the borehole when pumping horizontally. In general, when these increases occur, water or chemicals (thinners) or both may be added to control them.[11, 16, 17]

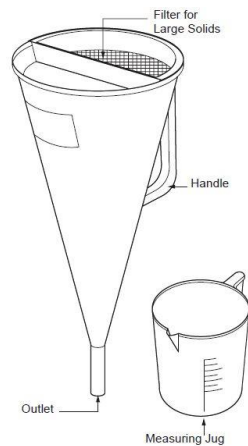


Figure 2.6: March Funnel and Graduated Cup for Quick Test of Viscosity of Drilling Mud[17]

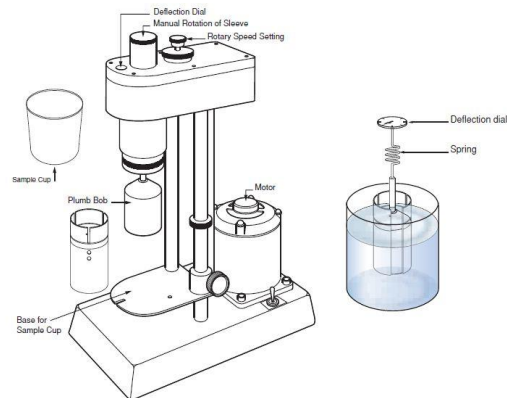


Figure 2.7: Multi-rate Viscometer for more Accurate Representation of Viscosity Measurement[17]

### 2.4.3 Filtration Loss

The Filtration property of a drilling fluid is the ability of the solid components of the mud to form a filter cake and magnitude of cake permeability. The effect of permeability establishes the size of filter cake and volume of filtrate from mud. The physical state of the colloidal material in the mud is dependent on filtration property and is often subjected to hydrostatic pressure while it is in contact with porous and permeable formations.

If the diameter of the pores is greater than the diameter of the suspended clays, the formation will absorb the whole fluid. This can result to lost in circulation especially at the extreme case where the fluid flow is entirely absorbed by the formation without mud return to the surface.

Filtration happens when the diameter of the pores is smaller than part of the suspended particles and forming a cake as base liquid will invade the formation.

Nevertheless, an approved fluid loss value and deposition of a thin, impermeable filter cake are often the determining factors for successful performance of a drilling fluid. There are two types of filtrations namely dynamic filtration, when the mud is circulating, and static filtration when the fluid is at rest.

Filter cake and filtrate are determined with a filter press apparatus (Figure 2.8). Filter cake is reported in 32nd's of an inch. Filtrate is measured in cc's. [11, 16-18]

The following are measured during this test:

1. The rate at which fluid from a mud sample is forced through a filter under specified temperature and pressure, as this reflects the efficiency with which the solids in the mud are creating an impermeable filter cake.
2. The thickness of the solid residue deposited on the filter paper caused by the loss of fluids, for it indicates the thickness of the filter cake that will be created in the wellbore. This does not accurately simulate downhole conditions for only static filtration is being measured. In the wellbore, filtration is occurring under dynamic conditions with the mud flowing past the wall of the hole.[11]

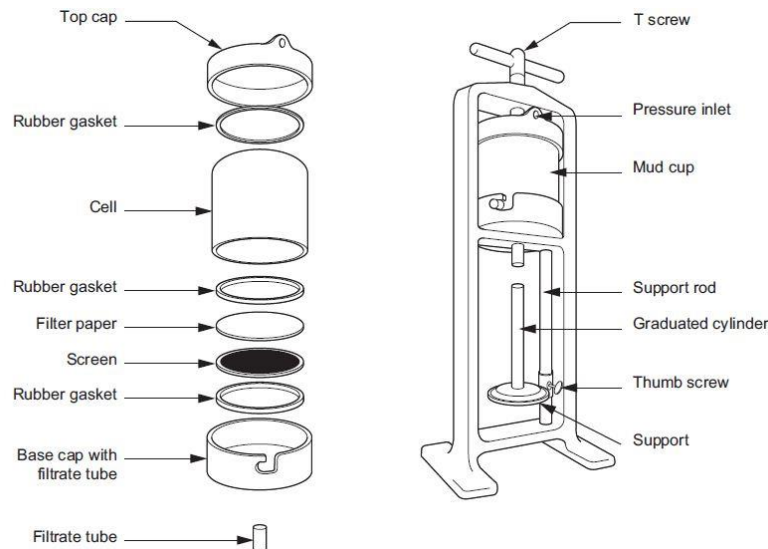


Figure 2.8: Filter Press Apparatus for Filtrate Verification [17]

### 2.4.4 Solids Content

Drilling mud are composed of both a liquid and a solid phase. It always important to avoid pipe sticking, a situation where annular velocities are reduced while drilling due to junk in the hole, and wellbore geometry anomalies resulting from accumulation of cuttings that eventually may result to hole packoff. This is often applicable around the Bottom-Hole Assembly (BHA) and can eventually stuck the drill string if not removed. Figure 2.9 shows a cutting bed formation, the proportion of solids in the mud should not exceed 10% by volume.

Equation 2.2, shows the expression of solids content

$$t = \frac{V_{Solids} \times 100}{V_{Mud}} \quad (2.2)$$

The two phases are separated by distillation where a carefully measured sample of mud is heated in a retort until the liquid components are vaporised, the vapours are then condensed, and collected in the measuring glass. The volume of liquids (oil and/or water) is read off directly as a percentage. The volume of solids (suspended and dissolved) is found by subtraction from 100%.  $t$  (Solids Content) is calculated by measuring the volume of liquid collected:[11, 16]

Equation 2.3, shows the expression on how the volume of solids are found.

$$t = 100 \times \left( \frac{1 - V_{Solids}}{V_{Mud}} \right) \quad (2.3)$$

In general, hole cleaning ability is enhanced by the following [19]:

- Increased fluid density
- Increased annular velocity
- Increased YP or mud viscosity at annular shear rates

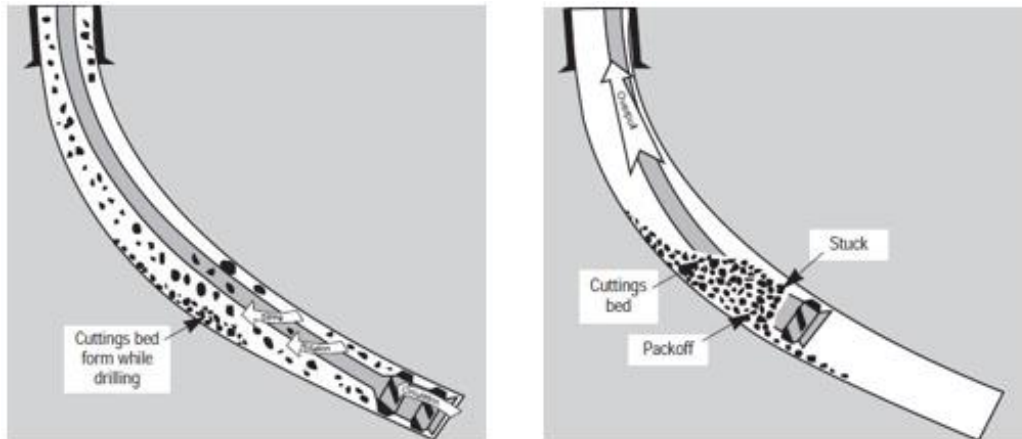


Figure 2.9: Cutting Bed Formation while Drilling that Results to Hole[19]

### 2.4.5 Sand Content

The amount of sand present in a fluid or slurry is determined by revealing solids larger than 200 mesh that are drawn in the fluid, and it is quite different from total solid's content. High proportion of sand in the mud is generally undesirable for this can damage the mud pumps. Therefore, mud Engineer measures the percentage of sand in mud regularly using a sand content kit and are expressed in percentage of total volume using the sand apparatus as seen in Figure 2.10[11, 16].

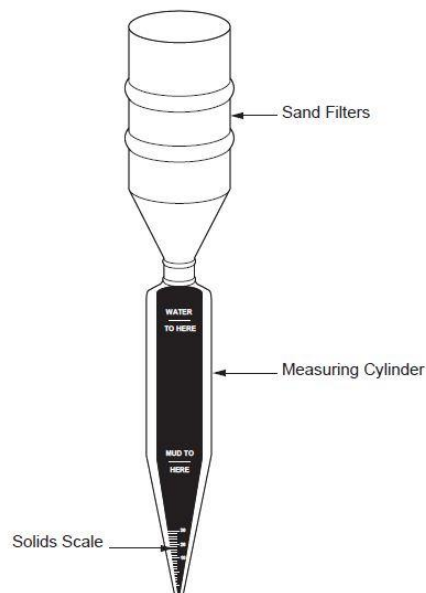


Figure 2.10: Sand content Apparatus for Measuring the Amount of Sand present in the Mud[17]

## 2.5 Acoustic Properties of Drilling Fluids

During drilling, as mud are injected down the drill pipe, they return via the annulus between the drill string and the formations in a circular manner. If the pore-fluid formation pressure exceeds that of the mud column, reservoir gas can enter the wellbore, creating a kick which can cause severe damage such as well blowout as is also seen in Figure 2.3.

Knowledge of the in-situ sound velocity of drilling mud can be useful for evaluating the presence and amount of gas invasion in the drilling fluid.

The use of ultrasonic sensor for fluid characterization is involved with in-situ characterization of downhole fluids in a wellbore using ultrasonic acoustic signals. This essentially involves measurements of the speed of sound, attenuation of the signal, and acoustic back-scattering.

Collectively this can be used in providing useful information as to the composition, nature of solid particulates, compressibility, bubble point, and the oil/water ratio of the fluid.[20]

Assuming a given drilling plan with pore pressure  $p$  represented as a function of depth  $z$ , The density of drilling mud required at each depth is given as Equation 2.4:

Equation 2.4: shows the expression for the density of mud required as each depth in drilling

$$\rho_{mud} = p/(gz) \quad (2.4)$$

Where;

$g$  : is the acceleration due to gravity

$\rho_{mud}$  is essentially as equivalent to density knowing that the density of the drilling mud depends on temperature and pressure through the depth  $z$ .

A constant geothermal gradient  $G$ , can be assumed such that the temperature variation with depth is expressed as Equation 2.5.

$$T = T_0 + Gz \quad (2.5)$$

Where;

$T_0$  is the surface temperature,

Typical value of  $G$  range from 20 to 30°C/km.

Drilling mud consists of suspensions of clay particles and high-gravity solids, such as barite (in water-based muds) and itabarite (an iron ore, in oil-based muds), whose properties are assumed to be temperature and pressure independent. The fluid properties depend on temperature and pressure, and on API number and salinity, if the fluid is oil or water, respectively.

The sound velocity of a drilling mud system changes when formation gas enters the well bore at a given drilling depth, also with the effect of gas absorption as in the case of oil-based muds. For water-based muds, the velocities are higher at low gas saturations and greater depths, with minimal value at midrange of saturations.

Oil-base muds have a different behavior when there is a gas invasion, for the velocity curves change clearly below a critical saturation, when all the gas goes into solution in the oil. This critical saturation decreases with decreasing depth, which implies that at shallow depths the gas is in the form of bubbles rather than dissolved in the oil.[21]

### 2.5.1 Biot Theory

Suspensions in drilling fluid can be derived using Biot theory, which generally considers the coupled motion of a porous elastic solid and a fluid, in the long wavelength limit. The properties of a suspension depend on two physical properties: the compressibility and the effective density. The compressibility can be obtained using Wood's formula as expressed in Equation 2.6

$$k = \sum_n k_n \phi_n \quad (2.6)$$

Where;

$\phi_n$  is the volume fraction, and  $k_n$  is the compressibility, of the component n.

This also can be applied in determining the inertial or effective density  $\rho_{eff}$ . The rule of thumb that are naturally observed is that for suspended particles which are denser than the fluid, their inertia tends to inhibit the oscillations of the fluid, while the fluid viscosity drags them along. The reduced particle momentum reduces the effective density of the suspension, while the viscous losses cause absorption of energy. The effective density of weighted muds can be significantly reduced at ultrasonic frequencies because of the inertia of the suspended particles. The limits of effective density in long-wave length region can be easily found, this are available in literatures.[22]



## 3 Ultrasonic Measurement Technique

Ultrasonic techniques of measurement offers possibility for environmental friendly and fast non-invasive testing, which has been well proven in various fields of studies ranging from medicine, industry and science. Online monitoring of fluid properties and particle sedimentation are continually being exploited using ultrasound. In oil and gas industries, much is still to be done with regards to real-time measurement in flow of liquid-solid particle suspension as it is a challenge in the metering world and also in ultrasound absorption with application in circulating drilling mud.

Ultrasound absorption is a critical parameter in investigation of an MWD acoustic level measurement. The technique is based on ultrasound signal reflection being dependent on the sound wave transfer in the base fluid, the longitudinal and transverse speed of sound in the material reflecting the signal as well as particle shape, size and concentration. This all together have dependency on ultrasound velocity and attenuation upon the material and structural properties. There are two basic types of ultrasonic testing, viz., pulseecho technique and through transmission technique, pulse-echo technique uses the same transducer as transmitter as well as receiver; whereas in through transmission technique, separate transducers are used for transmitting and receiving ultrasonic signals[23, 24].

In order to understand the measuring principle itself, it is necessary to understand some basic terms which are important in ultrasonic measurement.

### 3.1 Wave Propagation and Particle Motion

Ultrasonic testing uses sound waves which essentially is referred to as acoustics. This involves vibration in a material where the particle velocity of the material initiates motion as the wave resulting from the vibration reaches individual particles under test. This is usually achieved by a piezoelectric element that is pulsed with an appropriate voltage- versus- time profile, this converts electric energy into mechanical energy by piezoelectric effect.

The most common methods of ultrasonic examination which utilizes particle velocity motion resulting from wave as generated within material are longitudinal waves or shear waves. This classification of ultrasonic waves is based upon the direction of particle vibration when an ultrasonic wave travels through a medium. Other forms of sound propagation exist, such as surface waves and Lamb waves which also is involved with superposition of longitudinal and shear wave particle velocity component the summary on mode of propagation is as shown in Table 3.1[25].

#### 3.1.1 Longitudinal Wave

A longitudinal wave can be referred to as compressional wave in which the particle motion is in the same direction as the propagation of the wave. It always needs a medium in order to travel, an example is sound in the air or in water. As shown in Figure 3.1. The individual particles in the medium - atoms or molecules - oscillate in the direction of propagation. When the oscillation has passed the particles return to their rest position, the equilibrium position. No energy is lost when the oscillation is propagated, apart from the losses due to the friction between the particles. It travels fastest amongst the various modes of propagation, which is the reason why it is mostly used in NDT [25-27].

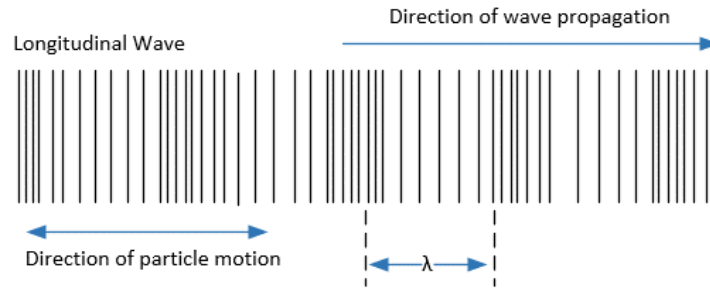


Figure 3.1: A Longitudinal Wave, The particles move in a direction parallel to the direction of wave propagation

### 3.1.2 Shear Wave

Shear wave which also can be referred to as horizontal or transverse wave looking at the coordinate used in its study is a wave motion in which the particle motion is perpendicular to the direction of the propagation. The particle vector is at 90° to the direction of wave vector; the depth of penetration is approximately equal to one wavelength. Shear waves can be found mostly in solid material and not in liquids or gasses and can convert to longitudinal waves through reflection or refraction at a boundary.

Figure 3.2, provides an illustration of the particle motion versus the direction of wave propagation for shear waves, though it has slower velocity and shorter wavelength as compared to longitudinal wave and are used mostly for angle beam testing in ultrasonic flaw detection.

In contrast to longitudinal waves, not all types of transverse wave are restricted to one medium. In gases and liquids ultrasound propagates only as a longitudinal wave or in other words: longitudinal waves compress and decompress the medium in the direction of the propagation[25-27].

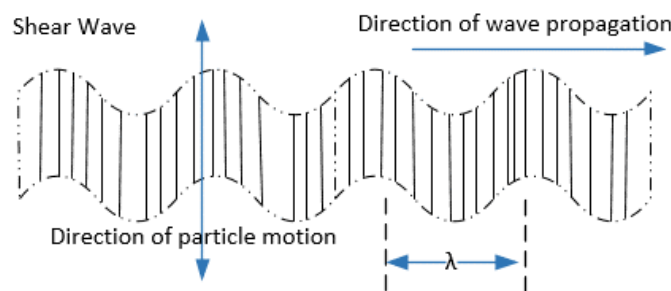


Figure 3.2: Shear Wave; as particle vibration is perpendicular to wave direction

Table 3.1: Summary of Wave Types used in Non-destructive Testing

Wave Type	Particle Vibration
Longitudinal (Compression)	Parallel to wave direction
Transverse (Shear)	Perpendicular to wave direction
Surface - Rayleigh	Elliptical orbit – symmetrical mode
Plate Wave - Lamb	Component perpendicular to surface

## 3.2 Properties of Acoustic Wave

Properties required for wave propagations in any medium are wavelength, frequency and velocity. The wavelength as expressed in equation (2.4) is directly proportional to the wave velocity and inversely proportional to the frequency at which the sound is propagated.

Equation 3.1, is an expression of acoustic wavelength for ultrasonic signals

$$\lambda = \frac{v}{f} \quad (2.4)$$

Where;

$\lambda$  : wavelength (m),  $v$  : velocity (m/s), and  $f$  : frequency (Hz)

Increase in frequency results to a decrease in wavelength as can be deduced from the equation. Velocity of sound is peculiar for different materials at different temperature ranges.[28]

### 3.2.1 Wave Velocity

Wave velocity an essential parameter for wave propagation in ultrasonics is the velocity at which disturbance travels in a medium, as shown in (Figure 3.3.), this are involved with oscillations which moves at a certain speed, frequency and amplitude and it's value depends on material, structure and form of excitation. Speed at which sound propagates in a medium is one of the properties of such medium and the value as used in ultrasonic NDE is derived from the bulk longitudinal wave velocity which is generally thought of as directly proportional to the square root of the elastic modulus over density.

At a specific temperature every medium has its own specific sound propagation velocity and it is affected by the medium's density and elastic properties, many tables of wave velocity values for different medium exist in literatures. Velocity of sound is greater in solids than in liquids and gases for the denser the molecular structure of a medium, the faster the sound waves propagate in such medium[25, 29].

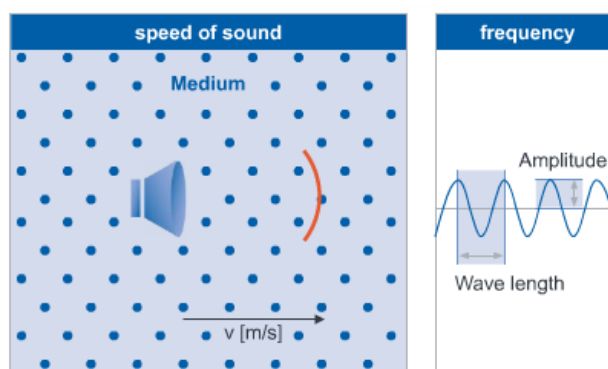


Figure 3.3: Medium propagation of wave velocity[29]

### 3.2.2 Frequency of Sound

Ultrasonic wave have frequency ranges usually in megahertz this are naturally higher than audible sound. At such ranges sound energy can only travel effectively through most liquids and some materials such as metals, plastics, ceramics, and composites but not in air or other gasses. Ultrasounds are usually more directional due to shorter wavelengths resulting from

their high frequency ranges and as such are more sensitive to any reflectors along its path. This makes it a very useful concept in oil industries for NDE and online monitoring of fluid properties and particle sedimentation such as in drilling operations.

Figure 3.4 shows some ranges of sound and their various applications. Humans can only hear up to a range of 18 to 20 kHz. Above 20 kHz denotes ultrasound, which can no longer be perceived by the human ear though some animals can still hear to some extent. The lower the velocity of sound of a medium, the lower the frequency with which ultrasonic flowmeters work. Different frequencies affect the penetrating power in the media, beam spread and the divergence of the acoustic beam[27-29].

Frequency of transducer also have effect on the shape of ultrasonic beam, beam spread, or the divergence of the beam from the center axis of the transducer

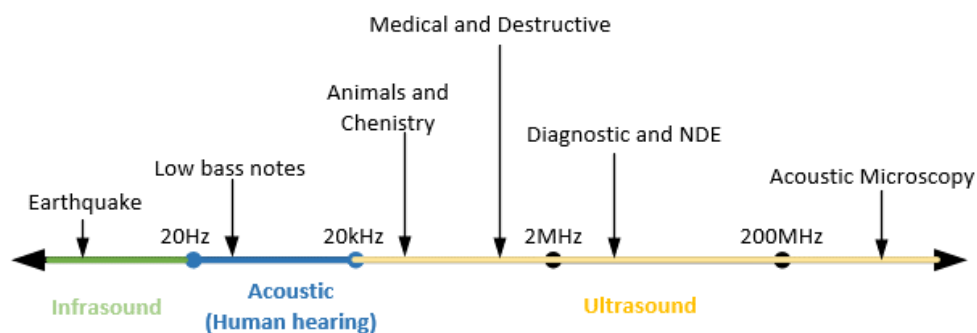


Figure 3.4: Sound Ranges and its Applications

### 3.2.3 Wavelength and Defect Detection

Frequencies of ultrasonic transducers are inversely proportional to the wavelength as expressed in (Equation 3.1), this on the other hand influences the penetrating power of the wave as well as how reflections are resolved.

The higher the wavelength or lower frequencies the further the penetration of the wave into a medium because of less absorptions. Higher frequencies decay more rapidly in a medium but with greater resolution capability. Ultrasonic techniques for flaw detection in measurements are often governed by two basic terms which are Sensitivity and resolution. This effect all together guides in decision making while selecting transducers for different applications.

- Sensitivity is the ability of the ultrasonic transducer to locate small discontinuities, and this increases with shorter wavelengths.
- Resolution is the response capability of a transducer in locating discontinuities that are close together within material/medium or located near the part surface.[28]

### 3.3 Ultrasonic Field Analysis

Sound wave beam emanating from ultrasonic transducers probe usually spreads out in the form of an elongated cone shape like the beam of light from a torch which widens and weakens as it travels over a distance from point source. This is as shown in (Figure 3.5). The weakening of sound intensity is because of energy loss, for ultrasonic beam are attenuated as it progresses through a material, this can be caused by the effect of: [30]

- Absorption of energy due to molecules vibration of the medium
- Scattering of sound waves as reflected from particle boundaries
- Interference effects around the transducers
- Beam Spreading which is the energy spread over an area with distance.

This concept of beam spreading aid in the understanding of ultrasonic field analysis. More also, with the ideas on how the beam affects an inspection one can perform and modify tests on an interactive basis following the changes in intensity of the beam along its axis and across the beam, thereby providing one with an effective feedback process for improving data acquisition, signal interpretation and so forth[25].

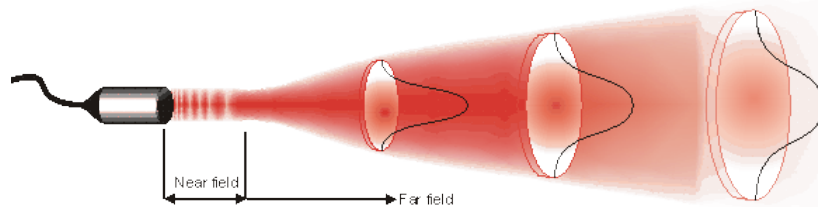


Figure 3.5: Sound Beam as it travels from a transducer probe [31]

#### 3.3.1 Ultrasonic Waveform Field Pressure

The pressure variation of ultrasonic field in drilling fluid system are three dimensional but are usually presented in two-dimensional form just as in every other medium. Several modified techniques exist in literatures for representing the variation but the most beneficial ones that are more applicable in field analysis problems are:[25]

**Axial pressure profile:** This is involved with the plots of the maximum pressure of an ultrasonic waveform as a function of the axial coordinate which originates from the center line of the transducer element, the changes in the signal intensity is observed when the transducers are taking apart over varying distances. The maximum pressure value is extracted as a peak-to-peak magnitude feature of the entire amplitude-versus-time profile as it passes the coordinate axis  $z$ . This can be shown from the center line of (Figure 3.6).

**Polar coordinate diffraction-type presentation:** This is involved with the plots of the maximum pressure against an angle  $\theta$ , basically as the transducers are taking apart along transversal direction in examining the rays as it projects from the coordinate center point. The maximum pressure value occurring at that angle can be measured along the radial coordinate, as shown in (Figure 3.6). This usually produce side lobes of pressure energy due to constructive and destructive interference phenomena occurring in the superposition process of ultrasonic waveforms.

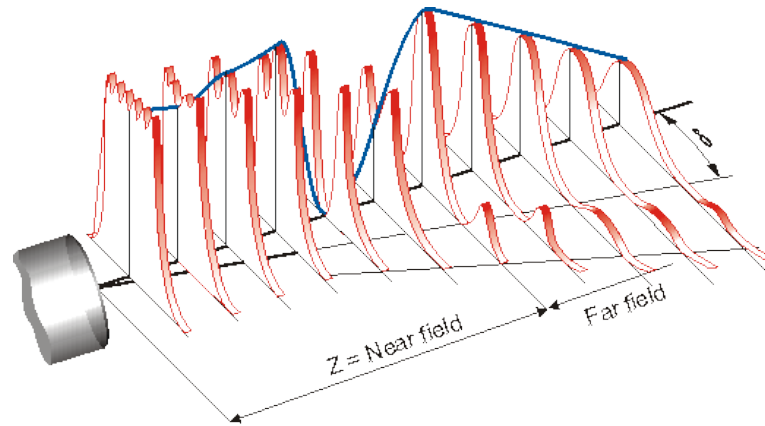


Figure 3.6: Ultrasonic Field Presentation[31]

### 3.3.2 Computational Model of a Single Point Source

Ultrasonic field in solid media such as drilling fluid is based on the computational model of a single point source. Pressure variations resulting from ultrasonic wave interaction with a small reflector are calculated by considering a known point source solution in the fluid in connection with Huygens's principle.[25] The expression of point-source excitation in a fluid which produces a spherical field is given in Equation 3.2

$$p(r, t) = \frac{A_0}{r} e^{i(kr - \omega t)} \quad (3.2)$$

Where;  $A_0 = \rho c U_0$ ,  $\omega = 2\pi f$ ,  $U_0$  is the amplitude of the outgoing wave,  $c$  is the wave velocity, and  $\rho$  is density.

Transducers, however, are not a point source, but a plate of piezoelectric material of finite dimensions. Huygens uses the concept of finite source to be made up of an infinite number of point sources in generating a computation mode. Once transducers are powered, sound will radiate out from each of these point sources, like stone dropping into a pond.[30]

### 3.3.3 Interference Effect

Interference' occurs whenever energy arrives at different wavelength intervals at a particular point in ultrasonic evaluation and this can be constructive or destructive. There is a zone near the source that is characterized by high variation in the field intensity especially for continuous wave operations. This zone is termed the near zone; beyond this we have the far zone where the field intensity decreases smoothly as also is shown in (Figure 3.6.). [25, 30]

**Near field:** is the point on the axis of transducer separating the region of large oscillation from the region of a smooth decay. This point can be located from the last of several local maxima, and this can be calculated from Equation 3.3.

$$N = \frac{D^2}{4\lambda} \quad (3.3)$$

Where;

$N$  is the Near field distance

$D$  is the element(crystal) diameter

$\lambda$  is the wavelength

**Angle of Divergence:** The relative intensity distribution of ultrasonic wave is characterized by the beam angle of divergence and this can also affect attenuation of the sound as it travels through a medium. Angle of divergence are controlled by varying transducer geometry, frequency and sizes. The expression for beam spread are theoretically in three slices as shown in (Figure 3.7). The intensity of sound falls at this different edges from the beam. These are grouped as – one defining the absolute edge of the beam; another defining the 6-dB edge; and the third defining the 20-dB edge. These three edges can be expressed as equation (3.4-3.6)

Equation 3.4: Defines the absolute edge of the beam

$$\sin \frac{\alpha}{2} = \frac{1.22\lambda}{D} \quad (3.4)$$

Equation 3.5: Defines the 6dB edge

$$\sin \frac{\alpha}{2} = \frac{0.56\lambda}{D} \quad (3.5)$$

Equation 3.6: Defines the 20dB edge

$$\sin \frac{\alpha}{2} = \frac{1.08\lambda}{D} \quad (3.6)$$

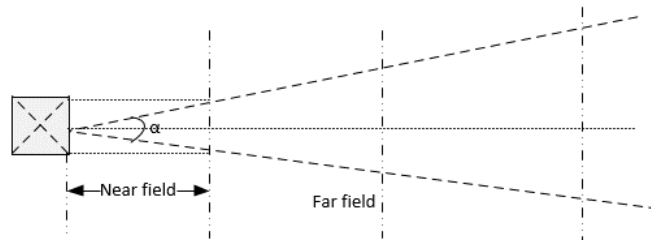


Figure 3.7: Ultrasonic Beam Control

Small angle of divergence is usually desirable and this can be obtained with smaller wave length transducer or higher frequency with larger transducer radius, though this can increase the near field effect. A balance between the transducer frequency and radius must be agreed upon in order to avoid confusion zone of constructive and destructive interference[25].

## 3.4 Additional parameters of wave propagation

Early kick detection methods in oil and gas industries can be improved upon once the varying parameters of wave velocity and attenuation which are essentially the nonlinear features of the drilling mud are monitored in real time[32]. The additional parameters for wave propagations are as described below;

### 3.4.1 Attenuation

Attenuation of ultrasonic signal is the decay rate of wave as it propagates through a media. This is a very useful quantity in characterization of ultrasonic wave in drilling operations. The intensity of sound waves usually decreases with distance as it travels through a medium this is because of internal friction (acoustic impedance) or energy absorption in the medium.

Attenuation can be seen as a function of frequency, however this is applicable to both dispersive and nondispersive media, as in drilling fluid system, for pulse spreading from acoustic waves essential leads to magnitude reduction[25]. The values for attenuation are often given for a single frequency of transducer, however the actual value of attenuation coefficient for a given material depends mainly on how the material was designed. Thus, the quoted values of attenuation only give a rough indication, a more trusted value can only be obtained by determining the attenuation experimentally for the material being used. Attenuation can be determined by evaluating the multiple backwall reflections seen in a typical A-scan display as shown in Figure 3.8.

Further effects that weakens Ultrasonic waves are scattering and absorption of sound, and their combined result gives rise to attenuation of wave propagation which is proportional to square root of sound frequency. [30]

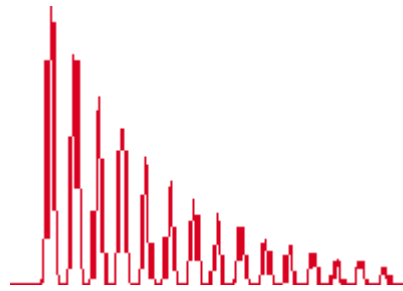


Figure 3.8: Wave Attenuation as it is propagated over distance[28]

Equation 3.7: Shows the expression for the amplitude change of a decaying plane wave

$$A = A_0 e^{-\alpha z} \quad (3.7)$$

Where;

$A_0$  : Initial (unattenuated) amplitude

$A$  : is the reduced amplitude as the wave travels over a distance from an initial point

$e$  :  $e$  is the exponential (or Napier's constant) which is approximately 2.71828.

$\alpha$  : Attenuation coefficient (Np/m); Np = Neper a logarithmic dimensionless quantity

$z$  : Distance traveled (m)

Attenuation is measured in decibel (dB), a logarithmic unit that describes the ratio between two measurements say  $X_1$  and  $X_2$  and their differences as expressed in Equation 3.8

Equation 3.8: shows the expression between two measurement

$$\Delta X (dB) = 10 \log \frac{X_2}{X_1} \quad (2.6)$$

The variation in sound pressures for ultrasonic transducers can be also be quantified as intensity of sound waves ( $I$ ), and this can be converted to a voltage signal since the intensity of sound waves is proportional to the square of pressure amplitude and is generally not measured directly. In decibels it is expressed as in Equation 3.9[28]:

Equation 3.9: shows the expression for change in intensity of sound waves ( $I$ )

$$\Delta I (dB) = 10 \log \frac{I_2}{I_1} = 10 \log \frac{P_2^2}{P_1^2} = 20 \log \frac{P_2}{P_1} = 20 \log \frac{V_2}{V_1} \quad (2.10)$$



Where;

$\Delta I$  : is the change in sound intensity between two measurements expressed in decibels (dB)

$P_1$  &  $P_2$  : are two different sound pressure amplitude measurements, and the log is to base 10

$V_1$  &  $V_2$  : the two transducer output voltages.

**Scattering:** Scattering is the reflection of the sound in directions other than its original direction of propagation, as this can produce both magnitude reductions as well as pulse spreading due to wave transmission from a transducer or from wave interaction with small obstacle as can be applicable to mud compositions (see Figure 3.9). The larger the particle size, present in a drilling mud the greater the scatter.

**Absorption:** Absorption is the conversion of the sound energy to other forms of energy; this usually occurs as the energy are lost which has correlations with the elastic properties of the medium. Lower frequency transducer overcomes the effect of high absorption and scatter for it tends to propagate sound wave father into the medium. Attenuation (absorption and scatter) decreases as test frequency decreases.

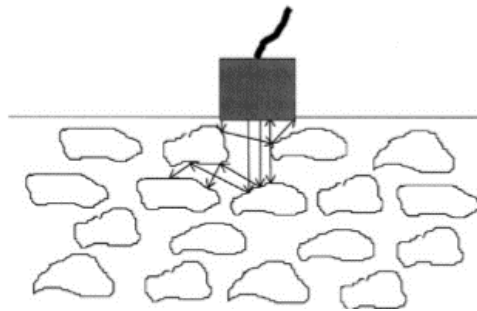


Figure 3.9: Effect of scattering from particle, as can be applicable to mud system[30]

### 3.5 Material Properties Affecting Speed of Sound in Drilling Mud

Drilling muds essentially exhibit a non-Newtonian characteristic when compare with Newtonian fluid such as water this generally influences their flow behaviours. Adequate understanding of rheological properties such as shear stress, shear strain and shear rate, based on the fluid viscosity dependence and the rate of deformation, is also useful in evaluating the presence and amount of gas invasion in the drilling fluid.

Take for instance, two parallel solid planes dipped in the fluid and separated by a distance, while keeping one of it at static position and moving the next one at constant velocity ( $V$ ).

Shear rate ( $\gamma$ ) is the rate of change of velocity at which one layer of fluid passes over an adjacent layer. It has reciprocal seconds as its unit.

The shear stress ( $T$ ) is defined as the force per unit area required to keep the plane moving at constant velocity  $V$ . The relationship between shear stress and shear rate for Newtonian fluids is given in Equation 3.10

$$T = \eta_s \gamma \quad (3.5)$$

Where;

$\eta_s$  is the shear viscosity.

Figure 3.11 (a) shows the flow curve for a Newtonian fluid. For those fluids, viscosity is only dependent on temperature and it has a linear relationship between shear stress and shear rates where their slope is given by the viscosity of the fluid which literally remains constant at any instance no matter how fast they are forced to flow through a pipe or channel which implies that viscosity is independent of the rate of shear, this is also shown in Figure 3.10.

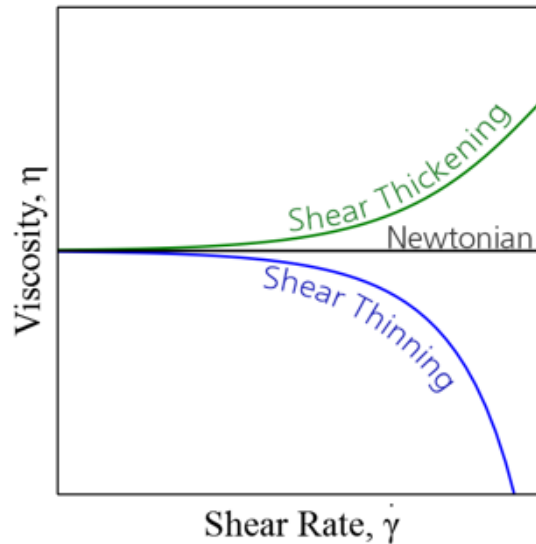


Figure 3.10: Viscosity of Newtonian, shear thinning and shear thickening fluids as a function of shear rate.[33]

In some other fluids, such as mayonnaise, however, shear stress is not proportional to shear rate. Rather, it needs a large initial shear stresses to move the adjacent planes at low shear rates. This can be approximated by the Bingham expression as given in Equation 3.11

$$T = \eta_{sco} \dot{\gamma} + T_0 \quad (3.6)$$

Where;

$T_0$ ; is the amount of shear stress required to produce initial shear motion and is called yield point and has dimensions of force per unit area.

Figure 3.11 (b) shows the flow curve in the Bingham model. The effective viscosity for a given shear rate is the slope of the line from the point of interest on the Bingham curve to the origin. Such behaviour may have interesting consequences on the measured ultrasound attenuation.[24, 33, 34]

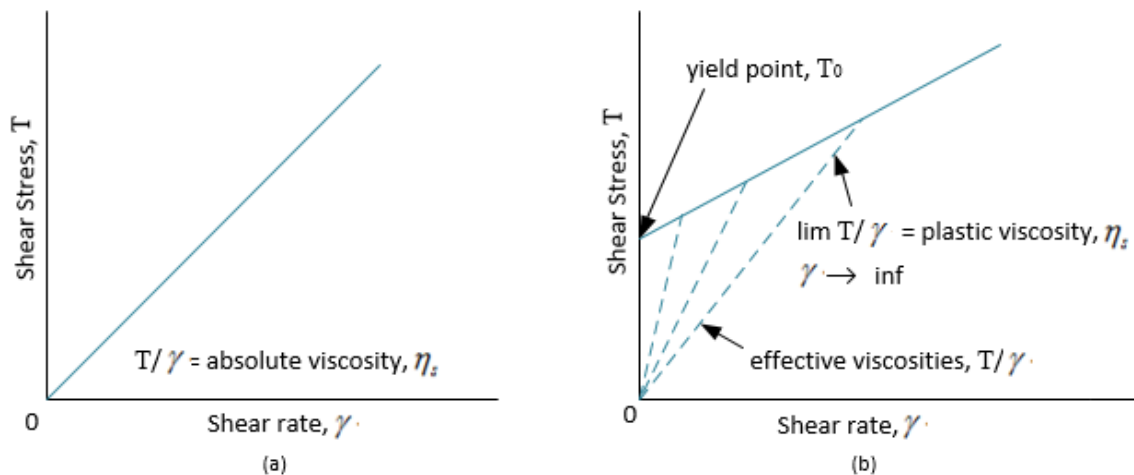


Figure 3.11: Shear stress versus shear rate for Newtonian (a) and non-Newtonian (b) fluid

### 3.5.1 Acoustic Impedance

Acoustic impedance is the opposition of a medium to a longitudinal wave motion. Knowing that sound travels through medium such as in drilling fluid under the influence of sound pressure and the medium molecules or atoms are bounded elastically to one another, this essentially will require some amount of pressure for wave to propagate through it. Acoustic impedance is as expressed in (Equation 3.7). The unit of acoustic impedance is “Rayls”  $\text{kg/m}^2\text{s}$

$$z = \rho * V \quad (3.7)$$

Where;

$\rho$  ; is the medium density in  $\text{kg/m}^3$

$V$  ; is the speed of sound in  $\text{m/s}$ .

Shear related physical properties of fluid can be measured through the acoustic impedance, in obtaining information with regards to the waves attenuation coefficient since the propagation of shear wave in fluid are strongly damped. Measurement of acoustic impedance can be used in characterizing viscosity and rheological properties of drilling fluids hence useful in evaluating the presence and amount of gas invasions. The energy absorbed by the fluid depends on the fluid mechanical properties such as viscosity. [28, 35]

Experimentally, acoustic impedance can be found in two ways:

- Measurement of the energy loss and the phase shift of the reflected wave, and
- by measuring the resonant frequency and the quality factor of a quartz crystal resonator immersed in the fluid.

### 3.5.2 Viscosity and Thermal Conductivity

Modern theories account that viscosity and thermal conductivity are essentially the two mechanism that causes attenuation when ultrasound propagates through homogeneous medium. The same effect is applicable to drilling fluid but with negligible thermal conduction contribution because of its low compressibility. However, ultrasound attenuation in drilling fluid depends on its rheological nature that is viscosity-related effect. Bulk viscosity is critical in evaluating the longitudinal rheology of Newtonian fluids and on the flip side it is also not

important for low-frequency shear rheology which is applicable with incompressible liquids where;

$$\text{div } v = 0$$

Navier-Stokes equation on attenuation of sound wave has been modified in [36] to accommodate the effect of longitudinal and shear rheology. This can also be useful in characterization of ultrasonic wave in drilling fluid. Stress is normal and not tangential considering that “longitudinal” viscos-elastic properties differ from traditional “shear” viscos-elastic properties, these are measured at high frequency which leads to much higher values than usual rheological data[37].

## 3.6 Measuring Principle of Ultrasonic

To detect flow in devices such as pipe, flumes etc., ultrasonic flowmeters use acoustic waves of a frequency >20 kHz. Depending on the design, they use either immersion or nonwetted transducers on the pipe perimeter to couple ultrasonic energy with the fluid flowing in the pipe. The two different technologies applicable with ultrasonic flow measurement: are the Doppler effect and Transit time difference.

### 3.6.1 Doppler Effect

An Australian physicist named Christian Doppler in 1842 predicts that the frequencies of received sound waves influences the motion of the source and observer relative to the propagating medium and at such this principle of measurement was named after him. This effect is heard on daily bases such as the change in pitch of an ambulance siren or an approaching train, where only a frequency shift takes place.

Doppler ultrasonic flowmeter works on this principle that the transmitter frequency changes linearly when it is reflected by particles and gas bubbles in a medium, the net result is a frequency shift between the Doppler signal transmitter and the signal receiver. This frequency shift is in direct proportion to the velocity of the liquid and can be precisely measured by the instrument to calculate the flow rate. This measuring principle requires some percentage of solid particles or air in the medium referred to as reflectors to achieve an optimal measurement results and are particularly suitable for applications with very dirty water, slurry and drilling fluids[38].

Figure 3.12 shows Doppler Effect basic measurement principle, having the Ultrasonic sensor installed at an Angle  $\alpha$ , where  $c$  represents the ultrasonic velocity in fluid, and  $u$  is fluid velocity,  $f_1$ ,  $f_2$ , and  $f_3$  are the ultrasonic frequency of transmitting sensor, the receiving ultrasonic frequency of particles in the fluid, and the ultrasonic frequency from the receiving sensor respectively and as such this can be expressed as in (Equation 3.13-3.15) [4].

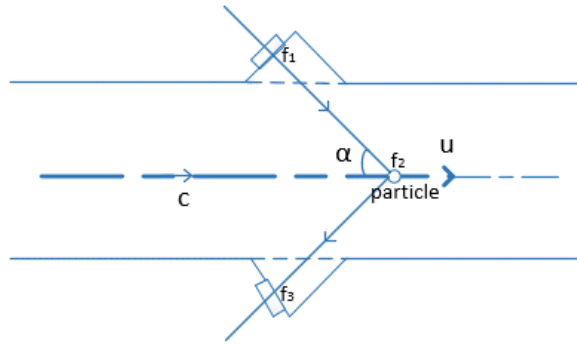


Figure 3.12: Doppler Effect measuring principle basic technique

$$f_2 = f_1 \left(1 - \frac{u \cos \alpha}{c}\right) \quad (3.13)$$

$$f_3 = f_2 \frac{c}{c + u \cos \alpha} \quad (3.14)$$

Equation 3.15 is obtained from equations (3.14 and 3.13)

$$f_3 = f_1 \frac{c - u \cos \alpha}{c + u \cos \alpha} \quad (3.15)$$

Doppler frequency shift  $\Delta f$  is the difference between the transmitting and receiving frequency, for liquids the propagations are usually faster and with this concept changes in rheological properties of drilling fluids can be detected and as such it can be effective for early kick detection.

$$\Delta f = f_1 - f_3 = f_1 \frac{2u \cos \alpha}{c + u \cos \alpha} = f \frac{2u \cos \alpha}{c} \quad (3.16)$$

The velocity of the fluid flow is can be expressed as equation (3.17), assuming  $A$  is the cross-sectional area of the pipeline.

$$V = \frac{Ac}{2f_1 \cos \alpha} \Delta f \quad (3.17)$$

knowing the ultrasonic propagation velocity in fluid  $c$ , the transmitting ultrasonic transducer frequency  $f_1$ , and the angle of installations the velocity of the fluid can be calculated[4].

### 3.6.2 Transit Time Difference

Transit time difference ultrasonic flow measurement essentially requires a pair of transducers for it's application. It is based on comparison between upstream and downstream measurements in observing the time it takes for an ultrasonic signal transmitted from one transducer, to cross a pipe and be received by a second transducer. It is also called time of flight and time of travel meter.

With no flow, the transit time would be equal in both directions. With flow, sound will travel faster in the direction of flow and slower against the flow. Ultrasonic signals from the transducers are easily attenuated by the presence of bubbles or particles for their reflecting qualities interfere with the transmission and receipt of the applied ultrasonic pulses.[38]

### 3.6.3 Pulsed Measurement Principle

Ultrasonic dopplers works on this principle, using a single transducer element which contains both the transmitting and receiving crystals on a single plate. At the initial measurement process, an ultrasonic burst of a given frequency and duration is sent into the medium. The transducer immediately switches to reception mode at the end of the emission. The transmitted signal from the transducer travels along the beam axis while encountering particles, partially backscattering the acoustic wave as shown in Figure 3.13. If the particle is motion within the medium, a frequency shift would be seen in the backscattered wave (so-called Doppler shift). This assumes that the velocity of the suspended particles is equal to the flow velocity. This principle of operation guarantees the precise knowledge of the position in the flow of a given backscattered signal amplitude at a given time stamp.[39]

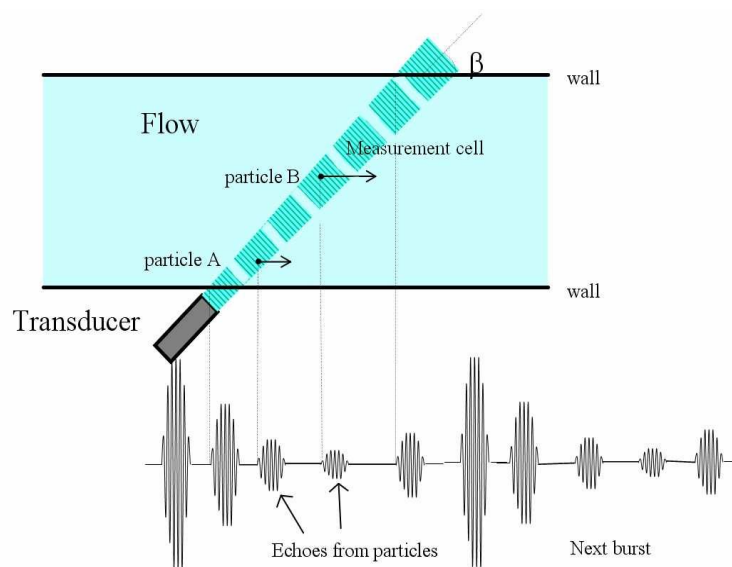


Figure 3.13: Pulsed Doppler principle: initial pulse and echoes from particles[39]

## 3.7 Interpretation of the Acoustic Spectrometer Raw Data

Flow behavior of drilling mud systems which can be categorized as a complex fluid is characterized through the fluid's viscosity dependence on the rate of deformation and the rate of shear which is a clear distinction between Newtonian and non-Newtonian fluid. Proper understanding of rheological properties are vital for measurement and characterization of liquid-particle flow, especially in terms of on-line measurement of particle concentration using the ultrasonic spectroscopy technique.

Interpretation of the acoustic raw data can be done using several approaches while observing how the signal intensity diminishes as shown in (Figure 3.14) depending on the level of dispersed system modeling involved. The transmitted ultrasound pulses through a test samples as generated by piezo-crystal of certain frequency and intensity diminishes in intensity due to the interaction with the sample. The receiving transducer converts this weaker pulse back to electric pulse and sends it to electronics for comparison with the initial pulse. This implies that

the raw data is equivalent to the intensity of the pulse after propagation through the sample, in addition one can also measure the time and phase of the pulse propagation.

The first step in interpretation of raw data is the empirical relationship which essentially requires no assumptions or models of the system that is under investigation, this includes calculation of either Acoustic or Rheological parameters of the system as expressed in Equation (3.18-3.21). Rheological parameters can be used for empirical correlations with observed processes.[37]

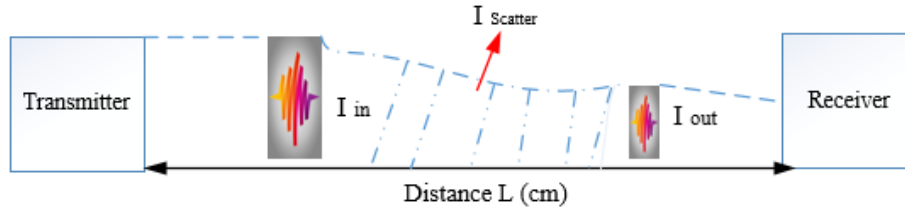


Figure 3.14: Interpretation of acoustic raw data

With no model assumptions, raw data corresponds to the intensity of ultrasound pulse after propagation  $I_{out}$ , which are;

- time of of the pulse flight  $t$  and
- phase of the sound after propagation

### 3.7.1 Time of the Pulse Flight $t$

Acoustic parameters can be characterized with attenuation  $\alpha$  and sound speed  $V$  as expressed in Equation (3.18 and 3.19), variation of these two properties of ultrasound depends on the properties of the system. Measuring the variations can provide insight to some information about properties of the system.

$$\alpha = \frac{10}{f[MHz]L[cm]} \log \frac{I_{in}}{I_{out}} \quad (3.18)$$

$$V = \frac{L[cm]}{t[sec]} \quad (3.19)$$

### 3.7.2 Phase of Sound after Propagation

Rheological parameters can be characterized with elastic modulus  $G'$  and viscous loss modulus  $G''$  as expressed in Equation (3.20 and 3.21).

$$G' = \rho V \quad (3.20)$$

$$G'' = \frac{2\rho\alpha V^3}{\omega} \quad (3.21)$$

Model assumptions is more applicable when the effect of particle size distribution and connections with specific forces are taken into consideration[37]. This thesis focused on the phenomenological interpretation of acoustic raw data with emphasis on attenuation along propagation distances resulting from different ultrasonic transducer frequencies.

## 4 Experiments

This section of the report describes ultrasonic technique of measurement, with focus on how ultrasonic waves attenuate as it propagates through different fluids over varying distances with different transducers frequency.

The attenuation spectra are suitable for characterizing hard solid particles that can essentially influence the rheological properties of the fluid in relation to early kick and loss detection.

The experiment was performed at USN Sensor Laboratory and Process Hall, with startup in February and ended in early April 2017. The goal intended to be attained with the performed tests was to acquire experimental data for characterizing the wave propagation in the fluids at static state with respect to propagated distance and transducer frequency which essentially will be an introduction to utilizing ultrasonic Doppler measurements for determining mud flow rate.

### 4.1 Setup

The experimental setup is shown in Figure 4.1. This set-up comprises of pair of Parametric wideband transducers of about 25 mm diameter taken apart over varying distances. The fluid tank has a dimension of about 35cm and 45cm thick and a length of 60 cm that contains about 170 liters of fluid sample. The measurement system consists of an Olympus Epoch 1000i signal transceiver with display showing the UTDR waveforms with adjustable gain level that allows for adjustment higher or lower from reference gain.

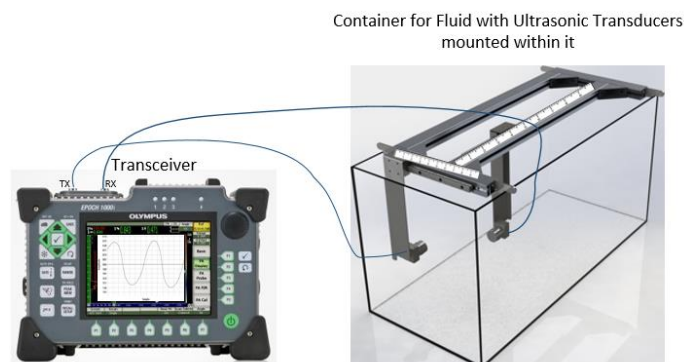


Figure 4.1: Setup of the Ultrasonic Measurement for both Axial and Transversal Direction

0.5MHz, 1MHz and 2.25MHz ultrasonic transducer frequency were tested out in through transmission mode for the various fluids (see Table 4.1) as contained for the setup. This test was performed over varying distances in both axial and transversal directions and the gain on how the amplitude of the ultrasonic wave diminishes over the specified distances are recorded manually in an excel sheet. This was used in determining the attenuation coefficient of the various fluid samples.



Table 4.1: Fluid Composition used

Fluid Type	Concentration of fluid	Viscosity [cP]	Density [kg/m <sup>3</sup> ]
Water	Water	1	1000
Water-Based Drilling Mud	As contained in Appendix C	19	1320
Simulated Mud (Fluid2)	1000 kg of K <sub>2</sub> CO <sub>3</sub> in 1000 liters of water.	4.1	1405

## 4.2 Procedure

The experiment was performed by connecting a pair of ultrasonic transducers of same frequency to the transmitter and receiver BNC connector of OLYMPUS transceiver after they are mounted on a movable handle in the tank with test fluid as is shown in Figure 4.4.

The frequency of the transducer is configured on the transceiver to conform to its design frequency through the pulser button and are placed in through transmission mode using a rotating knob for the same page.

- The transducers are varied within an axial range between 3cm to 45cm in the step of 1cm. and transversal range from 0cm to 4cm at the step of 1cm.
- Before varying the transducer distances the reference gain is set on the transceiver and ensuring that the starting point for the receiving transducer is at 100% of the set gain.
- The percentage change in gain is observed as the transducers are taken apart and recorded manually in an excel sheet while ensuring that the time of flight for the transducer differences conforms at a specific distance, in order not to record noise signal, this same dB gain setting is used in adjusting the system sensitivity.
- Data were collected by clearly ensuring errors due to parallex were minimized by observing the markings in the metric rule for distance measurement in a straight line directly above it while moving the transducer holder.

### 4.2.1 Experimental Test Matrix

A test matrix is a tabular documentation and definition of test cases to be implemented during experimentation. This test matrix contained the different combination of each test case that was conducted, using least possible resource and time in covering all the permutation [40]. Table 4.2 shows the test matrix used for data collection.

Table 4.2: Experimental Test Matrix

EXPERIMENTAL TEST MATRIX		
Control Variables	Design Variable	Response Variables
Distance [cm]	Axial and Transversal distance directions	Amplitude gain [dB]
Transducer Frequency [MHz]	Fluid in static state	% of Attenuated signal
Fluid Type	Fluid Density	
<b>Water</b>		
Control variables changes		
Axial distance [cm]	(3,4,...,45)	Steps of 1
Transversal distance [cm]	(3,6,...,45)	Steps of 3
Transducer Frequency [MHz]	(0.5, 1, 2.25)	
No. Observations	42 * 5 samples* 3 Tf + 15*3Tf	675
<b>Simulated Mud</b>		
Control variables changes		
Axial distance [cm]	(3,4,...,45)	Steps of 1
Transducer Frequency (MHz)	(0.5, 1, 2.25)	
No. Observations	42 * 3 samples* 3 Tf	378
<b>Drilling Mud</b>		
Control variables changes		
Axial distance [cm]	(3,4,...,45)	Steps of 1
Transversal distance [cm]	(3,4,...,45)	Steps of 3
Transducer Frequency [MHz]	(0.5, 1, 2.25)	
No. Observations	42 * 5 samples* 3 Tf + 15*3Tf	675

Original experimental setup which involves the use of ultrasonic pulse receiver and oscilloscope had a technical problem midway into the thesis period. A new arrangement was made which involves the use of Olympus transceiver. In this case, it requires manually inputting observed data into an excel sheets used for data collection.

As consequence to the technical problem, more test matrix was required to be observed

### 4.2.2 Devices used

**Ultrasonic transducer:** Videoscan immersion transducer of three different ultrasonic frequency as shown in (Figure 4.2 and Table 4.3) was used for the experiment which provides heavily damped broadband performance as it is the best choice in applications where good axial or distance resolution is necessary or in tests that require improved signal-to-noise in attenuating or scattering materials such as drilling fluids.[41]

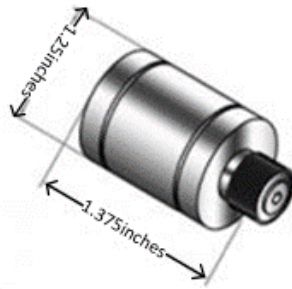


Figure 4.2: Modified image of an Immersion transducer of 1inch element diameter[41]

The wavelength of the different transducer frequency used is as calculated in Table 4.3, this shows that 2.25MHz has the lowest wavelength.

Table 4.3: Calculated details of the transducer in water at sound speed of 1480 [m/s]

Frequency [MHz]	Element Diameter [mm]	Near zone [cm]	Wavelength [ $\lambda$ ] mm/cycle
0.5	25	5.3	3
1	25	10.6	1.5
2.25	25	23.8	0.7

**Ultrasonic transceivers:** Olympus EPOCH 1000i as shown in Figure 4.3 was used with display showing the UTDR waveforms. This device is a fully integrated transceiver made for industrial settings, it works excellently in determining the acoustic propagation of the various transducers in the fluid samples[42].



Figure 4.3: Ultrasonic Transceiver

**Containers for fluid samples:** Figure 4.4, shows the container utilized for the experimental setup, the transducers are mounted in the movable slides as shown in Figure 4.4 (a). Water sample was used in figure (a) which is made of a transparent aquarium glass while the drilling fluids were used with figure (b) which is made of a steel tank following the same experimental arrangement.

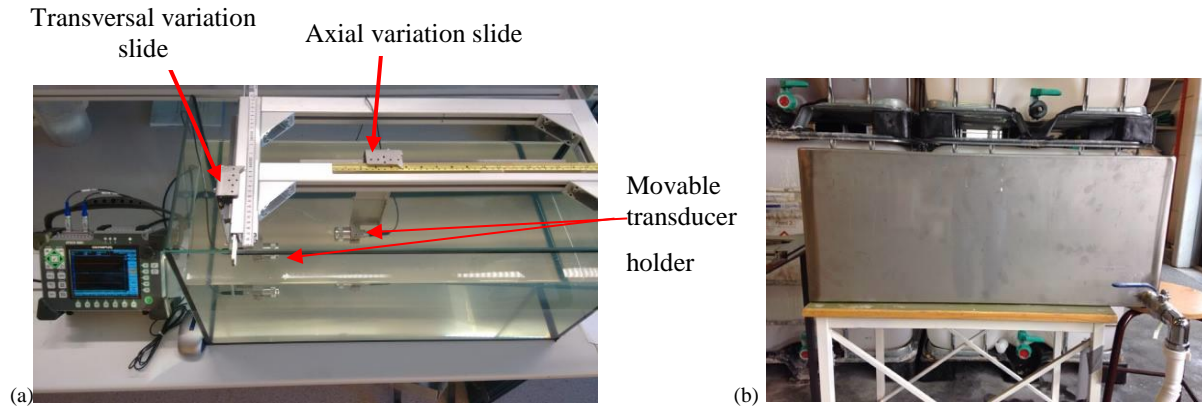


Figure 4.4: Container for the Fluid Samples (a) was used for water and (b) was used for Drilling Fluids

## 4.3 Description of Statistical Analysis Tools Used

In order to minimize the effect of variability in result as introduced in measurement processes, statistical approach was used in planning and interpretation of the experimental data. This section of the report explains some of the statistical methods used in the experiment.

### 4.3.1 Univariate Linear Regression

Mathematical function such as straight line or exponentials was used to fit experimental data in finding correlations between its dependable and independent variables, in this case amplitude and distance for the various transducer frequencies. In fitting data from experimentation, they were transformed approximately to linear best fit of the form of (Equation 4.1).

$$y = ax + b \quad (4.1)$$

The approach used in this report is the method of least squares to fit the data. The attenuation coefficient of the ultrasonic transducers in various fluid samples as used in this experiment were predicted as well as the unattenuated signal as expressed in the functional form of (Equation 4.2).

$$A_d = K_1 e^{-K_2 x} \quad (4.2)$$

Where;

$K_1$  : Initial (unattenuated) amplitude [dB]

$A_d$  : is the reduced amplitude as the wave travels over a distance [dB]

$e$  :  $e$  is the exponential (or Napier's constant) which is approximately 2.71828.

$K_2$  : Attenuation coefficient (Np/m)

$x$  : Distance traveled (cm)

This essentially is the expression for the amplitude change of a decaying plane wave of ultrasonic transducers. The best-fit values was found from (Equation 4.3 and 4.4) using the functional form of (Equation 4.2).

$$a = \frac{n \sum x_i y_i - (\sum x_i)(\sum y_i)}{n \sum x_i^2 - (\sum x_i)^2} \quad (4.3)$$

$$b = \frac{n \sum x_i^2 \sum y_i - (\sum x_i)(\sum x_i y_i)}{n \sum x_i^2 - (\sum x_i)^2} \quad (4.4)$$

Where;  $K_2 \approx b$ , and  $K_1 \approx a$ , and  $A_d \approx y_i$ , [43, 44].

**Coefficient of determination ( $r^2$ ):** In determining how good a regression line fits a data sample, coefficient of determination ( $r^2$ ) was used in examining and interpreting the regression model. This was observed using the straight line passing through the data as a best line fit, a good fit of  $r^2$  should be close to unity.  $r^2$  is given by Equation 4.5

$$r^2 = 1 - \frac{\sum (ax_i + b - y_i)^2}{\sum (y_i - \bar{y}_i)^2} \quad (4.5)$$

Where; the expression of the numerator of the second term is the sum of the square deviations of the data from the best fit, and the denominator expresses the sum of the squares of the variation of the data ( $y$ ) about the mean. [43]

**Standard error of estimation  $S_{y,x}$ :** This quantifies how best the line fit represents the data, it is expressed as Equation 4.6

$$S_{y,x} = \sqrt{\frac{\sum (y_i - Y_i)^2}{n - 2}} \quad (4.6)$$

Where;  $S_{y,x}$  is standard deviation of the differences between the data points and the best-fit line, it has the same unit as the measured data ( amplitude decibel),  $n$  is the number of sample,  $y_i$  is the data points and  $Y_i$  is the regression model[43].

**Root Mean Square Error (RMSE):** This was also used in verification of experimental results, it is the measure of the standard deviation of the prediction errors (Residuals). The residual is seen as the estimation of how far from the regression line that the data points are. The formula is is similar to standard error of estimation and is as expressed in (Equation 4.7).

$$RSME = \sqrt{\frac{\sum (y_i - Y_i)^2}{n}} \quad (4.7)$$

The lower the value the more correlated the model is to the data, just like standard error of estimation, this have the same unit as the measured data.

**Student's t distribution:** This is used in estimating the confidence intervals for the parameter acquired from the regression model, it is expressed in terms of the level of significance in understanding how reliable the model is. The use of student's t distribution is applicable

when the samples size from the experimentation is less than 30, it is used in similar form as the normal distribution and the approximation for the value of  $v$  can be read from the table in Appendix B. following the curve for the appropriate value of  $v$  as shown in (Figure 4.5).  $1 - \alpha$  is the probability that  $t$  falls between  $-t_{\alpha/2}$  and  $t_{\alpha/2}$  and is stated in (Equation 4.4). The table shows only the most common values of  $t$  that correspond to confidence levels. For example the probability of a 95% confidence level can be quantified as  $\alpha = 1 - 0.95 = 0.05$  and  $\alpha/2 = 0.025$ . [43]

$$P[-t_{\alpha/2} \leq t \leq t_{\alpha/2}] = 1 - \alpha \quad (4.4)$$

The two-sided  $(1-\alpha)$  confidence interval for the slope parameter  $a$  and  $b$  are given in (Equation 4.4 and 4.6)

$$a \pm \frac{S_{y,x} t_{\alpha/2, n-2}}{\sqrt{x_i^2 - n\bar{x}^2}} \quad (4.5)$$

$$b \pm S_{y,x} t_{\alpha/2, n-2} \sqrt{\frac{1}{n} + \frac{(\sum x_i)^2}{n^2 (\sum x_i^2 - n\bar{x}^2)}} \quad (4.6)$$

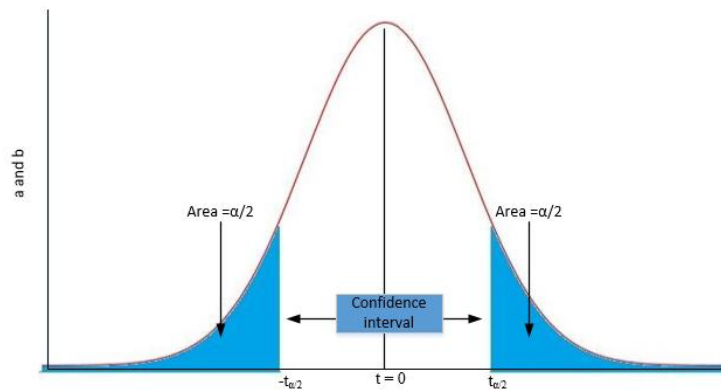


Figure 4.5: Confidence Interval for t-distribution

### 4.3.2 Multivariate Data Analysis

Multiple linear regression was performed on the combined data using *Unscramber-X* software where multiple correlated dependent variables was inspected.

Firstly, the data was analyzed using principal component analysis (PCA). In this method, the data matrix was decomposed into two parts “structure” and noise as expressed in Equation 4.5

$$X = tp^T + e$$

Where;  $X$  is the data matrix,  $t$  is the score (map of samples),  $p^T$  is the loading (map of variables) and  $e$  is the noise part.

The loading plots is always interpreted together with the corresponding score plot in describing the variables correlation. [45]

The reason behind reducing the multidimensional data set into a new data set of lower dimension is to determine factors influencing the attenuated signal from the sensors.

Furthermore, a regression model was calibrated, and was used to predict the output  $Y$  for the respective transducer frequencies. The calibration was implemented using multivariate

calibration techniques, which is partial least square regression (PLS-R). This method is involved with a linear decomposition of both Input and output data simultaneously in maximizing covariance between them.

### 4.3.3 Multivariate Data Presentation

The data collected was stored in the excel file ‘Multivariate2’, thereafter, the *UnscramblerX* software is used to load the data for further analysis. The sample for the experimental data is as shown in Figure 4.6.

Multivariate2		Distance [cm]	0.5MHz [dB]	1MHz [dB]	2.25MHz [dB]	Water	Sim_Mud	Real_Mud	0.5MHz Attenuation	1MHz Attenuation	2.25MHz Attenuation
		1	2	3	4	5	6	7	8	9	10
W03	1	3.0000	0.0000	0.0000	0.0000	1.0000	0.0000	0.0000	0.0000	0.0000	0.0000
W04	2	4.0000	-0.2730	-0.1580	-0.1581	1.0000	0.0000	0.0000	0.2730	0.1580	0.0351
S_M03	3	3.0000	0.0000	0.0000	0.0000	0.0000	1.0000	0.0000	0.0000	0.0000	0.0000
S_M04	4	4.0000	-0.2637	-0.2349	-0.1755	0.0000	1.0000	0.0000	0.2637	0.2349	0.1755
M03	5	3.0000	0.0000	0.0000	0.0000	0.0000	0.0000	1.0000	0.0000	0.0000	0.0000
M04	6	4.0000	-3.6896	-4.6358	-5.7323	0.0000	0.0000	1.0000	3.6896	4.6358	5.7323

Figure 4.6: Presentation of Data in Unscrambler Software

PCA Uses only the input variables (X), which are:

- Distance [cm] which varies from 3 to 45 in the steps of 1cm
- Amplitude variations in [dB] for the various transducer frequencies

The PLS-R uses both the input and output variables (Y). The output variables is:

- The attenuated signals [dB/cm] for the various transducer frequencies

## 5 Results and Discussions

This section of the report presents the result and analysis of the experiments performed in the characterization of ultrasonic sound wave with propagation distances for three different ultrasonic transducers.

The data were collected for both axial and transversial direction, the transversial direction was not fully accompanied due to some technical problems associated with the initial experimental setup and as such there are no sufficient data for its characterization.

The regression coefficient for both the linear and logarithmic scale gave an equivalent result, once the Neper quantity of the linear scale (slope (b)) is divided with 0.1151 when converting to decibels as can be derived from Equation 5.1

Equation 5.1: Shows the relationship between decibel and Neper quantity[46]

$$1dB = \frac{1}{20 \log_{10} e} Np \quad (5.1)$$

The raw data for the different results as presented in this section can be found in Appendix D.

Table 5.4 shows the summary of calculated values of sound speed for the different transducer in the fluid samples. This was used in the interpretation of some of the results in this chapter, though the focus of this thesis is on attenuation of ultrasonic wave. Analysis of the data was done with Matlab, Unscrambler-X and Microsoft Excel software. The decibel plot for each transducers was mean centered in other to resolve the intercept as zero, the MATLAB code is found in Appendix E.

### 5.1 Ultrasonic Propagation in Water

Propagation of sound wave in water is the basis for much instrumentation. Having water as the main component of water-based drilling fluid as used in this report and also as the simplest reference medium in which NDE ultrasound experimentation is performed, accurate determination of ultrasound attenuation in water helps in interpretation of corresponding measurements in a more complex media, such as in drilling fluid.

The Acoustic propagation loss in water is basically as result of losses due to a number of factors ranging from geometric spreading, surface interactions, and the viscosity of water to ionic relaxation of chemicals that may be present in it.[47]

Using a four degree of freedom regression model at 95% confidence interval in estimation of the attenuation coefficient for water at different ultrasonic frequency. The results as seen in

Table 5.1, shows that 2.25MHz transducer frequency attenuates more compared to 1MHz and 0.5MHz transducer, while 0.5MHz transducer is the least attenuated frequency for the same propagation distances in water at a room temperature. This is also seen by comparing their results in Figure 5.4 and 5.5. This agrees with the theory, that the higher the frequency (smaller wavelength), the greater the attenuation of sound wave or the lower frequencies the further the penetration of the wave in a medium because of less absorptions. Higher frequency ultrasounds decay more rapidly in a medium but with greater resolution capability.



Table 5.1: Regression Result in Water Sample for the Different Transducers

Regression Analysis – Linear model :  $y = ax + b$  using a function form of  $A_d = K_1 e^{-K_2 x}$

---

Dependent variable: Amplitude Independable variable: Distance

---

Estimated parameter for the various ultrasonic transducers in water

Tf [MHz]	Intercept (a)	Slope (b)	$K_1$ [v]	$K_2$ [Np/m]	$\alpha$ [dB/m] (2 <sup>nd</sup> Model)
0.5	0.0590 ±0.0039	-0.0198 ±0.0027	1.04	0.0198	0.1719
1	0.0534 ±0.0086	-0.0140 ±0.0067	1.06	0.0140	0.1207
2.25	0.0307 ±0.0073	-0.0121 ±0.0058	1.03	0.0121	0.1049

---

Analysis of Variance, with degree of freedom of 4, using 5 samples of experimentation

Tf [MHz]	$r^2$	RMSE	$S_{y,x}$	t - Values	
0.5	0.9967	0.0014	0.0015	±0.0039	±0.0027
1	0.9840	0.0025	0.0026	±0.0086	±0.0067
2.25	0.9884	0.0017	0.0018	±0.0064	±0.0050

### 5.1.1 Measurements with 0.5MHz Transducer in Water

Figure 5.1 shows the results of the raw attenuation data for water at 0.5MHz ultrasonic frequency. From the regression plots the field intensity of the ultrasonic wave tends to decrease smoothly along the propagation distance, this probably is due to the transducer having its near field distance at about 5cm as is seen in

Table 5.4. This equally implies that there is no much interferences from point source since the initial startup distance for the measurements is at 3cm. The resultant effect gave a higher correlation coefficient value as compared with other transducers with farther near zone distances. It also shows a very low standard error of deviation value as the signal tends to decay in a smooth linear form.

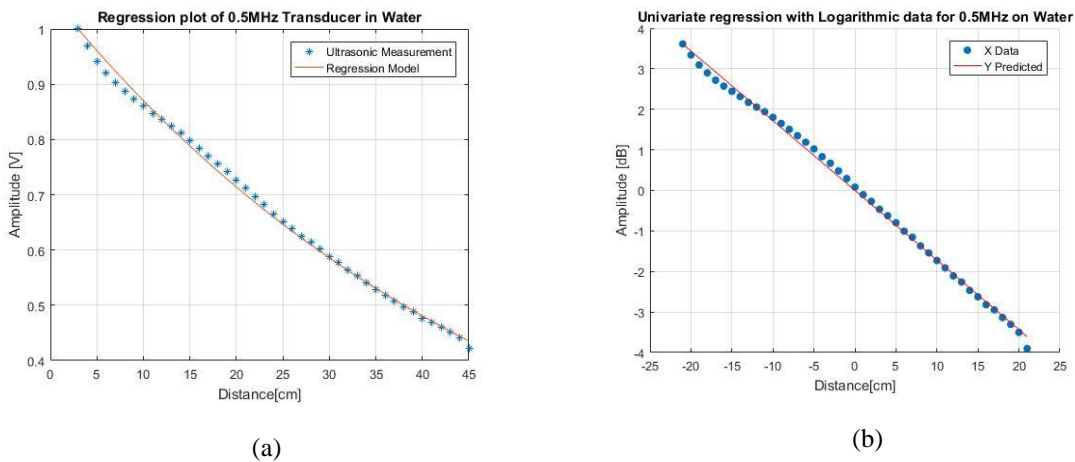


Figure 5.1: Regression plot for Linear (a) and Logarithmic Scale (b) of Amplitude Variation of 0.5MHz Transducer versus Distance

### 5.1.2 Measurements with 1MHz Transducer in Water

Figure 5.2 shows the results of 1MHz ultrasonic propagation in water at various distances. The ultrasonic wave decay is not clearly in a smooth manner since it has the near field distance at about 11cm. This essentially reduces the correlation rate of the amplitude signal with distance and as such it gave a much higher standard error of deviation. The average attenuation value as computed from the raw data is 0.115 dB/cm which is about 0.05 dB/cm lower than the estimated attenuation coefficient for the transducer. The change in amplitude along the propagation path for this transducer is in the range of -5dB which is lower than that of 0.5MHz transducer.

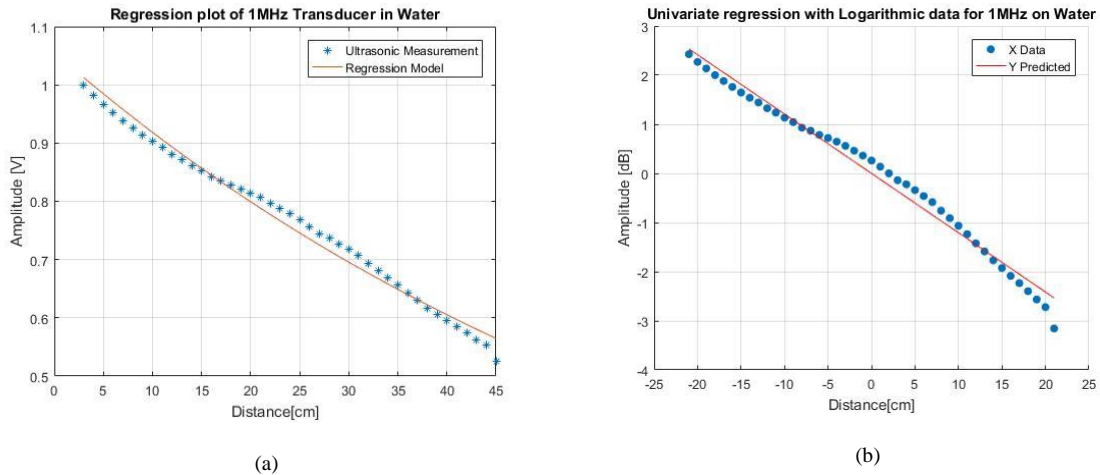


Figure 5.2: Regression plot for Linear (a) and Logarithmic scale (b) of Amplitude Variation of 1MHz Transducer versus Distance

### 5.1.3 Measurements with 2.25MHz Transducer in Water

Figure 5.3 shows the results of 2.25MHz ultrasonic propagation in water at various distances. This transducer has the highest attenuation coefficient value and as such the signal diminishes faster compared to 0.5MHz and 1MHz transducer and this influences a better resolution result from the regression fit for the unattenuated amplitude ( $K_1$ ). It also shows a lower RMSE value from the estimations in the regression models as compared to the other frequencies.

At 45cm distance this frequency shows a step decrease of amplitude this obviously could be due resolution of object relative to the size of its wavelength along the propagation path or reflections resulting from the interferences of the fluid container boundary.

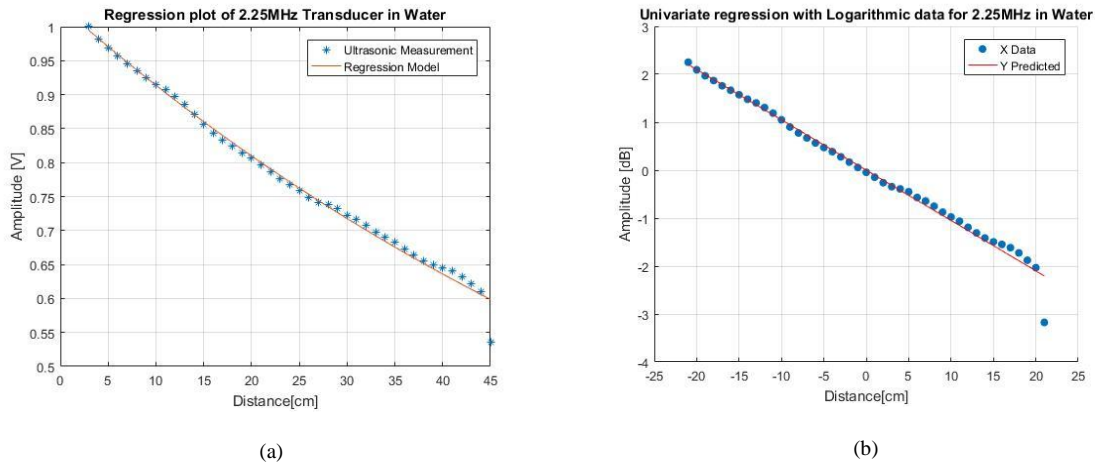


Figure 5.3: Regression plot for Linear (a) and Logarithmic Scale (b) of Amplitude Variation of 2.25MHz Transducer versus Distance

### 5.1.4 Combined Results of the Measurements in Water

Figure 5.4 Shows the amplitude changes of the various ultrasonic frequencies in water over the specified propagation distances. From the plot 0.5MHz transducer penetrates farther than the other transducers, this essentially is as a result of its higher wavelength. Though in

Table 5.1 it shows the highest correlation rate with regards to propagation distances, it is still the transducer with the lowest resolution capability as this can be verified from the sound speed calculation of

Table 5.4.

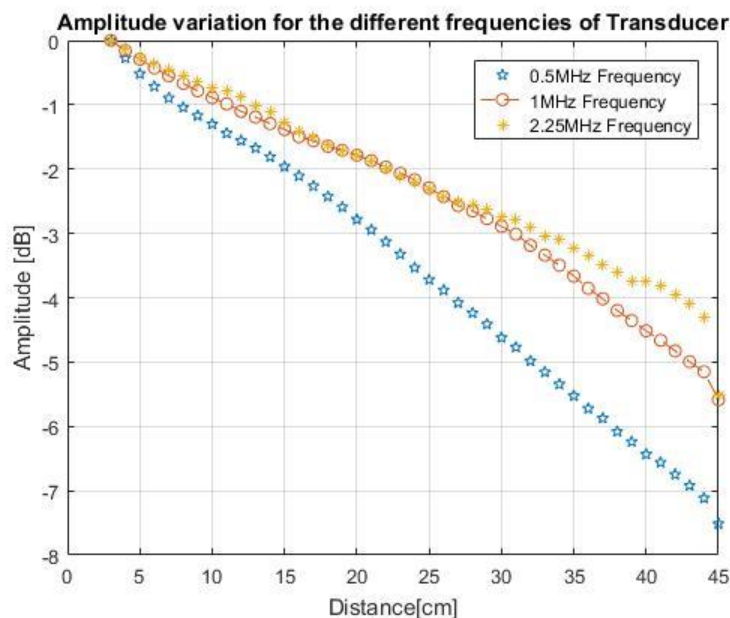


Figure 5.4: Combined plots of Amplitude Changes in Propagation Distances for the Various Ultrasonic Transducer in Water

Figure 5.5 shows the combined attenuation response of the transducers. This clearly reveals the differences between the attenuation coefficient of the various frequencies. 2.25MHz is seen to be the most attenuated transducer, followed by 1MHz while 0.5MHz transducer has the least attenuated signal.



### 5.2.1 Measurements with 0.5MHz Transducer in Simulated Mud

Table 5.2 and Figure 5.6 shows the results of 0.5MHz ultrasonic propagation in simulated mud at various distances. The amplitude drop is within the range of -9dB, and it is the least attenuated frequency within the same fluid sample because of its higher wavelength. This transducer voltage diminishes from 1v to approximately 0.35v along the propagation path as the sounds are absorbed by the medium.

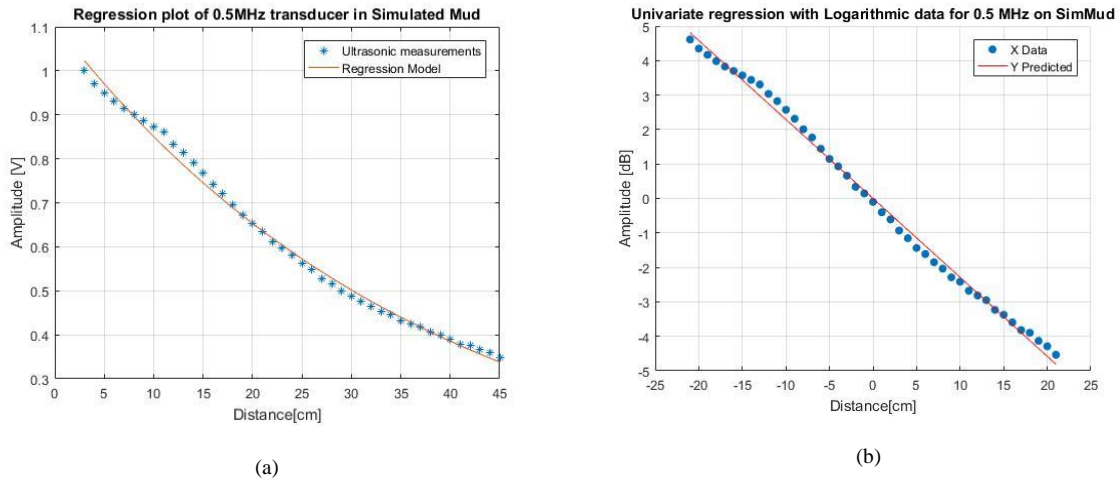


Figure 5.6: Regression plot for Linear (a) and Logarithmic scale (b) of Amplitude Variation of 0.5MHz Transducer versus Distance

### 5.2.2 Measurements with 1MHz Transducer in Simulated Mud

Figure 5.7 shows the results of 1MHz ultrasonic propagation in simulated mud at various distances. There is much variations in the field intensity as this influences the correlation rate and as such it is seen to have the highest error of prediction as can be obtained in Table 5.2, this certainly is because of the near field distance.

More also, the reduction in amplitude is in the range of -6dB and as such this confirms that 0.5MHz transducer penetrates more than it in the same fluid sample.

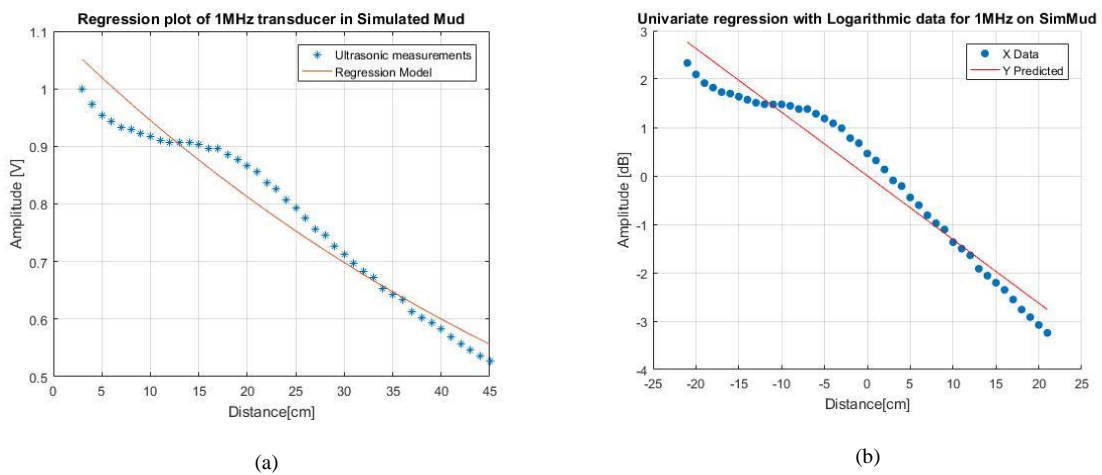


Figure 5.7: Regression plot for Linear (a) and Logarithmic Scale (b) of Amplitude Variation of 1MHz Transducer versus Distance

### 5.2.3 Measurements with 2.25MHz Transducer in Simulated Mud

Figure 5.8 shows the results of 2.25MHz ultrasonic propagation in simulated mud at the various distances. This transducer has a better correlation coefficient result along the propagation path when compared to 0.5MHz and 1MHz transducer in the same fluid sample. The reduction in amplitude is in the range of -4dB, this clearly reveals that it is the most attenuated transducer this basically is because of its resolution capability resulting from a shorter wave length. It also gives a better correlation result with respect to propagation distance this can be seen in Table 5.2

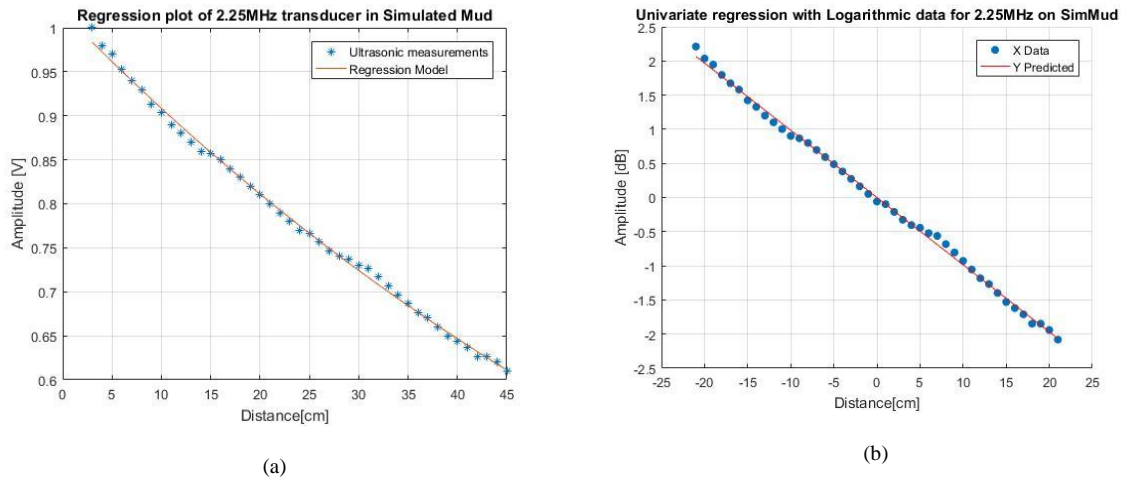


Figure 5.8: Regression plot for Linear (a) and Logarithmic Scale (b) of Amplitude Variation of 2.25MHz Transducer versus Distance

### 5.2.4 Combined Result of the Measurements in Simulated Mud

Figure 5.9 Shows the amplitude changes of the various ultrasonic transducers in simulated mud over the specified propagation distances. From the plot 0.5MHz transducer penetrates farther than the other transducers, similar effect was equally observed with water. Generally attenuation of sound wave is greater in this fluid than in water, this obviously is as a result of the soluble salt substance that was used in its design which altogether influences its acoustic properties.

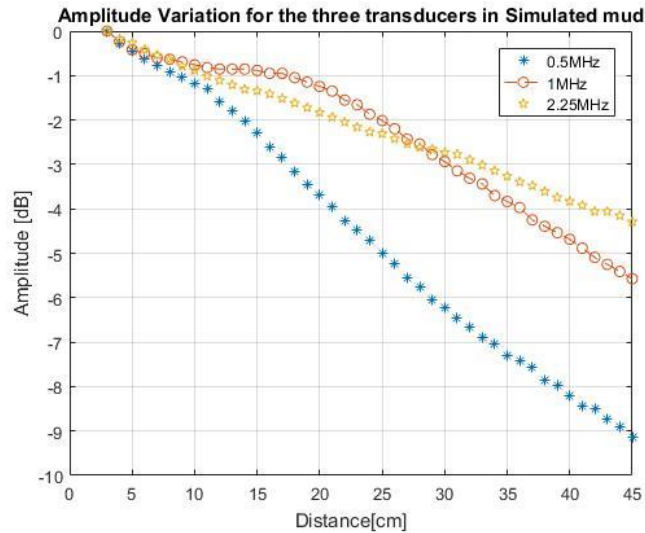


Figure 5.9: Combined plots for Amplitude Changes with Propagation Distances for the Various Ultrasonic Transducers in Simulated mud

Figure 5.10 shows the combined attenuation response of the transducers in simulated mud. There is a high variation in the field intensity for 0.5MHz and 1MHz transducer. While 2.25MHz transducer tends to be more stable and sensitive in the propagation distance, which is an indication of point source interferences as a result of near field distances. The plot also showed that 2.25MHz attenuates more than the other frequencies.

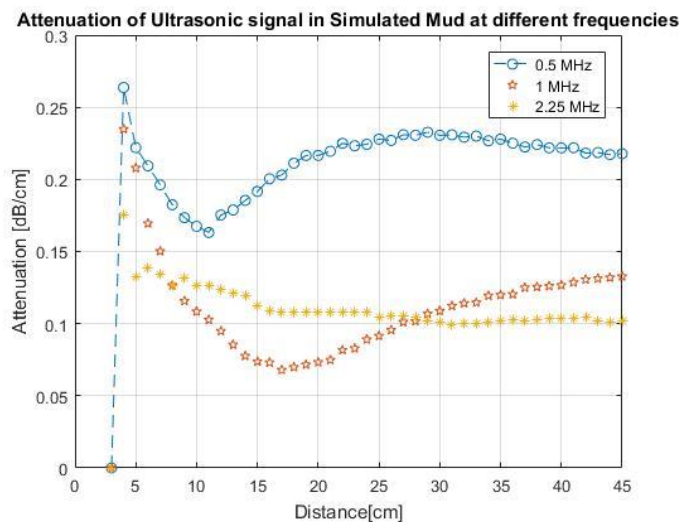


Figure 5.10: Attenuation of Ultrasonic Wave in Simulated Mud versus Propagation Distance

### 5.3 Ultrasonic Propagation Result in Mud

The drilling mud exhibited a very different characteristic when compared with the other fluid samples. This is due to the non-linear nature of the fluid resulting from high viscous or elastic property. This influences much attenuation of sound wave. The propagation distance of the various transducers was greatly reduce in the mud sample, though 0.5MHz transducer tend to propagate farther than the other transducers.

This confirms the theory that attenuation (absorption and scatter) decreases as test frequency reduces for higher wavelength transducer could overcome the effect of high absorption and scatter that are peculiar with the mud.

Figure 5.11, 5.12, and 5.13 (a). Shows the amplitude variation in the fluid samples at different frequencies, and Table 5.3 provides the analysis result for the various transducers in the mud sample.

Table 5.3: Regression result in Real mud sample for the different transducers

Regression Analysis – Linear model :  $y = ax + b$  using a function form of  $A_d = K_1 e^{-K_2 x}$

---

Dependent variable: Amplitude			Independable variable: Distance		
Estimated parameter for the various ultrasonic transducers in Real mud					
Tf [MHz]	Intercept (a)	Slope (b)	$K_1$ [v]	$K_2$ [Np/m]	$\alpha$ [dB/m] (2 <sup>nd</sup> Model)
0.5	0.7090 ±0.0239	-0.3555 ±0.0079	2.03	0.3555	0.3225
1	1.502 ±0.0072	-0.520 ±0.0021	4.49	0.520	4.5134
2.25	2.004 ±0.0028	-0.681±0.0115	7.42	0.681	5.9147

---

Analysis of Variance, with degree of freedom of 4, using 5 samples of experimentation

Tf [MHz]	$r^2$	RMSE	$S_{y,x}$	t - Values	
0.5	0.914	0.0129	0.0139	±0.0239	±0.0079
1	0.997	0.0033	0.0037	±0.0072	±0.0021
2.25	0.998	0.0042	0.0051	±0.0028	±0.0115

### 5.3.1 Measurements with 0.5MHz Transducer in Water-based Mud

0.5MHz transducer has the largest error in resolution of object along the propagation distances as is seen in Table 5.3, this effect can also be observed in the regression fit of Figure 5.11. The attenuates coefficient of this transducer in the fluid sample is lower as compared with the other higher frequency transducers this essentially is due to its higher wavelength and this tends to influence much penetration, though with lower resolution capability when identifying objects along it path.

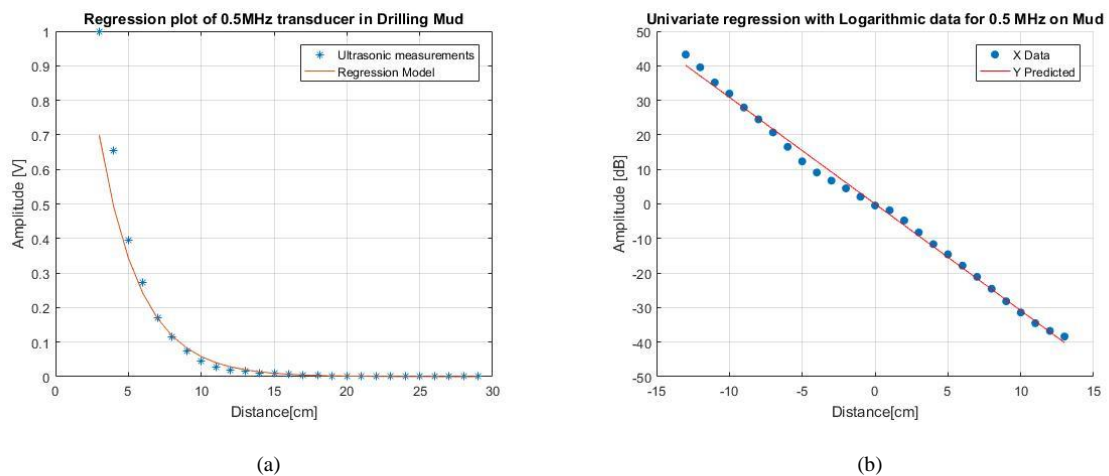


Figure 5.11: Regression plot for Linear (a) and Logarithmic Scale (b) of Amplitude Variation of 0.5MHz Transducer versus Distance



### 5.3.2 Measurements with 1MHz Transducer in Water-based Mud

The effect of attenuation is higher in 1MHz transducer than in 0.5MHz, but better resolution capability was realized as the reduced wavelength brings about reduction prediction error as can be seen in linear scale of Figure 5.12.

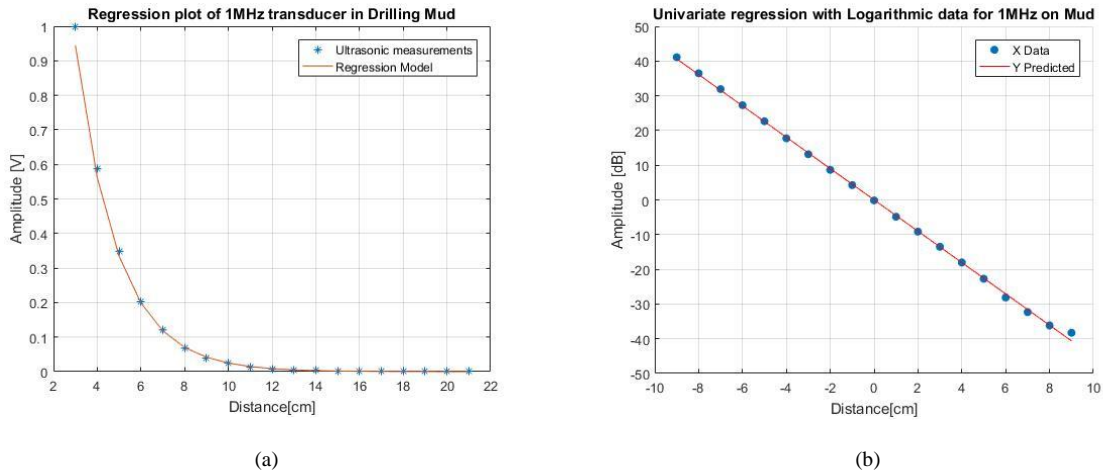


Figure 5.12: Regression plot for Linear (a) and Logarithmic Scale (b) of Amplitude Variation of 1MHz Transducer versus Distance

### 5.3.3 Measurements with 2.25MHz Transducer in Water-based Mud

This transducer has the highest attenuated signal with lowest penetration capability as compared with other frequency but with better resolution results as can be seen in Table 5.3

Figure 5.13 shows the amplitude variation of 2.25MHz transducer with better resolution capability as compared with the other transducers. This tends to be the most attenuated frequency in the mud sample as the signal could only travel a short distance before completely attenuated. Obvious reason is due to resolution of back-scattering result from smaller particles used in formulation of the mud that is relative to the transducers shorter wavelength.

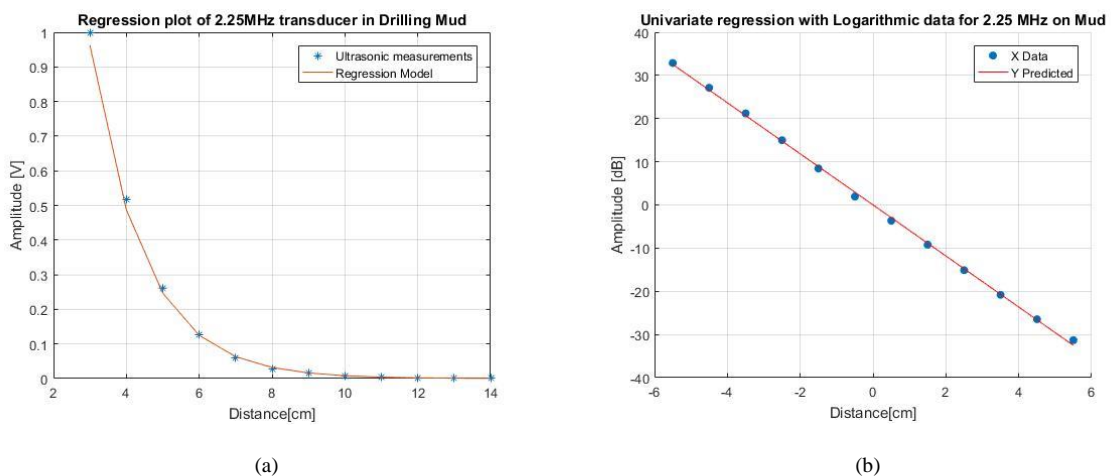


Figure 5.13: Regression plot for Linear (a) and Logarithmic Scale (b) of Amplitude Variation of 2.25MHz Transducer versus Distance

### 5.3.4 Combined Result of the Measurements in Real Mud

Figure 5.14 shows the amplitude variation in decibel for the different transducers in mud sample. 2.25MHz transducer was more attenuated than the other frequencies and also with very low penetration capability. From the plot it is seen that it could only travel upto about 14cm before the signal is completely attenuated while 1MHz transducer got to 22cm.

0.5MHz was the least attenuated frequency in the mud sample, as it could travel farther up to 28cm along the propagation distances.

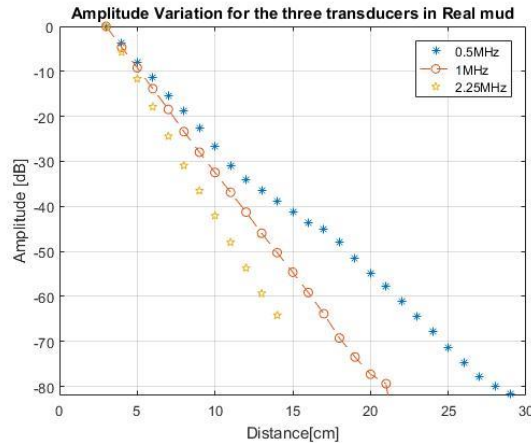


Figure 5.14: Combined plot for Amplitude Change with Propagation Distances for the various Ultrasonic Transducer in Mud

Figure 5.15 shows the attenuation of sound wave in the mud sample. 2.25MHz transducer is seen to be highly attenuated with a very short penetration capability, obviously due to its shorter wavelength, and the attenuation is certainly due to the transducer high sensitivity in resolution of object along its propagation path.

In the case of real mud it is essentially due to its ability to resolve smaller particles in the mud composition which influences back scattering thereby causing much attenuation of ultrasound.

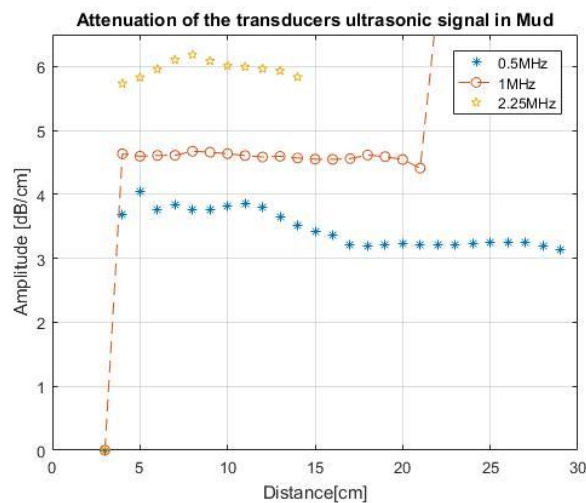


Figure 5.15: Attenuation of Ultrasonic Wave in Mud versus Propagation Distance

## 5.4 Multivariate Data Analysis

Multiple correlation of the collective data from all the fluid samples and transducers were analyzed using unscrambler software. The effect of the acoustic property was observed through the different Attenuation Spectroscopy resulting from the fluid samples.

Table 5.4 shows the calculated results of the sound speed  $V$  of the different fluid and their rheological parameters. This was used in the interpretation of the multivariate results and plots.

Prior to the analysis, it's essential to find out with the help of matrix plot, whether the variables within the data set needs to be scaled in other to provide all the variable equal chances of influencing the oncoming analysis.

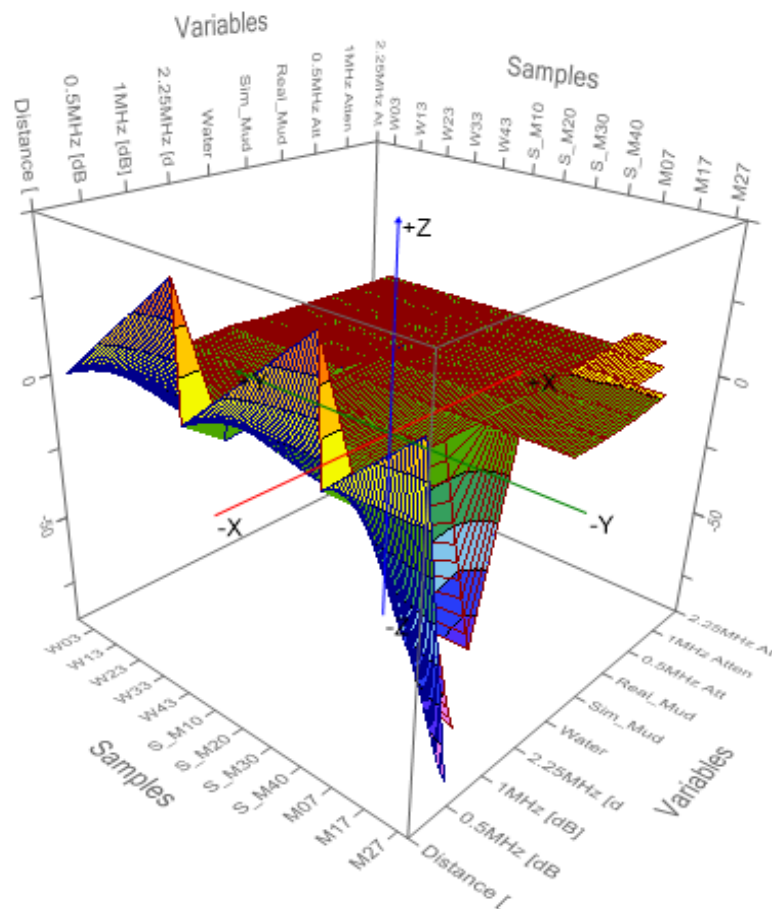


Figure 5.16: Matrix Plot of Data set

Most variables do not have same variance as seen in the matrix plot of Figure 5.16, therefore, Scaling was done on the data matrix, to ensure contribution from all the variables.

Table 5.4: Summary of Sound speed Results for the Various Fluid samples, Transducers attenuation values and Near zone Distances

Acoustic impedance; $Z = \rho V$ , N = Near zone							
Sample	Tf (MHz)	V [m/sec]	$\alpha$ [dB/cm]	N [cm]	$\rho$ [kg/m <sup>3</sup> ]	Z [kg/m <sup>2</sup> s]	$\eta$ [cP]
Water	0.5	1432 $\pm$ 0.69	0.17	5.5	1000	1.43x10 <sup>6</sup>	0.98
	1	1448 $\pm$ 0.17	0.12	10.8	1000	1.45x10 <sup>6</sup>	0.98
	2.25	1467 $\pm$ 0.13	0.10	24.0	1000	1.47x10 <sup>6</sup>	0.98
Simulated Drilling fluid	0.5	1970 $\pm$ 0.09	0.23	4.0	1405	2.77x10 <sup>6</sup>	4.1
	1	2015 $\pm$ 0.06	0.13	7.8	1405	2.83x10 <sup>6</sup>	4.1
	2.25	2050 $\pm$ 0.05	0.10	17.2	1405	2.88x10 <sup>6</sup>	4.1
Water-based Drilling fluid	0.5	1487 $\pm$ 0.32	0.3	5.3	1320	1.96x10 <sup>6</sup>	19
	1	1536 $\pm$ 0.15	4.5	10.2	1320	2.03x10 <sup>6</sup>	19
	2.25	1587 $\pm$ 0.09	5.9	22.2	1320	2.09x10 <sup>6</sup>	19

### 5.4.1 PCA Results

For PCA analysis in finding the hidden information and relationship between samples, variables, and as well as their cross-relationship. This is done by decomposition of the data set into structural part and noise part, by using Principal Component Analysis (PCA) from the software.

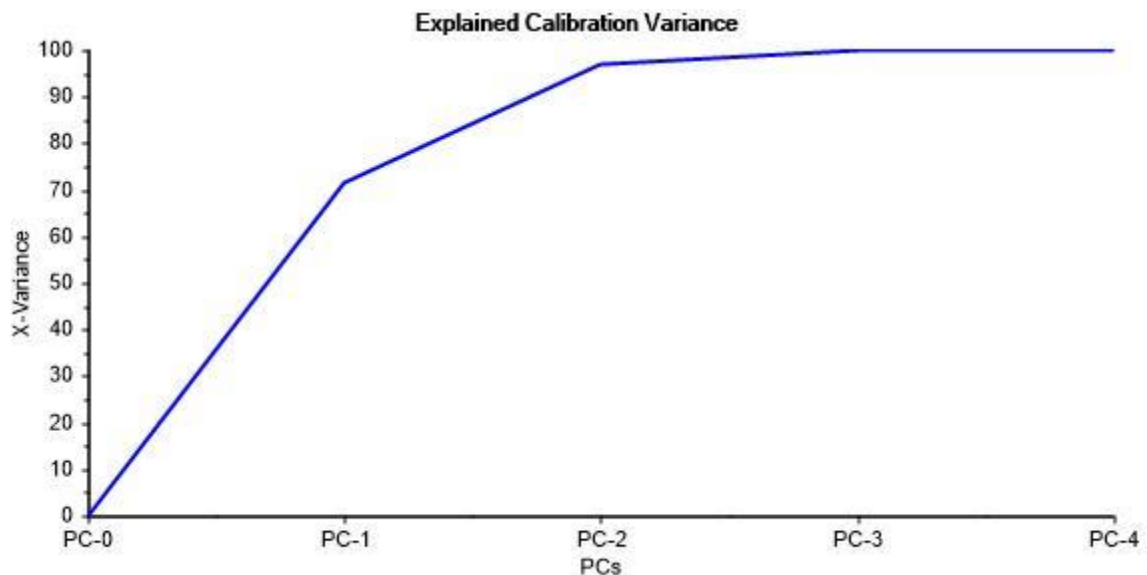


Figure 5.17: Explained Variance for the Decomposed Dataset

Figure 5.17, shows the explained variance plot for the correlation between the fluid samples, and the different transducer along their various propagation distances. PC1 and PC2 explains

over 75% of the variations, and as such was used in interpreting the scores and loading plots of Figure 5.18.

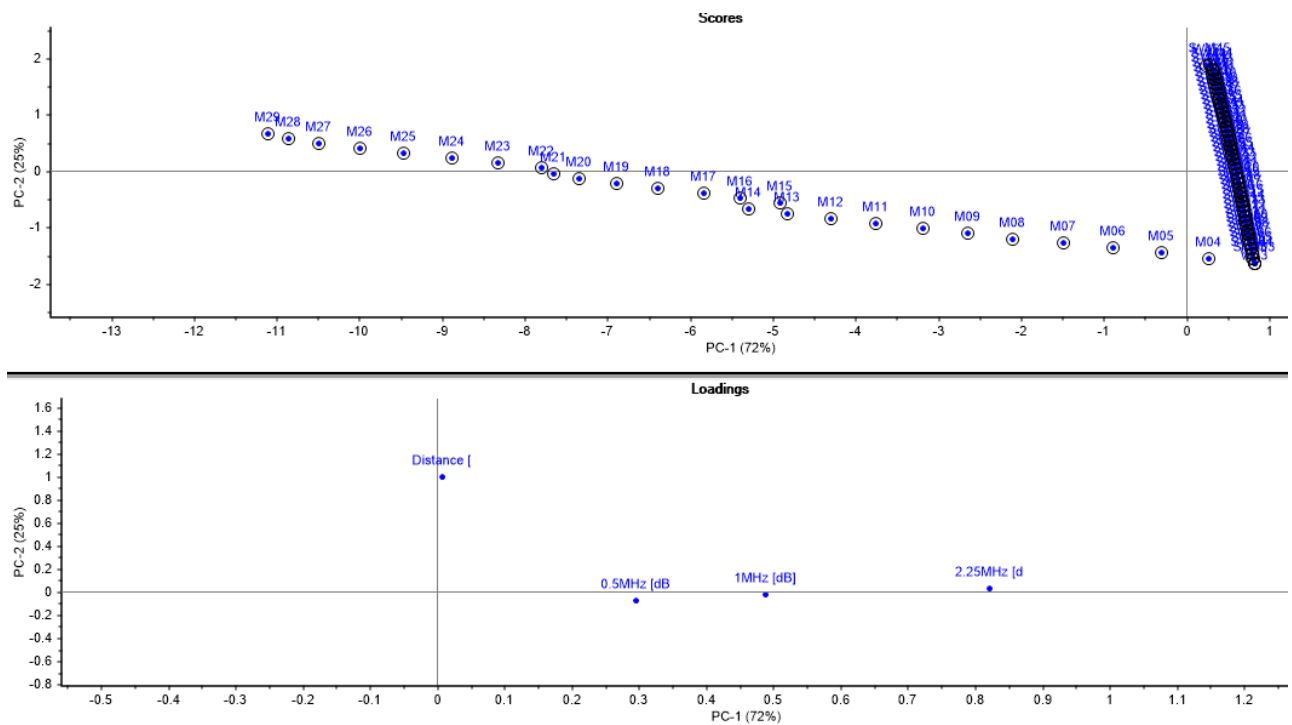


Figure 5.18: Scores and Loading plot

In PC-1 direction the most important variable is the transducer frequencies, while in PC-2 direction shows propagation distance, this is seen in the loading plot of Figure 5.18.

The plot reveals a very large distinctions between the acoustic property of the drilling fluid which is inversely correlated to that of simulated mud and water. The obvious reason is due to how highly attenuated the ultrasound is in the mud as a result of the drilling fluid greater viscous property as is seen in

Table 5.4. Moreover the acoustic back-scattering from particle used in its formulation influences the attenuation of ultrasound.

Water and simulated mud exhibit similar characteristics even though the density of simulated mud seems to be higher than that of water. This shows that viscosity has more effect to the attenuation of ultrasound than density.

The density of the simulated mud is higher than that of the real mud as well. The effect of high density in simulated mud increases the velocity of sound of the fluid. Two physical properties of the medium are crucial in this respect, these are the density and the compressibility of the medium. Denser medium such as the simulated mud is made up of more massive particles which are formulated from dissolved salt in its concentration. This however will require greater force to initiate particle motions (inertia).

The acoustic impedance was calculated using the relation;  $Z = \rho V$ . Where, ‘Z’ is acoustic impedance, ‘ρ’ is material density and ‘V’ is the velocity of sound in the medium.

The response from the plot also reveals that mud has a very small propagation distance. This is also a clear indication of how strongly attenuated the ultrasonic sound is in it. This is caused by acoustic back-scattering from particle used in its formulation.

The effect of Frequency as was also observed from the plot showed how inversely correlated the 2.25MHz frequency varies from the Mud. This was actually the transducer that was

highly attenuated due to its shorter wavelength. Other fluids showed a little similar effect, on 2.25MHz transducer by tilting away at an angle from it as is seen in the scores and loading plot of Figure 5.18.

### 5.4.2 PLS-R Results

In performing the PLS-R modelling cross validation was used instead of test set validation since clear distinctions were already observed from the PCA analysis, and also there was no sufficient data to be used for test set validation.

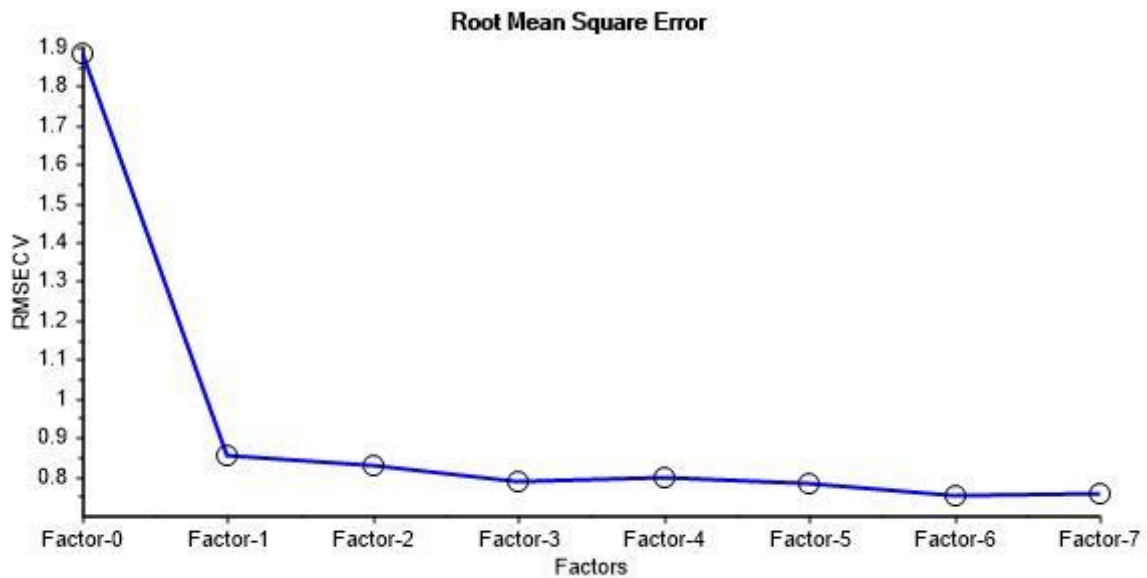


Figure 5.19: Root Mean Square Error Plot

The model choose 2 component factors from the Root Mean Square Error plot of Figure 5.19. This produces X- and Y- Loadings for the input and output data as seen in Figure 5.20. The plot consists of factor 1 and factor 2. Factor 1 has a contribution of 55% on Y variance and factor 2 has about 14%. Therefore, maximum of two components was required to predict the Y variable which in this case is the attenuation coefficient of the various transducers in the fluid sample while the remaining components are considered as noise for they provide little or no information for the model.

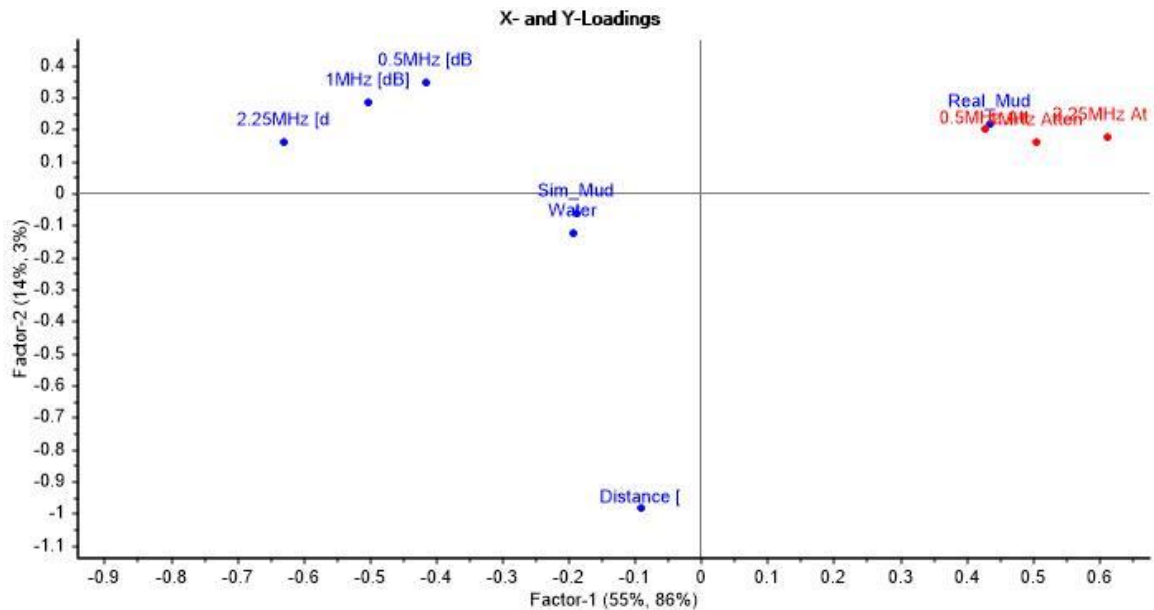


Figure 5.20: X- and Y- Loadings Plot

From the analysis of the first factor, it was discovered that propagation distance has greater contribution in determining how the different transducers attenuate in the fluid samples. This was found to be correct for the same effect was already observed in the PCA analysis where the drilling mud shows different correlation compared to the other fluid samples. The indications from x- y- loadings of Figure 5.20 now confirms the indications from the PCA plots that drilling mud has very different acoustic properties compared to simulated mud and water.

Water has the lowest ultrasonic sound absorption along its propagation distance compared to the other fluids samples.

Table 5.4 reveals that it has the lowest acoustic impedance as well as sound speed, and other rheological parameters, this gives an insight to its acoustic property resulting from probably the molecular structure of water as compared to other fluid samples.

Simulated mud attenuates a little more than water due to ionic influence from the salt used in formulating the fluid.

In the same figure Distance is seen to be inversely proportional to transducer frequency. For the higher the transducer frequency the lower the distance travelled by the ultrasound. This is a clear indication of a shorter wave length, and greater resolution capability.

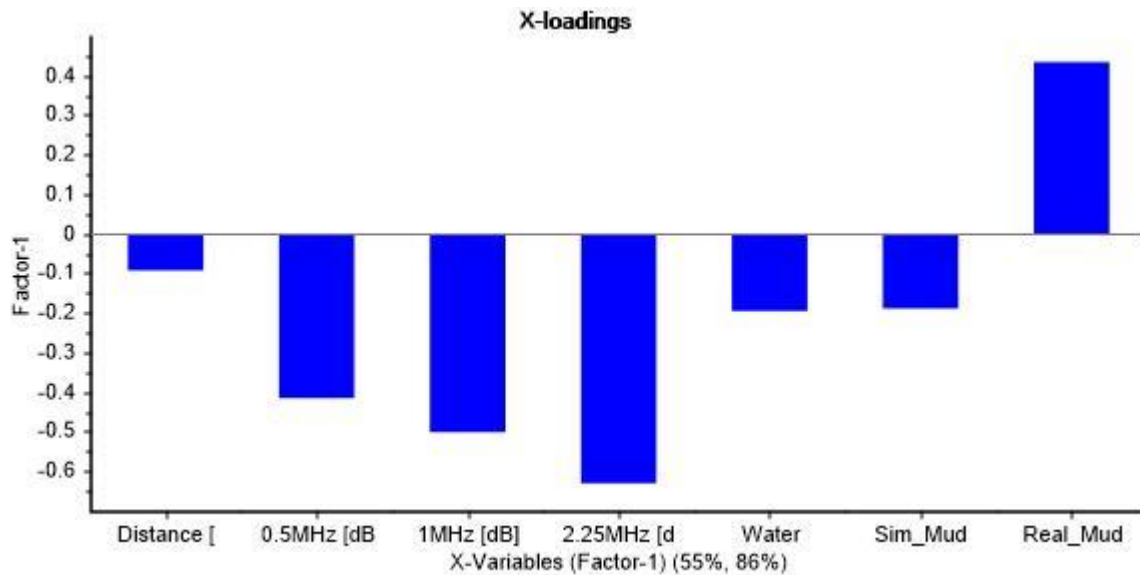


Figure 5.21: Loading Weight

From the loading weight as seen in Figure 5.21, the acoustic influence of the various fluid properties as explained in X- Y- loadings plot is also indicated here. The effect of attenuation in drilling mud is greater than in the other fluid samples, reason is due to high viscosity effect as can be seen in the rheological parameter of

Table 5.4 and also scattering resulting from particles used in the design of the mud.

In this figure, the important variables are:

**2.25MHz transducer** ; This has the highest negative contribution (-0.6) to the attenuation of ultrasound wave in the propagation distance, followed by **1MHz** transducer and then **0.5MHz** transducer is the lowest attenuated frequency in all fluid samples, this obviously is as a result of its high wavelength.

**Real\_Mud** ; is inversely correlated to transducer frequencies in the propagation distance, with a positive contribution of about (4). For the higher the transducer frequency the lower the distance travelled by the ultrasound in the mud. This effect is also applicable to other fluid samples. Water is observed to have lowest effect with negative contribution of about (-0.2) and simulated mud is (-0.17).



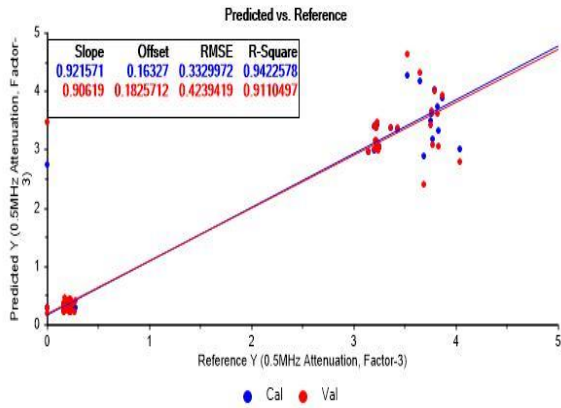


Figure 5.22: Predicted vs. Reference Plot of 0.5MHz

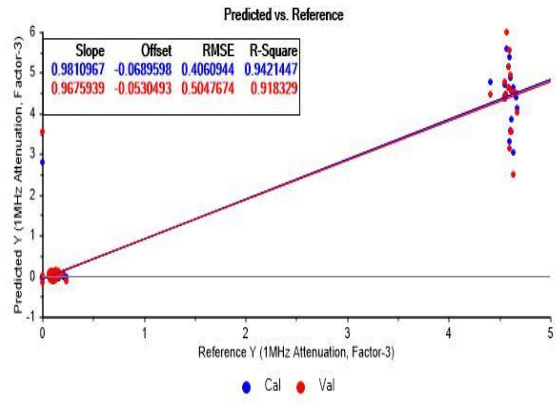


Figure 5.23: Predicted vs. Reference Plot of 1MHz

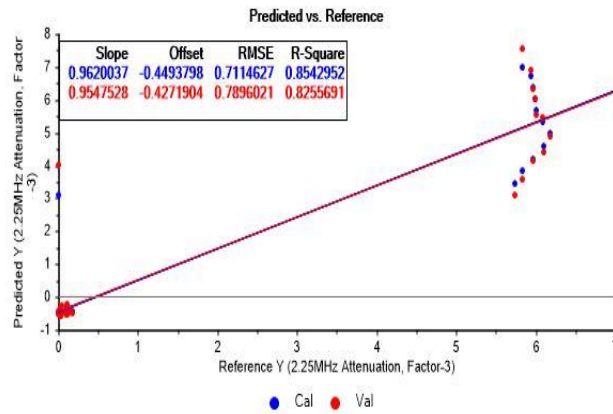


Figure 5.24: Predicted vs. Reference of 2.25MHz

Figure 5.22, 5.23, and 5.24 shows the predicted vs. reference plot of the three different frequencies resulting from the model form factor of 1 as selected by the Root Mean Square error plot.

0.5MHz transducers has better RMSE result that is **0.33**, than the other frequencies this essentially is due to all the fluid samples provided more data with regards to the propagation distance at this frequency. This can be observed from the MATLAB plot of Figure 5.25

2.25MHz has highest prediction errors of about **0.7**.

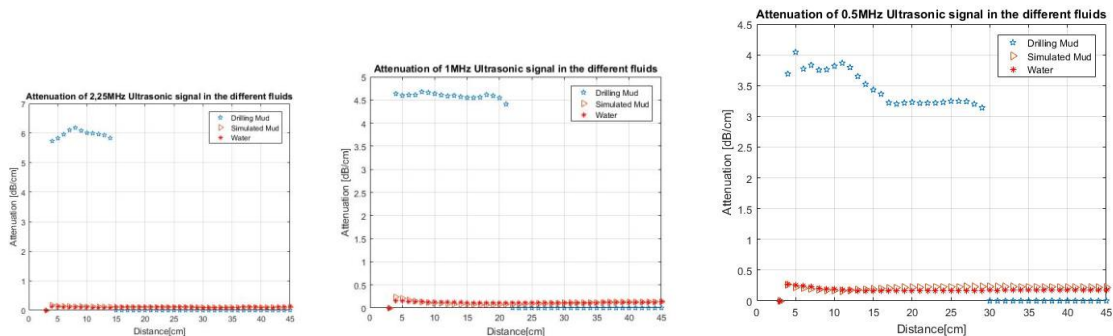


Figure 5.25: The plot of the collective fluids attenuation and frequency versus distance

## 6 Conclusion

The focus of this master thesis is to perform an experimental test and characterization of the wave propagation in different fluid samples at static state with respect to propagated distance using ultrasonic techniques which essentially will be an introduction to utilizing ultrasonic Doppler measurements for determining mud flow rate in the test rig at USN.

The project gives a theoretical background of the acoustic properties of the different fluids samples before the corresponding analysis using the ultrasonic attenuation effects.

From the interpretation of the experimental results, two different fluid samples that was compared with real drilling mud exhibit a similar trend with regards to the attenuation of sound wave, and as such their rheological parameters were calculated to verify this result.

It was observed that the sound speed in simulated mud is larger than in real mud and water due to its higher density. This effect does not have much significance to attenuation of sound wave as compared to real mud which has a lower density but higher viscosity, this revealed that viscosity of medium has more effect to attenuation than density.

Among other effect of attenuation could be back scattering resulting from particles of different sizes that was used in formulating the drilling fluid but this have not been completely investigated. Simulated mud was designed with salt concentrate, the effect of ionic motion applicable to the dissolved salt in it composition seems not to have much influence to attenuation of sound wave as compared to the real mud.

Therefore, based on my observations, real mud would be preferable to be used on the Doppler test on flowrate measurement than using simulated mud.

Also, the test essentially should be performed in flow conditions rather than in static state for Doppler meters rely on reflectors in the flowing liquid.

### 6.1 Further Works

Based on the observation from the effects of the drilling mud acoustic properties as compared with the simulated mud samples, I would recommend the investigation of variations in the concentration and additive used in the design of fluid samples as it influences attenuation and speed of sound.

Measurements was done in static state, the acoustic effects of the fluid samples when flowing should be investigated.

Finally, I would recommend the investigation of the rheological parameters of the fluid samples based on the experimental results acquired, which already provided some insight on the intensity of ultrasound pulse after propagation, which are; attenuation  $\alpha$  and sound speed  $V$  as it relates to the acoustic property of the fluids. This is highlighted in (chapter 3.7). and Table 5.4.

Based upon ultrasonic measurement principles, a model that categorizes the fluid viscosity can be developed for estimation of viscosity of the fluid samples, where the input could be fixed distance measurement and attenuation is measured.

# References

- [1] R. Caenn, H. C. H. Darley, and G. R. Gray, "Chapter 1 - Introduction to Drilling Fluids," in *Composition and Properties of Drilling and Completion Fluids (Sixth Edition)*, ed Boston: Gulf Professional Publishing, 2011, pp. 1-37.
- [2] G. E. L. D. M. Schafer, D. A. Glowka, and D. D. Scott, "An Evaluation of Flowmeters for the detection of Kicks and Lost Circulation During Drilling," 1992.
- [3] Stéphane Fischer, Claude Rebattet, Thibault Lalande, Damien Dufour, and N. Bachellier, "Applicability of Ultrasonic Pulsed Doppler for Fast Flow-Metering," in *Proceedings of the 8th International Symposium on Ultrasonic Doppler Methods for Fluid Mechanics and Fluid Engineering, Dresden-Rossendorf, Germany, 2012*.
- [4] Q. Zhou, H. Zhao, H. Zhan, H. Zhang, and C. Lu, "The application of ultrasonic based on Doppler effect used in early kick detection for deep water drilling," in *2013 International Conference on Communications, Circuits and Systems (ICCCAS)*, 2013, pp. 488-491.
- [5] S. A. Africk, C. K. Colton, W. H. Dalzell, D. T. Wu, J. L. Albritton, and L. R. Daum, "Ultrasonic pulsed Doppler (USPD): A backscatter technique for characterization of particles and nanoparticles; Non-invasive measurement of fluid flow velocity," in *Proceedings of the 39th Annual Symposium of the Ultrasonic Industry Association*, 2010, pp. 1-7.
- [6] K. Mohanarangam, K. Simic, A. Brent, and P. Fawell., "Fluid flow characterization of process equipment using ultrasonic pulsed Doppler technique," presented at the Proceedings of the 8th International Symposium on Ultrasonic Doppler Methods for Fluid Mechanics and Fluid Engineering, Dresden-Rossendorf, Germany, 2012.
- [7] "Front Matter," in *Composition and Properties of Drilling and Completion Fluids (Sixth Edition)*, ed Boston: Gulf Professional Publishing, 2011, pp. i-ii.
- [8] A. J. Hayman, "Ultrasonic Properties of Oil- Well Drilling Muds," in *ULTRASONICS SYMPOSIUM* 1989.
- [9] T. a. A. M. Geehan. Drilling Mud: Monitoring and Managing It. *1(2)*. Available: [http://www.slb.com/resources/publications/industry\\_articles/oilfield\\_review/1989/or1989jul04\\_drilling\\_mud.aspx](http://www.slb.com/resources/publications/industry_articles/oilfield_review/1989/or1989jul04_drilling_mud.aspx)
- [10] Schlumberger. (2013, 17/05/17). *Drilling Fluid Basics*. Available: [http://www.slb.com/resources/oilfield\\_review/~media/Files/resources/oilfield\\_review/ors13/spr13/defining\\_fluids.ashx](http://www.slb.com/resources/oilfield_review/~media/Files/resources/oilfield_review/ors13/spr13/defining_fluids.ashx).
- [11] A. S. S. Committee, *Drilling Fluids Processing Handbook (1)*. Saint Louis, US: Gulf Professional Publishing, 2011.
- [12] T. H. Omland, "Particle settling in non-Newtonian drilling fluids," no. 80, University of Stavanger, Faculty of Science and Technology, Department of Petroleum Engineering, Stavanger, 2009.
- [13] L. D. Maus, J. D. Tannich, and W. T. Ilfrey, "Instrumentation Requirements for Kick Detection in Deep Water."
- [14] PetroWiki. (2017, 30/04/2017). *Drilling fluid types*. Available: [http://petrowiki.org/Drilling\\_fluid\\_types#cite\\_note-r1-1](http://petrowiki.org/Drilling_fluid_types#cite_note-r1-1)

- [15] N. G. Oil. (2017). *Drilling Fluid Technology*. Available: <http://www.netwasgroup.us/fluid-technology/relationship-of-mud-properties-to-functions.html>
- [16] J. P. Nguyen, *Fundamentals of Exploration and Production*: Technip, Paris, 1996.
- [17] O. a. G. P. Petroleum Support. (2015, 13/05/17). *Drilling Fluid Test on Field*. Available: <http://petroleumsupport.com/drilling-fluid-test-on-field/>
- [18] K. E. Solutions. (2013). *Properties of Drilling fluid*. Available: [knowenergysolutions.com/conventional-energy/oil-and-gas/drilling/mud-engineering/properties-of-drilling-fluid](http://knowenergysolutions.com/conventional-energy/oil-and-gas/drilling/mud-engineering/properties-of-drilling-fluid)
- [19] N. G. Oil. (2013). *Drilling Fluid Technology*. Available: <http://www.netwasgroup.us/fluid-technology/functions-of-a-drilling-fluid.html>
- [20] W. Han, J. R. Birchak, B. H. Storm, and T. E. Ritter, "Acoustic sensor for fluid characterization," ed: Google Patents, 2004.
- [21] J. M. Carcione and F. Poletto, "Sound velocity of drilling mud saturated with reservoir gas," *GEOPHYSICS*, vol. 65, pp. 646-651, 2000.
- [22] A. J. Hayman, "Ultrasonic properties of oil-well drilling muds," in *Proceedings., IEEE Ultrasonics Symposium*, 1989, pp. 327-332 vol.1.
- [23] J. Aho and N. R. Society, *Papers Presented at the Nordic Rheology Conference, Stavanger, Norway, June 13-15, 2007: General Papers and Papers from the Special Sessions on Emulsions and Suspension*: Nordic Rheology Society, 2006.
- [24] E. Motz, D. Canny, and E. Evans, "Ultrasonic Velocity And Attenuation Measurements In High Density Drilling Muds."
- [25] J. L. Rose, *Ultrasonic waves in solid media*. Cambridge [u.a.]: Cambridge University Press, 1999.
- [26] R. Prakash, *Non-Destructive Testing Techniques*. Kent, GB: New Academic Science, 2011.
- [27] OLYMPUS. (2017, 04/04/17). *Ultrasonic Flaw Detection Tutorial*. Available: <http://www.olympus-ims.com/en/ndt-tutorials/flaw-detection/wave-propagation/>
- [28] N. R. Center. (2017). *Introduction to Ultrasonic Testing*. Available: <https://www.nde-ed.org/EducationResources/CommunityCollege/Ultrasonics/Physics/defectdetect.htm>
- [29] KROHNE, "Ultrasonic flowmeters - Liquids," ed, 2017.
- [30] J. C. Drury, "NDT FUNDAMENTALS: Ultrasonics, Part 7. The ultrasonic beam," vol. 5, pp. 297-299, 2005.
- [31] S. Processing. (2017, 10/03/17). *The Ultrasonic Field*. Available: <http://www.signal-processing.com/transducers.php>
- [32] J. Frank-Michael, "Early kick detection and nonlinear behavior of drilling mud," ed: Unpublished, 2014.
- [33] RheoSense. (2016, 02/05/2017). *Viscosity of Newtonian and non-Newtonian Fluids*. Available: <http://www.rheosense.com/applications/viscosity/newtonian-non-newtonian>
- [34] Schlumberger. (2017). *Oilfield Glossary*. Available: [http://www.glossary.oilfield.slb.com/Terms/s/shear\\_rate.aspx](http://www.glossary.oilfield.slb.com/Terms/s/shear_rate.aspx)

- [35] S. H. Sheen, K. J. Reimann, W. P. Lawrence, and A. C. Raptis, "Ultrasonic techniques for measurement of coal slurry viscosity," in *IEEE 1988 Ultrasonics Symposium Proceedings.*, 1988, pp. 537-541 vol.1.
- [36] A.S.Dukhin and P.J.Goetz, "Characterization of Liquids, Nano- and Microparticulates, and Porous Bodies using Ultrasound," vol. 24, p. 518, 2002.
- [37] A.S.Dukhin and P.J.Goetz. ULTRASOUND FOR CHARACTERIZING LIQUID BASED FOOD. *PRODUCTS. 1. Acoustic Spectroscopy.* . Available: <http://www.nihon-rufuto.com/science/pdf/Newsletter14%20food%20product.pdf>
- [38] J. Flood. (1997, 04/05/2017). *Ultrasonic Flowmeter Basics.* Available: <http://www.sensorsmag.com/components/ultrasonic-flowmeter-basics>
- [39] A. Pallarès, S. Fischer, X. France, M. N. Pons, and P. Schmitt, "Acoustic turbidity as online monitoring tool for rivers and sewer networks," *Flow Measurement and Instrumentation*, vol. 48, pp. 118-123, 4// 2016.
- [40] J. W. Einax, "Steven D. Brown, Roma Tauler, Beata Walczak (Eds.): Comprehensive chemometrics. Chemical and biochemical data analysis," *Analytical and Bioanalytical Chemistry*, vol. 396, p. 551, 2010.
- [41] OLYMPUS. (2017). *Immersion Transducers.* Available: <http://www.olympus-ims.com/en/ultrasonic-transducers/immersion/>
- [42] H. Viumdal, m. o. e. Norges teknisk-naturvitenskapelige universitet Fakultet for informasjonsteknologi, and f. Høgskolen i Telemark Fakultet for teknologiske, "Dynamic estimators using laser and ultrasonic instrumentation for determining the metal and bath heights in aluminium electrolysis cells : a combination of hard/soft sensor approach," 2015:15, Norwegian University of Science and Technology, Faculty of Information Technology, Mathematics and Electrical Engineering Telemark University College, Faculty of Technology, Trondheim, 2015.
- [43] A. J. Wheeler and A. R. Ganji, *Introduction to engineering experimentation*, 3rd ed. ed. Boston: Pearson, 2010.
- [44] W. MathWorld. (2017). *Least Squares Fitting--Exponential.* Available: <http://mathworld.wolfram.com/LeastSquaresFittingExponential.html>
- [45] K. H. Esbensen, D. Guyot, F. Westad, L. P. Houmøller, and A. S. A. Camo, *Multivariate data analysis - in practice : an introduction to multivariate data analysis and experimental design*, 5th ed. ed. Oslo: Camo, 2001.
- [46] <https://en.wikipedia.org/wiki/Neper>. (2016, 10/05/2017). *Neper.* Available: <http://www.radio-electronics.com/info/formulae/decibels/dB-decibel-neper-conversion.php>
- [47] C. Jensen and T. Anderson, "Sound Attenuation in Water," 2009.
- [48] G. Knowing. (2017). *StatsBookStudentTTable.* Available: <http://growingknowing.com/GKStatsBookStudentTTable.html>

# Appendices

## Appendix A: Task Description

**HSN** University College  
of Southeast Norway  
Faculty of Technology, Natural Sciences and Maritime Sciences, Campus Porsgrunn

### FMH606 Master's Thesis

**Title:** Characterization of ultrasonic waves in various drilling fluids

**HSN supervisor:** Håkon Viumdal (main-supervisor) and Saba Mylvaganam (co-supervisor).

**External partner:** Geir Elseth (Statoil), Tor Inge Waag (Teknova) and Espen Oland (Teknova)

**Task background:**

Drilling operations for oil and gas are becoming more and more advanced, due to desired real time monitoring and control of the involved processes. The wells to be constructed are becoming more complex leading to new and complex types of drilling procedures with increased need for various specialized tools and equipment.

Thus, there is currently an increased research activity on improving the drilling operation by enhancement of sensor and control systems. As a part of the sensor research, estimations of the flow rates using ultrasonic Doppler measurements are evaluated in mud flow applications.

The Faculty of Technology at USN has in collaboration with Statoil designed and assembled a flow loop in the process hall. The rig represent the first step in a potential R&D activity where different advanced sensor applications are to be developed and tested with respect to flow rate and rheological properties in drilling operations. The research group at USN aim at utilizing ultrasonic Doppler measurements for determining the mud flow rate. As a basis for this research, this master thesis emphasize on static measurements with reference to how the ultrasonic wave attenuates in various fluids and specifically in drilling fluids.

**Task description:**

Feasibility study on ultrasonic Doppler flow rate measurement in drilling mud.

- 1) Literature research on Ultrasonic Doppler flow rate measurements and its usage in mud flow in particular.
- 2) Experimental research on acoustic properties in water, artificial drilling fluid(s) (from test rig) and actual drilling fluid(s), with three different ultrasonic transducers.
- 3) Analysing the experimental results and characterizing the wave propagation in the fluids with respect to the propagated distance and transducer frequency.
- 4) Submitting a report according to the guidelines of USN with a systematic documentation of codes developed and data gathered


**Student category:**

IIA students

**Practical arrangements:**

USN, campus Porsgrunn, has an ultrasonic Doppler sensor as a part of a flow loop, in the process hall. Measurements of acoustic properties in various fluids will be performed using appropriate containers and equipment available in the sensor lab.

**Signatures:**

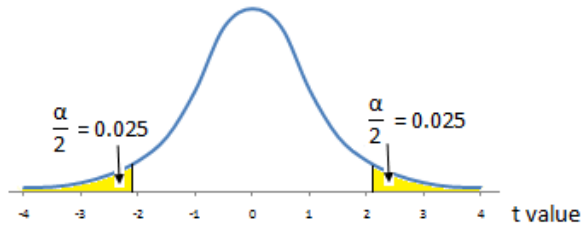
Student (date and signature): 03/02/17 

Supervisor (date and signature):  
03.02.2017 

Appendix B: Distribution Table

**Student's t Distribution Table**

For example, the t value for 18 degrees of freedom is 2.101 for 95% confidence interval (**2-Tail**  $\alpha = 0.05$ ).



	90%	95%	97.5%	99%	99.5%	99.95%	1-Tail Confidence Level
	80%	90%	95%	98%	99%	99.9%	2-Tail Confidence Level
	0.100	0.050	0.025	0.010	0.005	0.0005	1-Tail Alpha
<i>df</i>	0.20	0.10	0.05	0.02	0.01	0.001	2-Tail Alpha
1	3.0777	6.3138	12.7062	31.8205	63.6567	636.6192	
2	1.8856	2.9200	4.3027	6.9646	9.9248	31.5991	
3	1.6377	2.3534	3.1824	4.5407	5.8409	12.9240	
4	1.5332	2.1318	2.7764	3.7469	4.6041	8.6103	
5	1.4759	2.0150	2.5706	3.3649	4.0321	6.8688	
6	1.4398	1.9432	2.4469	3.1427	3.7074	5.9588	
7	1.4149	1.8946	2.3646	2.9980	3.4995	5.4079	
8	1.3968	1.8595	2.3060	2.8965	3.3554	5.0413	
9	1.3830	1.8331	2.2622	2.8214	3.2498	4.7809	
10	1.3722	1.8125	2.2281	2.7638	3.1693	4.5869	
11	1.3634	1.7959	2.2010	2.7181	3.1058	4.4370	
12	1.3562	1.7823	2.1788	2.6810	3.0545	4.3178	
13	1.3502	1.7709	2.1604	2.6503	3.0123	4.2208	
14	1.3450	1.7613	2.1448	2.6245	2.9768	4.1405	
15	1.3406	1.7531	2.1314	2.6025	2.9467	4.0728	
16	1.3368	1.7459	2.1199	2.5835	2.9208	4.0150	
17	1.3334	1.7396	2.1098	2.5669	2.8982	3.9651	
18	1.3304	1.7341	2.1009	2.5524	2.8784	3.9216	
19	1.3277	1.7291	2.0930	2.5395	2.8609	3.8834	
20	1.3253	1.7247	2.0860	2.5280	2.8453	3.8495	
21	1.3232	1.7207	2.0796	2.5176	2.8314	3.8193	
22	1.3212	1.7171	2.0739	2.5083	2.8188	3.7921	
23	1.3195	1.7139	2.0687	2.4999	2.8073	3.7676	
24	1.3178	1.7109	2.0639	2.4922	2.7969	3.7454	
25	1.3163	1.7081	2.0595	2.4851	2.7874	3.7251	
26	1.3150	1.7056	2.0555	2.4786	2.7787	3.7066	
27	1.3137	1.7033	2.0518	2.4727	2.7707	3.6896	
28	1.3125	1.7011	2.0484	2.4671	2.7633	3.6739	
29	1.3114	1.6991	2.0452	2.4620	2.7564	3.6594	
30	1.3104	1.6973	2.0423	2.4573	2.7500	3.6460	

[48]



Appendix C: Data Sheet for Water-Based mud used

**MI SWACO**  
 A Schlumberger Company  
 Væskerapport - utskipping (VU)

MR NUMMER:	
MUDTYPE:	LYDRIL SYSTEM-M0007251
LAGER / RIGG:	KSU
TIL RIGG:	
REKVIRERT AV:	
LEVERT VOLUM:	

DATO LEVERT	
TANK NUMBER:	K-17
TESTET AV :	
DATO TESTET:	7.3.17
LEVERT BÅT:	

Analysér		Enhet	Resultat
Tetthet		Sg	1.32+
Rheologiavlesninger:	600 rpm	lbs/100ft <sup>2</sup>	70
	300 rpm	lbs/100ft <sup>2</sup>	51
	200 rpm	lbs/100ft <sup>2</sup>	42
	100 rpm	lbs/100ft <sup>2</sup>	31
	6 rpm	lbs/100ft <sup>2</sup>	11
	3 rpm	lbs/100ft <sup>2</sup>	9
Gelstyrke	10 s	Pa	5
	10 m	Pa	10
Viskositet	PV	cP	19
	YP	Pa	15
HTHP filtertap	ved deg. C	ml	
Retorte	Solids	vol. %	
	Vann	vol. %	
	Olje	vol. %	
Olje- /vann-forhold( For Versapro LS: Olje/Brine )		OWR	
LGS		kg/m <sup>3</sup>	
Klorid		mg/ltr	
<b>Tester kun for oljebaserte væsker:</b>			
ES		Volt	
Excess Lime		kg/m <sup>3</sup>	
<b>Tester kun for vannbaserte væsker:</b>			
MBT		kg/m <sup>3</sup>	
KCl		kg/m <sup>3</sup>	
Glycol		%	
pH			8.2 - ved 15C
API Filtertap		ml / 30 min	
Refraktometer Glycol %		%	
<b>Andre tester for brine:</b>			
Temperatur		°C	
NTU			
pH			
Klarhet ( visuelt )			
Lukt			
Kommentarer:			



Sound Speed Calculation for 0.5MHz frequency in water										Sound Speed Calculation for 2.25MHz frequency in water										Sound Speed Calculation for 1MHz frequency in water									
Test 1	Test 2	Test 3	Test 4	Test 5	Std. Dev.	Mean	Tot V (m/sec)	Std. Dev.	Mean	Test 1	Test 2	Test 3	Test 4	Test 5	Std. Dev.	Mean	Tot V (m/sec)	Std. Dev.	Mean	Test 1	Test 2	Test 3	Test 4	Test 5	Std. Dev.	Mean	Tot V (m/sec)		
3.0	22.3	24.0	24.2	24.1	24.0	0.8	23.7	1254.4	0.8	23.7	21.24	21.17	21.22	21.24	0.04	21.20	1414.961	0.04	21.20	22.52	22.58	22.56	22.51	22.53	0.0	22.5	1331.0		
4.0	29.3	30.8	30.9	30.9	30.8	0.7	30.5	1310.4	0.4	28.06	27.91	27.97	28.14	27.97	0.09	28.01	1428.061	0.09	28.01	29.27	29.38	29.38	29.38	29.3	0.0	29.3	1363.2		
5.0	36.1	37.5	37.6	37.7	37.6	0.7	37.3	1340.9	0.5	34.7	34.67	34.67	34.7	34.72	0.02	34.692	1441.254	0.02	34.692	35.97	36.14	36.17	36.01	35.99	0.1	36.1	1386.7		
6.0	42.8	44.3	44.3	44.3	44.2	0.6	44.0	1364.1	0.6	41.42	41.37	41.49	41.46	41.51	0.06	41.45	1447.527	0.06	41.45	42.74	42.88	42.84	42.76	42.75	0.1	42.8	1402.1		
7.0	49.6	51.0	51.1	51.1	50.9	0.6	50.7	1390.0	0.7	48.24	48.18	48.09	48.22	48.21	0.06	48.188	1462.544	0.06	48.188	49.59	49.59	49.73	49.48	49.47	0.1	49.6	1412.4		
8.0	56.4	57.8	57.8	57.8	57.7	0.6	57.5	1391.1	0.8	55.04	54.99	55.02	55.03	54.98	0.03	55.012	1454.238	0.03	55.012	56.25	56.47	56.48	56.36	56.24	0.1	56.4	1419.4		
9.0	63.2	64.6	64.7	64.7	64.5	0.6	64.4	1398.5	0.9	61.74	61.78	61.79	61.78	61.78	0.02	61.778	1456.829	0.02	61.778	63.11	63.33	63.33	63.22	63.03	0.1	63.2	1424.0		
10.0	69.9	71.4	71.4	71.4	71.3	0.7	71.1	1406.9	1.0	68.54	68.46	68.54	68.57	68.61	0.06	68.544	1458.917	0.06	68.544	69.86	70.07	70.03	70.0	69.85	0.1	70.0	1429.3		
11.0	76.7	78.2	78.2	78.2	77.9	0.7	77.8	1412.2	11	75.32	75.26	75.34	75.24	75.05	0.05	75.304	1460.746	0.05	75.304	76.65	76.78	76.86	76.73	76.58	0.1	76.7	1433.8		
12.0	83.5	84.9	84.8	84.9	84.7	0.6	84.6	1419.1	12	82.13	81.96	82.1	82.07	82.04	0.07	82.06	1462.345	0.07	82.06	83.61	83.65	83.63	83.43	83.29	0.1	83.5	1437.7		
13.0	90.2	91.5	91.6	91.7	91.4	0.6	91.3	1424.0	13	88.81	88.89	88.85	88.74	88.81	0.06	88.82	1463.634	0.06	88.82	90.07	90.36	90.35	90.14	89.99	0.1	90.2	1441.5		
14.0	97.0	98.3	98.4	98.4	98.1	0.6	98.0	1427.9	14	95.58	95.42	95.51	95.56	95.48	0.06	95.51	1465.815	0.06	95.51	96.84	97.17	97.04	96.87	96.78	0.1	96.9	1444.2		
15.0	103.5	105.0	105.0	105.1	104.9	0.7	104.7	1432.7	15	102.24	102.13	102.24	102.19	102.16	0.05	102.192	1467.825	0.05	102.192	103.5	103.71	103.68	103.62	103.51	0.1	103.6	1447.8		
16.0	110.3	111.9	111.9	111.8	111.7	0.7	111.5	1435.1	16	108.96	108.79	108.92	108.99	108.95	0.08	108.922	1468.941	0.08	108.922	110.21	110.56	110.54	110.29	110.2	0.2	110.4	1448.8		
17.0	117.1	118.6	118.5	118.6	118.3	0.6	118.2	1437.8	17	115.76	115.61	115.7	115.81	115.77	0.08	115.73	1468.936	0.08	115.73	116.99	117.36	117.33	117.18	116.99	0.2	117.2	1450.9		
18.0	123.8	125.3	125.3	125.4	125.1	0.7	125.0	1440.3	18	122.52	122.34	122.53	122.5	122.53	0.08	122.484	1469.58	0.08	122.484	123.8	124.13	124.06	123.9	123.74	0.1	123.9	1452.5		
19.0	130.7	132.1	132.1	132.1	131.7	0.6	131.7	1442.2	19	129.23	129.13	129.15	129.26	129.21	0.05	129.196	1470.634	0.05	129.196	130.44	130.83	130.79	130.7	130.51	0.1	130.6	1454.1		
20.0	137.4	138.9	138.9	138.9	138.4	0.6	138.5	1444.0	20	136.04	135.93	136.03	136.07	136.04	0.06	136.01	1470.48	0.06	136.01	137.28	137.63	137.6	137.38	137.21	0.2	137.4	1455.4		
21.0	144.2	145.7	145.7	145.6	145.3	0.7	145.3	1445.4	21	142.76	142.59	142.77	142.85	142.82	0.10	142.758	1471.021	0.10	142.758	143.95	144.35	144.38	144.13	143.97	0.2	144.2	1456.8		
22.0	150.9	152.4	152.5	152.3	152.0	0.6	152.0	1447.2	22	149.69	149.48	149.55	149.56	149.55	0.08	149.568	1473.023	0.08	149.568	150.76	151.16	151.12	150.89	150.72	0.2	150.9	1457.6		
23.0	157.6	159.3	159.2	159.1	158.7	0.7	158.8	1448.7	23	156.37	156.11	156.38	156.35	156.39	0.12	156.32	1474.341	0.12	156.32	157.51	158.02	157.91	157.74	157.58	0.2	157.8	1458.0		
24.0	164.5	166.0	165.9	166.0	165.6	0.6	165.6	1449.5	24	163.08	162.77	163.1	163.11	163.11	0.15	163.034	1472.086	0.15	163.034	164.29	164.59	164.63	164.47	164.31	0.1	164.5	1459.3		
25.0	171.2	172.7	172.8	172.8	172.3	0.7	172.4	1450.3	25	169.92	169.66	169.89	169.9	169.86	0.11	169.846	1471.922	0.11	169.846	171.01	171.43	171.41	171.2	171.0	0.2	171.2	1460.2		
26.0	177.9	179.6	179.5	179.5	179.4	0.7	179.1	1451.9	26	176.73	176.3	176.55	176.55	176.55	0.15	176.536	1472.787	0.15	176.536	177.85	178.18	178.06	177.96	177.69	0.2	177.9	1461.1		
27.0	184.7	186.3	186.2	186.3	185.7	0.7	185.8	1452.9	27	183.34	182.93	183.3	183.22	183.34	0.17	183.226	1473.59	0.17	183.226	184.57	184.93	184.84	184.64	184.48	0.2	184.7	1461.9		
28.0	191.4	193.1	192.9	192.9	192.4	0.7	192.5	1454.4	28	189.97	189.56	189.96	189.96	189.97	0.14	189.928	1474.243	0.14	189.928	191.21	191.63	191.57	191.41	191.08	0.2	191.4	1463.1		
29.0	198.1	199.8	199.7	199.7	199.1	0.7	199.3	1455.2	29	196.71	196.51	196.72	196.75	196.71	0.10	196.68	1474.476	0.10	196.68	198.25	198.48	198.28	198.25	197.79	0.2	198.1	1463.6		
30.0	204.9	206.6	206.5	206.5	205.9	0.7	206.1	1455.8	30	203.59	203.19	203.58	203.56	203.62	0.18	203.508	1474.144	0.18	203.508	204.67	205.22	205.17	204.88	204.63	0.2	204.9	1464.0		
31.0	211.6	213.3	213.3	213.3	212.8	0.8	212.9	1456.2	31	210.38	210.03	210.38	210.39	210.34	0.15	210.304	1474.057	0.15	210.304	211.57	211.87	211.88	211.73	211.41	0.2	211.7	1464.4		
32.0	218.4	220.0	220.0	220.0	219.4	0.7	219.8	1457.6	32	216.99	216.63	216.98	216.94	217.07	0.18	216.938	1475.076	0.18	216.938	218.3	218.6	218.54	218.36	218.09	0.2	218.4	1465.3		
33.0	225.1	226.8	226.7	226.7	226.2	0.7	226.3	1458.2	33	223.72	223.38	223.72	223.72	223.68	0.17	223.664	1475.427	0.17	223.664	224.91	225.25	225.26	225.07	224.87	0.2	225.1	1466.2		
34.0	231.8	233.7	233.6	233.5	232.9	0.8	233.1	1458.7	34	230.52	230.15	230.54	230.46	230.5	0.16	230.434	1475.477	0.16	230.434	231.68	232.22	232.13	231.88	231.61	0.2	231.9	1466.1		
35.0	238.6	240.4	240.5	240.3	239.7	0.8	239.9	1459.9	35	237.33	236.94	237.33	237.29	237.38	0.24	237.31	1474.804	0.24	237.31	238.5	239.05	238.85	238.75	238.41	0.2	238.7	1466.8		
36.0	245.5	247.2	247.3	247.2	246.5	0.8	246.6	1461.2	36	244.15	243.75	244.15	244.17	244.17	0.28	244.124	1474.66	0.28	244.124	240.44	240.87	240.85	240.66	240.38	0.2	240.5	1466.3		
37.0	252.2	254.0	253.8	253.7	253.3	0.7	253.4	1460.1	37	250.81	250.41	251.14	250.79	250.85	0.26	250.8	1475.279	0.26	250.8	252.01	252.45	252.35	252.24	252.1	0.2	252.2	1466.9		
38.0	259.0	260.6	260.6	260.5	259.9	0.6	260.2	1460.5	38	257.61	257.29	257.86	257.46	257.63	0.21	257.57	1475.327	0.21	257.57	258.73	259.17	259.17	258.98	258.71	0.2	259.0	1467.4		
39.0	265.8	267.6	267.6	267.3	266.6	0.8	267.0	1460.7	39	264.33	263.98	264.7	264.65	264.45	0.29	264.422	1474.915	0.29	264.422	260.57	260.97	260.85	260.77	260.54	0.2	260.8	1468.2		
40.0	272.7	274.3	274.3	274.2	273.4	0.7	273.8	1461.1	40	271.13	270.64	271.47	271.43	271.45	0.30	271.304	1474.361	0.30	271.304	272.82	273.26	273.26	273.07	272.8	0.2	273.2	1468.7		
41.0	279.4	281.2	281.1	281.0	280.2	0.7	280.6	1461.3	41	278.18	277.92	278.42	278.18	278.23	0.12	278.13	1474.131	0.12	278.13	279.05	279.55	279.45	279.28	279.02	0.2	279.3	1468.1		
42.0	286.1	287.8	287.8	287.6	287.0	0.7	287.3	1462.1	42	284.76	284.41	284.93	284.77	284.81	0.19	284.736	1475.051	0.19	284.736	285.72	286.24	286.21	285.9	285.7	0.2	286.0	1468.8		
43.0	292.8	294.5	294.4	294.3	293.6	0.7	293.9	1463.0	43	291.39	291.07	291.52	291.52	291.52	0.21	291.42	1475.534	0.21	291.42	292.36	292.95	292.78	292.58	292.3	0.2	292.6	1469.6		
44.0	299.5	301.3	301.1	301.0	300.4	0.7	300.6	1463.5	44	298.15	297.																		

Raw Data with calculated Results for 1MHz Transducer in Simulated Drilling Mud

Distance	Test 1		Test 2		Test 2		Mean [dB]	Ad [dB]	Std. [dB]	Ad [dB]	Ln Ad [y]	x	x*y	x*x	Am [dB]	d[Np/m]	Sqr Resid.	Sum[y-ym]				
	Gain [dB]	Rel. Amp.	Gain [dB]	Rel. Amp.	Gain [dB]	Rel. Amp.																
3	12.9	100.0	12.3	100.0	100.0	100.0	0.00	0.00	1.00	1.0	0.00	0.0	0.00	3.0	0.0	9	-0.131588034	1.05	0.00	0.00	0.05	
4	13.1	99.8	12.6	99.7	12.6	99.7	99.8	-0.23	0.05	0.97	0.9	0.12	0.2	-0.03	4.0	-0.1	16		1.04	0.03	0.00	0.04
5	13.2	99.7	12.8	99.5	12.7	99.6	99.6	-0.42	0.14	0.95	0.9	0.10	0.2	-0.05	5.0	-0.2	25	Regression model	1.02	0.02	0.00	0.03
6	13.2	99.7	12.9	99.4	12.9	99.4	99.5	-0.51	0.21	0.94	0.9	0.08	0.2	-0.06	6.0	-0.4	36	a	0.86	0.01	0.00	0.01
7	13.3	99.6	13.0	99.3	13.0	99.3	99.4	-0.60	0.21	0.93	0.9	0.08	0.2	-0.07	7.0	-0.5	49	b	0.99	0.02	0.00	0.02
8	13.3	99.6	13.0	99.3	13.1	99.2	99.4	-0.63	0.25	0.93	0.9	0.06	0.1	-0.07	8.0	-0.6	64	k1	0.97	0.01	0.00	0.02
9	13.3	99.6	13.1	99.2	13.1	99.2	99.3	-0.69	0.22	0.92	0.9	0.06	0.1	-0.08	9.0	-0.7	81	k2	0.96	0.01	0.00	0.02
10	13.3	99.6	13.2	99.1	13.2	99.1	99.2	-0.76	0.27	0.92	0.8	0.05	0.1	-0.09	10.0	-0.9	100	Sum[y-ym]	0.95	0.01	0.00	0.02
11	13.4	99.5	13.2	99.1	13.3	99.0	99.2	-0.82	0.25	0.91	0.8	0.05	0.1	-0.09	11.0	-1.0	121	RMSE	0.93	0.01	0.00	0.02
12	13.4	99.5	13.3	99.0	13.3	99.0	99.1	-0.85	0.27	0.91	0.8	0.05	0.1	-0.10	12.0	-1.2	144	Sx,y	0.92	0.01	0.00	0.02
13	13.4	99.5	13.3	99.0	13.3	99.0	99.1	-0.85	0.27	0.91	0.8	0.04	0.1	-0.10	13.0	-1.3	169	Significan	0.90	0.01	0.00	0.02
14	13.4	99.5	13.3	99.0	13.3	99.0	99.1	-0.85	0.27	0.91	0.8	0.04	0.1	-0.10	14.0	-1.4	196	Critical t	0.89	0.01	0.00	0.02
15	13.5	99.4	13.3	99.0	13.3	99.0	99.1	-0.88	0.22	0.90	0.8	0.04	0.1	-0.10	15.0	-1.5	225	Student's t Calculation	0.88	0.01	0.00	0.02
16	13.5	99.4	13.4	98.9	13.4	98.9	99.0	-0.95	0.28	0.90	0.8	0.04	0.1	-0.11	16.0	-1.8	256	Sum[DB]^2	0.86	0.01	0.00	0.01
17	13.5	99.4	13.4	98.9	13.4	98.9	99.0	-0.95	0.28	0.90	0.8	0.03	0.1	-0.11	17.0	-1.9	289	nMean^2	0.85	0.01	0.00	0.01
18	13.6	99.3	13.5	98.8	13.5	98.8	99.0	-1.05	0.28	0.89	0.8	0.03	0.1	-0.12	18.0	-2.2	324	sum[DB]	0.84	0.01	0.00	0.01
19	13.7	99.2	13.6	98.7	13.6	98.7	98.9	-1.15	0.28	0.88	0.8	0.04	0.1	-0.13	19.0	-2.5	361	sum[DB]^2	0.82	0.01	0.00	0.01
20	13.8	99.1	13.7	98.6	13.7	98.6	98.8	-1.25	0.29	0.87	0.8	0.04	0.1	-0.14	20.0	-2.9	400	nMean^2	0.81	0.01	0.00	0.01
21	13.9	99.0	13.8	98.5	13.8	98.5	98.7	-1.35	0.29	0.86	0.7	0.04	0.1	-0.16	21.0	-3.3	441	sum[DB]	0.80	0.01	0.00	0.01
22	14.1	98.8	14.0	98.3	14.0	98.3	98.4	-1.55	0.30	0.84	0.7	0.04	0.1	-0.18	22.0	-3.9	484	sumx2[y]-	0.79	0.01	0.00	0.00
23	14.2	98.7	14.1	98.2	14.1	98.2	98.3	-1.66	0.30	0.83	0.7	0.04	0.1	-0.19	23.0	-4.4	529	++ (t-value	0.78	0.01	0.00	0.00
24	14.4	98.5	14.3	98.0	14.3	98.0	98.1	-1.87	0.31	0.81	0.7	0.04	0.1	-0.22	24.0	-5.2	576	++ (t-value	0.76	0.01	0.00	0.00
25	14.6	98.3	14.5	97.8	14.5	97.8	98.0	-2.01	0.25	0.79	0.6	0.05	0.1	-0.23	25.0	-5.8	625	++ (t-value	0.75	0.01	0.00	0.00
26	14.7	98.2	14.7	97.6	14.7	97.6	97.8	-2.20	0.32	0.78	0.6	0.05	0.1	-0.25	26.0	-6.6	676	++ (t-value	0.74	0.01	0.00	0.00
27	14.9	98.0	14.9	97.4	14.9	97.4	97.6	-2.43	0.33	0.76	0.6	0.05	0.1	-0.28	27.0	-7.5	729	++ (t-value	0.73	0.01	0.00	0.00
28	15.1	97.8	15.0	97.3	15.0	97.3	97.5	-2.54	0.33	0.75	0.6	0.05	0.1	-0.29	28.0	-8.2	784	++ (t-value	0.72	0.01	0.00	0.00
29	15.3	97.6	15.3	97.0	15.3	97.0	97.2	-2.78	0.34	0.73	0.5	0.05	0.1	-0.32	29.0	-9.3	841	++ (t-value	0.71	0.01	0.00	0.00
30	15.5	97.4	15.4	96.9	15.4	96.9	97.1	-2.94	0.28	0.71	0.5	0.05	0.1	-0.34	30.0	-10.1	900	++ (t-value	0.70	0.01	0.00	0.00
31	15.6	97.3	15.6	96.7	15.6	96.7	96.9	-3.14	0.36	0.70	0.5	0.06	0.1	-0.36	31.0	-11.2	961	++ (t-value	0.69	0.01	0.00	0.01
32	15.9	97.0	15.8	96.5	15.8	96.5	96.7	-3.31	0.29	0.68	0.5	0.06	0.1	-0.38	32.0	-12.2	1024	++ (t-value	0.68	0.01	0.00	0.01
33	16.0	96.9	15.9	96.4	15.9	96.4	96.6	-3.44	0.30	0.67	0.5	0.06	0.1	-0.40	33.0	-13.1	1089	++ (t-value	0.67	0.01	0.00	0.01
34	16.2	96.7	16.2	96.1	16.2	96.1	96.3	-3.70	0.30	0.65	0.4	0.06	0.1	-0.43	34.0	-14.5	1156	++ (t-value	0.66	0.01	0.00	0.02
35	16.4	96.5	16.3	96.0	16.3	96.0	96.2	-3.83	0.31	0.64	0.4	0.06	0.1	-0.44	35.0	-15.5	1225	++ (t-value	0.65	0.01	0.00	0.02
36	16.5	96.4	16.5	95.8	16.5	95.8	96.0	-3.97	0.31	0.63	0.4	0.06	0.1	-0.46	36.0	-16.5	1296	++ (t-value	0.64	0.01	0.00	0.02
37	16.8	96.1	16.7	95.6	16.7	95.6	95.7	-4.25	0.32	0.61	0.4	0.06	0.1	-0.49	37.0	-18.1	1369	++ (t-value	0.63	0.01	0.00	0.03
38	16.9	96.0	16.9	95.4	16.9	95.4	95.6	-4.39	0.33	0.60	0.4	0.06	0.1	-0.51	38.0	-19.2	1444	++ (t-value	0.62	0.01	0.00	0.03
39	17.1	95.8	17.0	95.3	17.0	95.3	95.5	-4.54	0.33	0.59	0.4	0.06	0.1	-0.52	39.0	-20.4	1521	++ (t-value	0.61	0.01	0.00	0.03
40	17.2	95.7	17.2	95.1	17.2	95.1	95.3	-4.69	0.34	0.58	0.3	0.06	0.1	-0.54	40.0	-21.6	1600	++ (t-value	0.60	0.01	0.00	0.04
41	17.5	95.4	17.3	95.0	17.3	95.0	95.1	-4.89	0.26	0.57	0.3	0.06	0.1	-0.56	41.0	-23.1	1681	++ (t-value	0.59	0.01	0.00	0.04
42	17.6	95.3	17.5	94.8	17.7	94.6	94.9	-5.09	0.32	0.56	0.3	0.07	0.1	-0.59	42.0	-24.6	1764	++ (t-value	0.58	0.02	0.00	0.05
43	17.8	95.1	17.7	94.6	17.8	94.5	94.8	-5.25	0.33	0.55	0.3	0.07	0.1	-0.60	43.0	-26.0	1849	++ (t-value	0.57	0.02	0.00	0.05
44	17.9	95.0	17.8	94.5	18.0	94.3	94.6	-5.41	0.33	0.54	0.3	0.07	0.1	-0.62	44.0	-27.4	1936	++ (t-value	0.56	0.02	0.00	0.06
45	18.1	94.8	18.0	94.3	18.1	94.2	94.4	-5.57	0.34	0.53	0.3	0.07	0.1	-0.64	45.0	-28.9	2025	++ (t-value	0.56	0.02	0.00	0.06
										0.72	26.9			-0.27	24	-377.3	31390		0.01	0.05	0.87	

Raw Data with calculated Results for 2.25MHz Transducer in Simulated Drilling Mud

Distance	Test 1		Test 2		Test 3		Mean [dB]	Ad [dB]	Std. [dB]	Ad [dB]	Ln Ad [y]	x	x*y	x*x	Am [dB]	d[Np/m]	Sqr Resid.	Sum[y-ym]				
	Gain [dB]	Rel. Amp.	Gain [dB]	Rel. Amp.	Gain [dB]	Rel. Amp.																
3	9.7	100.0	9.8	100.0	9.8	100.0	100.0	0.0	0.00	1.0	1.0	0.00	0.0	0.00	3.0	0.0	9	0.98	0.0000	0.0003	0.0471	
4	9.9	99.8	10.0	99.8	10.0	99.8	99.8	-0.2	0.00	1.0	1.0	0.04	0.03	-0.02	4.0	-0.1	16	Regression model	0.97	0.0002	0.0001	0.0388
5	10.0	99.7	10.1	99.7	10.1	99.7	99.7	-0.3	0.00	1.0	0.9	0.03	0.03	-0.03	5.0	-0.2	25	a	0.96	0.0152	0.0001	0.0350
6	10.1	99.6	10.2	99.6	10.2	99.6	99.6	-0.4	0.05	1.0	0.9	0.03	0.05	-0.05	6.0	-0.3	36	b	0.95	0.0159	0.0000	0.0290
7	10.2	99.5	10.3	99.5	10.3	99.5	99.5	-0.5	0.00	0.9	0.9	0.03	0.05	-0.06	7.0	-0.4	49	k1	0.94	0.0155	0.0000	0.0247
8	10.3	99.4	10.4	99.4	10.4	99.4	99.4	-0.6	0.00	0.9	0.9	0.03	0.06	-0.07	8.0	-0.6	64	k2	0.93	0.0145	0.0000	0.0216
9	10.5	99.2	10.5	99.3	10.5	99.3	99.2	-0.8	0.05	0.89	0.8	0.03	0.07	-0.09	9.0	-0.8	81	Sum[y-ym]	0.92	0.0151	0.0000	0.0170
10	10.6	99.1	10.6	99.2	10.7	99.1	99.1	-0.9	0.06	0.9	0.8	0.03	0.07	-0.10	10.0	-1.0	100	RMSE	0.91	0.0145	0.0000	0.0145
11	10.7	99.0	10.8	99.0	10.8	99.0	99.0	-1.0	0.00	0.9	0.8	0.03	0.07	-0.12	11.0	-1.3	121	Sx,y	0.90	0.0146	0.0001	0.0115
12	10.8	98.9	10.9	98.9	10.9	98.9	98.9	-1.1	0.00	0.9	0.8	0.03	0.07	-0.13	12.0	-1.5	144	Significan	0.89	0.0142	0.0001	0.0094
13	10.9	98.8	11.0	98.8	11.0	98.8	98.8	-1.2	0.00	0.9	0.8	0.03	0.08	-0.14	13.0	-1.8	169	Critical t	0.88	0.0139	0.0001	0.0076
14	11.0	98.7	11.1	98.7	11.1	98.7	98.7	-1.3	0.00	0.9	0.7	0.03	0.08	-0.15	14.0	-2.1	196	Student's t Calculation	0.87	0.0137	0.0001	0.0059
15	11.1	98.6	11.1	98.7	11.1	98.7	98.7	-1.3	0.06	0.9	0.7	0.02	0.07	-0.15	15.0	-2.3	225	Sum[DB]^2	0.86	0.0129	0.0000	0.0054
16																						

Sound Velocity for Sim_Mud at 2.25MHz										Sound Velocity for Sim_Mud at 1MHz										Sound Velocity for Sim_Mud at 0.5MHz															
Test 1		Test 2		Test 3		Std.		Mean		ToF [cm/sec]		Test 1		Test 2		Test 3		Std.		Mean		ToF [cm/sec]		Test 1		Test 2		Test 3		Std.		Mean		ToF [cm/sec]	
Distance	ToF [μsec]	ToF [μsec]	ToF [μsec]	ToF [μsec]	ToF [μsec]	ToF [μsec]	ToF [μsec]	ToF [μsec]	ToF [μsec]	ToF [μsec]	ToF [μsec]	Distance	ToF [μsec]	ToF [μsec]	ToF [μsec]	ToF [μsec]	ToF [μsec]	ToF [μsec]	ToF [μsec]	ToF [μsec]	ToF [μsec]	ToF [μsec]	Distance	ToF [μsec]	ToF [μsec]	ToF [μsec]	ToF [μsec]	ToF [μsec]	ToF [μsec]	ToF [μsec]	ToF [μsec]	ToF [μsec]	ToF [μsec]	ToF [μsec]	
3	14.8	14.9	14.9	14.9	0.06	14.9	0.06	14.9	0.06	14.9	0.06	3	15.7	15.7	15.8	0.1	15.7	0.1	15.7	0.1	15.7	0.1	3	15.7	15.7	15.8	0.1	15.7	0.1	15.7	0.1	15.7	0.1	15.7	0.1
4	19.8	19.8	19.8	19.8	0.00	19.8	0.00	19.8	0.00	19.8	0.00	4	21.1	20.6	20.7	0.3	20.8	0.3	20.8	0.3	20.8	0.3	4	21.1	20.6	20.7	0.3	20.8	0.3	20.8	0.3	20.8	0.3	20.8	0.3
5	24.5	24.6	24.7	24.7	0.10	24.6	0.10	24.6	0.10	24.6	0.10	5	25.9	25.5	25.6	0.2	25.7	0.2	25.7	0.2	25.7	0.2	5	25.9	25.5	25.6	0.2	25.7	0.2	25.7	0.2	25.7	0.2	25.7	0.2
6	29.4	29.4	29.4	29.4	0.00	29.4	0.00	29.4	0.00	29.4	0.00	6	30.9	30.8	31	0.1	30.9	0.1	30.9	0.1	30.9	0.1	6	30.9	30.8	31	0.1	30.9	0.1	30.9	0.1	30.9	0.1	30.9	0.1
7	34.3	34.3	34.4	34.4	0.06	34.3	0.06	34.3	0.06	34.3	0.06	7	35.7	35.7	35.8	0.1	35.7	0.1	35.7	0.1	35.7	0.1	7	35.7	35.7	35.8	0.1	35.7	0.1	35.7	0.1	35.7	0.1	35.7	0.1
8	39.1	39.2	39.3	39.3	0.10	39.2	0.10	39.2	0.10	39.2	0.10	8	40.6	40.5	40.6	0.1	40.6	0.1	40.6	0.1	40.6	0.1	8	40.6	40.5	40.6	0.1	40.6	0.1	40.6	0.1	40.6	0.1	40.6	0.1
9	44.1	44.1	44.0	44.0	0.06	44.1	0.06	44.1	0.06	44.1	0.06	9	45.6	45.4	45.5	0.1	45.5	0.1	45.5	0.1	45.5	0.1	9	45.6	45.4	45.5	0.1	45.5	0.1	45.5	0.1	45.5	0.1	45.5	0.1
10	49.0	49.1	49.0	49.0	0.06	49.0	0.06	49.0	0.06	49.0	0.06	10	50.4	50.2	50.4	0.1	50.3	0.1	50.3	0.1	50.3	0.1	10	50.4	50.2	50.4	0.1	50.3	0.1	50.3	0.1	50.3	0.1	50.3	0.1
11	53.9	53.8	53.9	53.9	0.06	53.9	0.06	53.9	0.06	53.9	0.06	11	55.3	55.2	55.3	0.1	55.3	0.1	55.3	0.1	55.3	0.1	11	55.3	55.2	55.3	0.1	55.3	0.1	55.3	0.1	55.3	0.1	55.3	0.1
12	58.7	58.7	58.7	58.7	0.00	58.7	0.00	58.7	0.00	58.7	0.00	12	60.1	60.1	60.1	0.0	60.1	0.0	60.1	0.0	60.1	0.0	12	60.1	60.1	60.1	0.0	60.1	0.0	60.1	0.0	60.1	0.0	60.1	0.0
13	63.6	63.5	63.6	63.6	0.06	63.6	0.06	63.6	0.06	63.6	0.06	13	64.9	64.9	65	0.1	64.9	0.1	64.9	0.1	64.9	0.1	13	64.9	64.9	65	0.1	64.9	0.1	64.9	0.1	64.9	0.1	64.9	0.1
14	68.4	68.4	68.4	68.4	0.00	68.4	0.00	68.4	0.00	68.4	0.00	14	69.8	69.8	69.8	0.0	69.8	0.0	69.8	0.0	69.8	0.0	14	69.8	69.8	69.8	0.0	69.8	0.0	69.8	0.0	69.8	0.0	69.8	0.0
15	73.1	73.2	73.2	73.2	0.06	73.2	0.06	73.2	0.06	73.2	0.06	15	74.6	74.5	74.6	0.1	74.6	0.1	74.6	0.1	74.6	0.1	15	74.6	74.5	74.6	0.1	74.6	0.1	74.6	0.1	74.6	0.1	74.6	0.1
16	77.9	78.1	78.1	78.1	0.12	78.0	0.12	78.0	0.12	78.0	0.12	16	79.5	79.5	79.5	0.0	79.5	0.0	79.5	0.0	79.5	0.0	16	79.5	79.5	79.5	0.0	79.5	0.0	79.5	0.0	79.5	0.0	79.5	0.0
17	82.8	83.0	82.9	82.9	0.10	82.9	0.10	82.9	0.10	82.9	0.10	17	84.3	84.3	84.3	0.0	84.3	0.0	84.3	0.0	84.3	0.0	17	84.3	84.3	84.3	0.0	84.3	0.0	84.3	0.0	84.3	0.0	84.3	0.0
18	87.7	87.7	87.8	87.8	0.06	87.7	0.06	87.7	0.06	87.7	0.06	18	89.2	89.2	89.1	0.1	89.2	0.1	89.2	0.1	89.2	0.1	18	89.2	89.2	89.1	0.1	89.2	0.1	89.2	0.1	89.2	0.1	89.2	0.1
19	92.6	92.7	92.5	92.5	0.10	92.6	0.10	92.6	0.10	92.6	0.10	19	94.1	94	94	0.1	94.0	0.1	94.0	0.1	94.0	0.1	19	94.1	94	94	0.1	94.0	0.1	94.0	0.1	94.0	0.1	94.0	0.1
20	97.4	97.6	97.4	97.4	0.12	97.5	0.12	97.5	0.12	97.5	0.12	20	99	98.9	98.9	0.1	98.9	0.1	98.9	0.1	98.9	0.1	20	99	98.9	98.9	0.1	98.9	0.1	98.9	0.1	98.9	0.1	98.9	0.1
21	102.3	102.3	102.3	102.3	0.00	102.3	0.00	102.3	0.00	102.3	0.00	21	103.7	103.8	103.7	0.1	103.7	0.1	103.7	0.1	103.7	0.1	21	103.7	103.8	103.7	0.1	103.7	0.1	103.7	0.1	103.7	0.1	103.7	0.1
22	107.3	107.2	107.1	107.1	0.10	107.2	0.10	107.2	0.10	107.2	0.10	22	108.5	108.6	108.6	0.1	108.6	0.1	108.6	0.1	108.6	0.1	22	108.5	108.6	108.6	0.1	108.6	0.1	108.6	0.1	108.6	0.1	108.6	0.1
23	112.1	112.2	112.1	112.1	0.06	112.1	0.06	112.1	0.06	112.1	0.06	23	113.4	113.5	113.5	0.1	113.5	0.1	113.5	0.1	113.5	0.1	23	113.4	113.5	113.5	0.1	113.5	0.1	113.5	0.1	113.5	0.1	113.5	0.1
24	116.9	116.9	116.9	116.9	0.00	116.9	0.00	116.9	0.00	116.9	0.00	24	118.2	118.4	118.3	0.1	118.3	0.1	118.3	0.1	118.3	0.1	24	118.2	118.4	118.3	0.1	118.3	0.1	118.3	0.1	118.3	0.1	118.3	0.1
25	121.7	121.7	121.7	121.7	0.00	121.7	0.00	121.7	0.00	121.7	0.00	25	123.1	123.2	123	0.1	123.1	0.1	123.1	0.1	123.1	0.1	25	123.1	123.2	123	0.1	123.1	0.1	123.1	0.1	123.1	0.1	123.1	0.1
26	126.6	126.7	126.7	126.7	0.06	126.7	0.06	126.7	0.06	126.7	0.06	26	128	128	127.9	0.1	128.0	0.1	128.0	0.1	128.0	0.1	26	128	128	127.9	0.1	128.0	0.1	128.0	0.1	128.0	0.1	128.0	0.1
27	131.5	131.5	131.4	131.4	0.06	131.5	0.06	131.5	0.06	131.5	0.06	27	132.8	132.8	132.8	0.0	132.8	0.0	132.8	0.0	132.8	0.0	27	132.8	132.8	132.8	0.0	132.8	0.0	132.8	0.0	132.8	0.0	132.8	0.0
28	136.2	136.2	136.3	136.3	0.06	136.2	0.06	136.2	0.06	136.2	0.06	28	137.5	137.5	137.7	0.1	137.6	0.1	137.6	0.1	137.6	0.1	28	137.5	137.5	137.7	0.1	137.6	0.1	137.6	0.1	137.6	0.1	137.6	0.1
29	141.1	141.1	141.1	141.1	0.00	141.1	0.00	141.1	0.00	141.1	0.00	29	142.4	142.5	142.5	0.1	142.5	0.1	142.5	0.1	142.5	0.1	29	142.4	142.5	142.5	0.1	142.5	0.1	142.5	0.1	142.5	0.1	142.5	0.1
30	146.0	145.9	146.0	146.0	0.06	146.0	0.06	146.0	0.06	146.0	0.06	30	147.3	147.4	147.4	0.1	147.4	0.1	147.4	0.1	147.4	0.1	30	147.3	147.4	147.4	0.1	147.4	0.1	147.4	0.1	147.4	0.1	147.4	0.1
31	150.9	150.8	150.8	150.8	0.06	150.8	0.06	150.8	0.06	150.8	0.06	31	152.1	152.2	152.4	0.2	152.2	0.2	152.2	0.2	152.2	0.2	31	152.1	152.2	152.4	0.2	152.2	0.2	152.2	0.2	152.2	0.2	152.2	0.2
32	155.7	155.7	155.6	155.6	0.06	155.7	0.06	155.7	0.06	155.7	0.06	32	157	157	157	0.0	157.0	0.0	157.0	0.0	157.0	0.0	32	157	157	157	0.0	157.0	0.0	157.0	0.0	157.0	0.0	157.0	0.0
33	160.5	160.5	160.4	160.4	0.06	160.5	0.06	160.5	0.06	160.5	0.06	33	161.8	161.9	161.8	0.1	161.8	0.1	161.8	0.1	161.8	0.1	33	161.8	161.9	161.8	0.1	161.8	0.1	161.8	0.1	161.8	0.1	161.8	0.1
34	165.3	165.2	165.4	165.4	0.10	165.3	0.10	165.3	0.10	165.3	0.10	34	166.7	166.7	166.7	0.0	166.7	0.0	166.7	0.0	166.7	0.0	34	166.7	166.7	166.7	0.0	166.7	0.0	166.7	0.0	166.7	0.0	166.7	0.0
35	170.3	170.2	170.2	170.2	0.06	170.2	0.06	170.2	0.06	170.2	0.06	35	171.6	171.6	171.6	0.0	171.6	0.0	171.6	0.0	171.6	0.0	35	171.6	171.6	171.6	0.0	171.6	0.0	171.6	0.0	171.6	0.0	171.6	0.0
36	175.1	175.1	175.1	175.1	0.00	175.1	0.00	175.1	0.00	175.1	0.00	36	176.5	176.5	176.5	0.0	176.5	0.0	176.5	0.0	176.5	0.0	36	176.5	176.5	176.5	0.0	176.5	0.0	176.5	0.0	176.5	0.0	176.5	0.0
37	180.0	180.1	180.0	180.0	0.06	180.0	0.06	180.0	0.06	180.0	0.06	37	181.3	181.4	181.3	0.1	181.3	0.1	181.3	0.1	181.3	0.1	37	181.3	181.4	181.3	0.1	181.3	0.1	181.3	0.1	181.3	0.1	181.3	0.1
38	184.9	184.9	184.9	184.9	0.00	184.9	0.00	184.9	0.00	184.9	0.00	38	186.1	186.2	186.2	0.1	186.2	0.1	186.2	0.1	186.2	0.1	38	186.1	186.2	186.2	0.1	186.2	0.1	186.2	0.1	186.2	0.1	186.2	0.1
39	189.8	189.7	189.6	189.6	0.10	189																													

